PRODUCTION OF NANO CALCITE IN LARGE SCALE

A Thesis Submitted to
the Graduate School of Engineering and Sciences of
İzmir Institute of Technology
in Partial Fulfillment of the Requirements for the Degree of

MASTER OF SCIENCE

in Chemical Engineering

by
Sezen Duygu ALICI

July 2013
İZMİR

We approve the thesis of **Sezen Duygu ALICI**

Examining Committee Members:

_____
Assoc. Prof. Dr. Ekrem ÖZDEMİR
Department of Chemical Engineering
İzmir Institute of Technology

_____
Prof. Dr. Mehmet POLAT
Department of Chemical Engineering
İzmir Institute of Technology

_____
Prof. Dr. METİN TANOĞLU
Department of Mechanical Engineering
İzmir Institute of Technology

1 July 2013

_____
Assist. Prof. Dr. Ekrem ÖZDEMİR
Supervisor, Department of Chemical Engineering
İzmir Institute of Technology

_____   _____
Pof. Dr. Fehime Seher ÖZKAN   **Prof. Dr. R. Tuğrul SENGER**
Head of the Department of   Dean of the Graduate School of
Chemical Engineering   Engineering and Sciences

ACKNOWLEDGEMENTS

ABSTRACT

PRODUCTION OF NANO CALCITE IN LARGE SCALE

Calcium carbonate ($CaCO_3$) has been used extensively as filling material in various industries in order to improve some mechanical properties of the composite materials and to reduce the product costs. There are mainly two methods for synthesizing $CaCO_3$ crystals: chemical method and carbonization method. The carbonization method is the most appropriate method for nano calcite production. A systematic study was conducted on the synthesis of calcite in nano sizes, homogeneous size distribution, and different morphologies by employing the newly developed small penetration method. The effects of various parameters on the particle size and morphologies such as flow rates of raw materials, concentration, pipe diameter, volumes of stabilization tank and reaction chamber, length in the reaction chamber, stirring rate, and temperature were investigated. Calcite particles of about 100-150 nm were achieved to produce in homogeneous size distributions for the developed method at large scale.

ÖZET

BÜYÜK ÖLÇEKTE NANO KALSİT ÜRETİMİ

Kalsiyum karbonat ($CaCO_3$), çeşitli sanayilerde kompozit malzemelerin bazı mekanik özelliklerini geliştirmek ve üretim maliyetini azaltmak amacıyla dolgu malzemesi olarak kullanılmaktadır. $CaCO_3$ temel olarak iki yöntem ile sentezlenmektedir: kimyasal yöntem ve karbonizasyon yöntemi. Nano kalsit üretimi için en uygun yöntem karbonizasyon yöntemidir. Yeni geliştirilmiş kısa penetrasyon yöntemi kullanılarak, nano boyutlarda, homojen boyut dağılımında ve farklı morfolojilerde kalsit üretmek üzere sistematik bir çalışma yapılmıştır. Ham maddelerin akış hızları, konsantrasyon, boru çapı, stabilizasyon tankı ve reaksiyon haznesinin hacimleri, reaksiyon haznesinin uzunluğu, karıştırma hızı ve sıcaklık gibi bazı parametrelerin tanecik boyutu ve morfolojileri üzerine etkileri incelenmiştir. Yaklaşık 100 – 150 nm boyutlarında ve homojen boyut dağılımınd kalsit taneciklerinin üretilmesi geliştirilen yeni yöntem ile büyük ölçekte başarılmıştır.

TABLE OF CONTENTS

LIST OF FIGURES

LIST OF TABLES

CHAPTER 1

INTRODUCTION

Nanotechnology is an essential research area that can be an alternative to perceive the development level of a country. Human beings have started to use nanotechnology for their own benefits only recently, although the nature has been using it for millions of years. This technology is known as an ability to manipulate, control and engineer the materials in the nanometer range. Properties of nanomaterials are not restricted to their structural or mechanical behaviors; and it is expected that nanomaterials would be the ground breaking improvement in the scientific areas such as information storage, pharmacy, metals, chemical, ceramics, polymers and catalysts etc.. Thus, Turkey, as the other countries, has been trying to form their own nanotechnology studies and areas focused on the advanced ceramics, nanostructured thin films, semiconductors, nanocomposites and advanced polymers. Nano calcium carbonate studies are one of those that came at the beginning of these nanotechnology researches.

Calcium carbonate ($CaCO_3$) has been used extensively as filling material in numerous applications such as electronics, paint, rubber, ink, ceramics, paper, metallurgy, optics, plastics and etc. (Cai, 2003; J. Carmona, 2004; Jung, Sung, Kim, Kim, & Chang, 2010; Matahwa, Ramiah, & Sanderson, 2008). Calcium carbonate has three different anhydrous crystalline polymorphs which have typical morphologies: aragonite (needles), vaterite (polycrystalline spheres), and the most thermodynamically stable calcite (rhomboidal). These polymorphs van be synthesized by adjusting the production conditions, and they can be used in different industries. Advanced applications of $CaCO_3$ essentially involve the synthesis of stable, homogeneous, and nano sized particles to be used as filler material in polyester films for magnetic types' productions, builder for detergent productions, coating pigment in the production of paper and cosmetic industries (J. Carmona, 2004). Using filling material in composite materials generally reduces the product cost and improves some of the mechanical properties of composite materials. For instance, when it is used in polypropylene (PP), the tensile yield strength of propylene-calcite composite material was decreased as the volume fraction of calcite was increased as shown in Figure 1.1. The decrease in tensile

yield strength is significant for the large particles. However, the decrease in tensile yield strength is less pronounced when smaller particles were used. As shown in the figure, as the diameters of the used calcite particles decrease, the tensile yield strength of the material is improved (J. F. W. Chen, Y. H., 2000). When 10 nm of calcite particles were used, there were no decrease in the tensile yield strength; on the other hand, it increased slightly. Consequently, by using this inorganic material as filler in composite materials, some of the structural features of them can be improved. The nature, shape and dispersion characteristics of the calcite particles effect the mechanical and other properties of the polymers (Tosun, 1988). Other advantages of using nano calcium carbonate are that, they can improve the air-tightness, opacity, resistivity and stiffness, and provide good stability, and good electricity insulation. Therefore, use of nano calcite is important in composite materials.
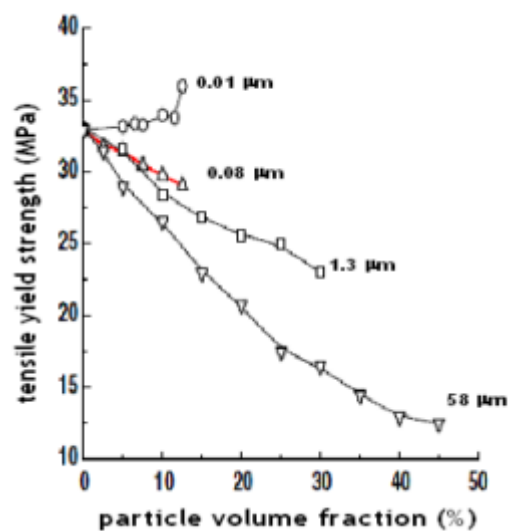
Figure 1.1. Tensile yield strength of polypropylene – calcite composite material
(Source : Chen 2000)

The calcium, carbon and oxygen atoms can arrange themselves in three different ways, to form three different calcium carbonate minerals. The most common arrangement is the hexagonal form known as calcite. A number of different calcite crystal forms are possible: scalenohedral, rhombohedral and prismatic. Also, less common form is aragonite, which has a discrete or clustered needle orthorhombic crystal structure. Rare and generally unstable one is called as vaterite mineral. These polymorphs can be synthesized by adjusting the production conditions and they can be

used in different industries. Also, soluble additives can be used and they alter the growth rates of crystal faces thus change in the overall crystal morphologies can be obtained (Cölfen, 2003; Pontoni, 2003). But, in this study, it is tried to produce nano sized calcite particles with optimum conditions and without additives.

There are basically three methods for calcite synthesis. These methods can be lime-soda, chemical and carbonization methods. The lime-soda process is the classical method of producing caustic soda, however, in this process, a solution of sodium carbonate is treated with excess $Ca(OH)_2$ producing liquid caustic and so, precipitated calcium carbonate (PCC) is produced as byproduct. Furthermore, the chemcal method utilizes Na_2CO_3 and $CaCl_2$. In both of these methods, the produced calcium carbonate particles' size is more than micron size, and so, nano $CaCO_3$ production is not possible by these methods especially in industrial scale (Islam, 2008). The only way to produce nano sized calcite particles is the carbonization method and it is widely used commercially. Because of the availability of raw materials and their low costs, carbonation method for producing nano calcite has advantages for large scale. The overall carbonation process generally consists of the following steps (Lin, Zhang, & Bai, 2006);

    a.   dissolution of calcium hydroxide ($Ca(OH)_2$):

$$Ca(OH)_2(s) \leftrightarrow Ca^{2+}(aq) + 2OH^-(aq);$$
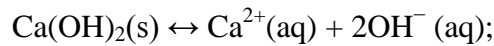
    b.   dissolution of carbon dioxide (CO_2) from gas phase into the liquid phase:

$$CO_2 \leftrightarrow CO_2(aq);$$
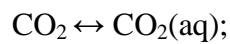
    c.   ionization of the dissolved CO_2:

$$CO_2(aq) + OH^-(aq) \rightarrow HCO_3^-(aq)$$
$$HCO_3^-(aq) + OH^-(aq) \rightarrow H_2O + CO_3^{-2}(aq);$$

    d.   and, crystallization:

$$Ca^{2+} + CO_3^{-2}(aq) \rightarrow CaCO_3(s). \text{ (Monchau, Hivart et al.)}$$
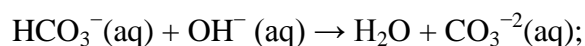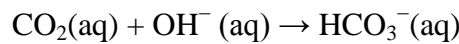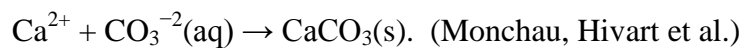
Generally, in literature, calcium carbonate crystallization has been studied extensively for a model system to other ionic crystallization processes and to understand the biological occurrences. However, no method has been suggested as of yet to produce calcite ($CaCO_3$) in nano sizes, homogeneous size distribution, and different morphologies especially in large scales. Therefore, the objective of this thesis is to produce nano calcite in homogeneous size distribution and different morphologies without using any additives.

CHAPTER 2

LITERATURE SURVEY

2.1   Forms of Calcium Carbonate and Usage Areas

Calcite is the most stable crystal form of the calcium carbonate and it has a wide range of applications. By using this inorganic material as a filler in thermoplastics, some of the structural features of them such as hardness, stiffness, toughness and heat distortion temperature, need to be improved. The nature, shape, aggregate size, degree of dispersion in the matrix form of composite materials, particle size and surface characteristics of the calcite effect the mechanical and other properties of the polymers (Tosun, 1988). When nano sized filling materials were used, the enhancement in the mechanical properties is especially significant, also, using this materials reduce the product costs (J. F. W. Chen, Y. H., 2000).

Calcium carbonate is classified by forms of presence as GCC (Ground Calcium Carbonate) and PCC (Precipitated Calcium Carbonate). PCC is generated by a method which uses CO_2 in a high concentration which is diffused through a $Ca(OH)_2$ solution. This method is generally called as carbonization method and it is also useful for sequestration of CO_2 from the waste gases (Ahn et al., 2003). Another method is chemical method which utilizes $CaCl_2$ as calcium source and Na_2CO_3 as carbonate source (Kang, Hirasawa, Kim, & Choi, 2005).

By changing the precipitation conditions and methods, the morphologies of calcium carbonate particles, that are categorized as calcite (rhombic), aragonite (needle-like) and vaterite (spherical), can be modified (Jung, 2000). Vaterite is generally formed in spherical, hexagonal, dihexagonal, and dipyramidal crystalline forms. Needle-like, orthorhombic and dipyramidal forms of calcium carbonates are called as aragonite. On the other hand, calcite is formed in rhombohedral, trigonal, hexagonal and scalenohedral morphologies (Coto, Martos, Peña, Rodríguez, & Pastor, 2012; Monteshernandez, Fernandezmartinez, Charlet, Tisserand, & Renard, 2008). Although, all of these crystal forms have the same composition of atoms, these atoms are differently arranged. So, these minerals contain different features. For example, one

major difference is that, in water aragonite is about %16 more soluble than calcite at 15°C. Usually, calcite crystals were characterized as {1 0 4} forms (García-Carmona, Morales, & Clemente, 2003). General crystal structures of calcite and its difference from the other $CaCO_3$ forms were given in Figure 2.1. Also, from the SEM images of $CaCO_3$ crystals, morphological differences of these crystals can be seen easily in Figure 2.2.
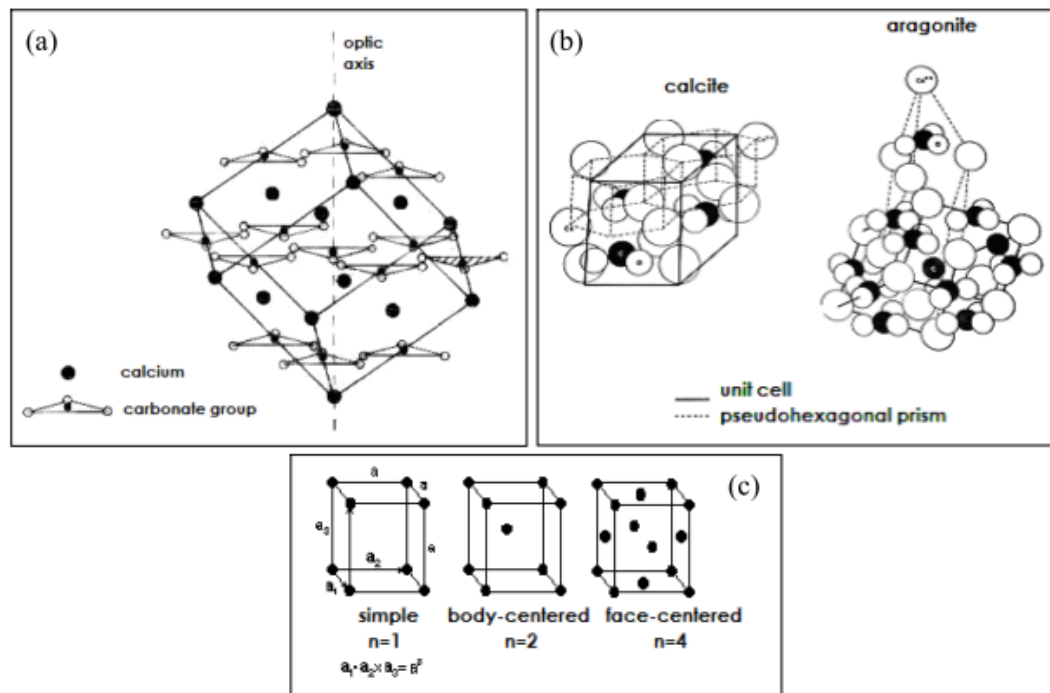
Figure 2.1. Lattice structure of calcite crystal (a) Calcite structure (b) Differences of calcite and aragonite crystal structures (c) Different atomic arrangements of calcite crystals
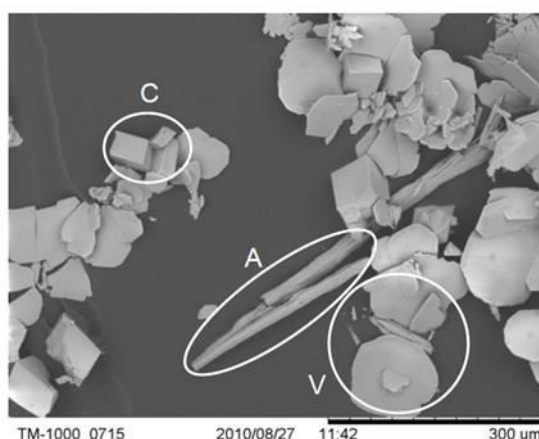
Figure 2.2. SEM images of CaCO$_3$ crystals (A) aragonite, (C) calcite and (V) vaterite
(Source : Tang, 2012)

The precipitation of calcium carbonate particles of different sizes, surface properties and morphologies have been intensively studied because of their application areas such as plastics, textiles, rubbers, adhesives, paints, paper, drug delivery, optics and wastewater treatment industries (Feng, Yong, & An, 2007; Jung, 2000; Nefyodova, 2000). These features of particles play a considerable role in determining the product's mechanical properties (Hrnjak-Murgic, 2002). The most important properties have been sizes and morphologies. For example, rhombohedral shaped calcite has been used as filler or pigment for paper industry to improve the brightness, opacity and smoothness of the papers (García-Carmona et al., 2003). On the other hand, plastic and rubber industries have required needle-like precipitated calcium carbonate particles with defined parameters, such as specific surface area, brightness, oil adsorption and chemical purity (Ye & Chen, 2011). Because of the increase of the interfacial area between the polymer and nano calcites, natural rubber latex film's tear strength, tensile strength and modulus can be efficiently improved by CaCO$_3$ nanocrystals (Cai, 2003). If nano calcites used as coating layer in the paper industry, they improve the gloss, opacity, absorption of ink, flatness, and spread (Laudone, 2004).

Calcite particles in nano sized and with low aggregation and agglomeration states exhibit better particle distribution while they are used in printing inks as additive or in cellulose fibers for paper fabrication as a brightness additive. Also, because of their dissolution in a solvent is faster than that of micro sized particles, nano calcite particles are used for antacid tablets (Montes-Hernandez, Daval, Findling, Chiriac, & Renard, 2012).

Besides these usage areas, other advanced applications have been investigated. Calcite particles in nano sized and homogeneous size distribution are used in detergent industry as builder, cosmetics industry as coating of pigments, and magnetic tapes industry as filler in polyester films. Hereby, development of production methods which can be easily scaled up to industrial scale should be provided (G. a. Carmona, 2003).

In 2011, grade calcium carbonate consumption was nearly 74 megatons in the world. 81 percent of this consumption was ground (GCC), and 19 percent of it was precipitated $CaCO_3$ (PCC). The largest markets for calcium carbonate have been paper and plastics which were accounting for around 39% and 26%, respectively, of total consumption of GCC and PCC in 2011(Roskill Information Services, 2012). The industries and their calcium carbonate consumption rates and also expected rates of them up to 2016 were given in Figure 2.3 (Roskill Information Services, 2012).
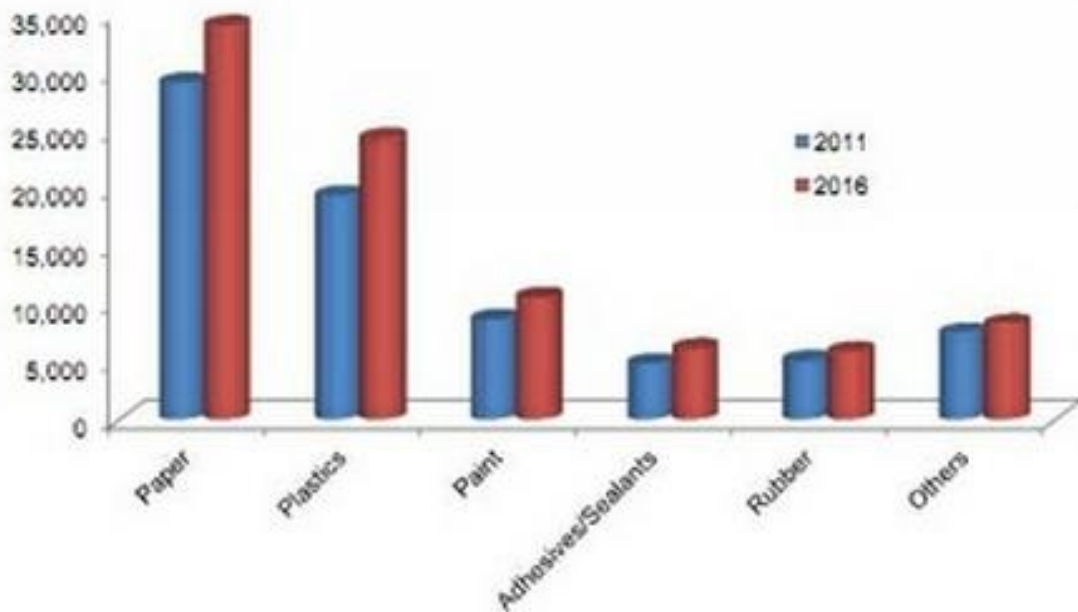
Figure 2.3. Consumption and forecast demand for GCC and PCC by end use, 2011 and 2016 (Source : Roskill Information Services, 2012)

2.2 Methods of CaCO₃ Production

Calcium carbonate precipitation methods are classified in two groups. The first method is chemical method which utilizes sodium carbonate (Na_2CO_3) as a carbonate source and calcium chloride ($CaCl_2$) as a calcium source (Zhu, Luo, Luo, & Liang,

2010). In this method, these two solutions are placed in a vessel with specific quantities. Both calcium chloride and sodium carbonate are completely soluble in water, therefore, Ca^{++} and $CO_3^{=}$ ions are dispersed easily in water and $CaCO_3$ crystallization occurs in the aqueous phase. This method has been used to explore the first step of the precipitation process by time dependent XRS (Pontoni, 2003; Rieger, 2000). But, this common technique has an important disadvantage that the initial growth and nucleation time scale is similar magnitude as the mixing time scale. Because of this situation, before nucleation will start, achieving homogeneous conditions is difficult (Faatz, Gröhn, & Wegner, 2005). Also, the produced calcium carbonate particles' size is more than micron size, and so, nano $CaCO_3$ production is not possible by the chemical method especially in industrial scale. However, because of the parameters can be controlled easily, chemical method is an applicable technique (Molva, 2012).

The second method is carbonization method which is the most suitable technique for the nano $CaCO_3$ production in industrial scale. The reason is that the raw materials are cheaper. Carbonization method utilizes calcium hydroxide ($Ca(OH)_2$) as a calcium ion source and carbon dioxide (CO_2) as a carbonate ion source. In the carbonization technique, an initial solution is prepared in a predetermined amount and then CO_2 gas is contacted through this solution. In literature, lots of different methods about carbonization route were attempted. By using pH and temperature controlled crystallizers of stirred tank (H. Konno, 2003), Couette-Taylor tank (Jung, 2000), spinning disc reactor (Burns & Jachuck, 2005), CSTR and fluidized-bed type (Tai, 2001), the crystal growth of $CaCO_3$ particles were studied. In one case, CO_2 gas was directly sent through the solution surface and reaction was controlled by stirring rates. in another case bubbling method was used (García-Carmona et al., 2003). In the bubbling method, $Ca(OH)_2$ solution was prepared in a batch and a bubbler was placed in the reactor. CO_2 gas was sent through this bubblers and diffusion occurs on the bubbles' surfaces (J. Carmona, 2004; Dagaonkar, Mehra, Jain, & Heeres, 2004; Domingo, Loste, Gómez-Morales, García-Carmona, & Fraile, 2006; García-Carmona et al., 2003). A schematic reactor designed by Jiang et al was given in Figure 2.4. Here, the reactor was filled with $Ca(OH)_2$ slurry and a micropore disperser was located in the reactor which had a gas inlet at the bottom. The CO_2 gas was dispersed into the mixture at a specific flow rate and reaction was not stopped until pH value dropped to 7. CO_2 gas bubbles' sizes were controlled by the micropore disperser with mean size of 20 μm (Jiang et al.,

2011). However, with this technique, obtained nano particles were quite clustered and process was not fully-controllable.
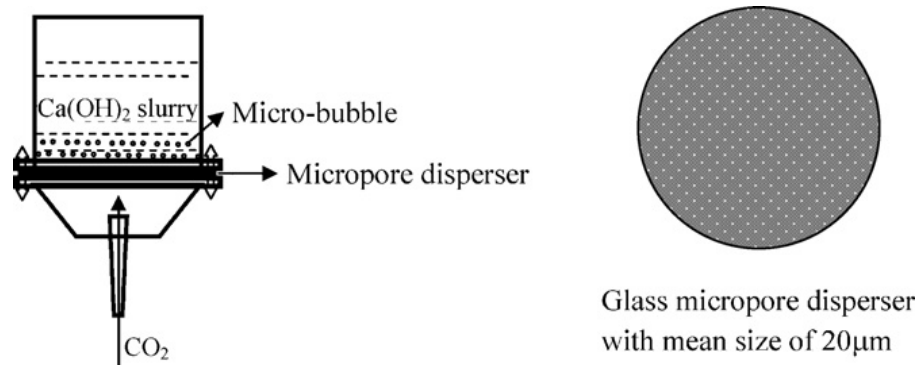
Figure 2.4. A schematic design of bubbling reactor for carbonization technique
(Source : Jiang et al., 2011)

In general, when the chemical and the carbonization methods are compared, in chemical method, obtained $CaCO_3$ particles are in micron size, but their morphologies are distinctly shaped (Faatz et al., 2005; Trippa & Jachuck, 2003). On the other hand, the particles obtained by carbonization method are in nano size and they have homogeneous particle size distributions depending on the method applied (Dagaonkar et al., 2004; Lin, 2002).

In literature, the researches were generally done at the laboratory scales. Only a few large scale studies were done in 5, 7 and 15 L reactors. Carbonization method was studied by Sonawane et. al with a 5 L reactor and they investigated the effects of diameter and geometry of orifice, CO_2 flow rate, and $Ca(OH)_2$ concentration. They demonstrated that very small calcite particles can be synthesized by using hydrodynamic cavitation reactor (Sonawane & Gumfekar, 2010). But, this study may not be scaled up for the industrial production because of the lime collected on the orifice can cause the system not to work continuously.

Chen et. al tried to produce hydrophobic calcium carbonate particles by using additives via carbonization route with a 7 L reactor. The amount of Ca^{++} ions they used was nearly saturation concentration amount and by using stearic acid (SA) in the presence of polyethylene glycol phosphate, they obtained nano calcite particles. Their particles were covered with stearic acid on their surfaces. They claimed that, when the weight ratio of $SA/CaCO_3$ reaches 2 % or more, $CaCO_3$ particles were covered by the

intact organic structure formed which makes $CaCO_3$ particles hydrophobic (X. Chen et al., 2010). But, the obtained particles were agglomerated and using additives would increase manufacturing costs. So, this technique may not be scaled up for the industrial production, too.

Another large scale study was reported by Cho et. al, which is about synthesis of calcium carbonate using limestone with 15 L reactor. They synthesized homogeneous PCC by calcinations, carbonation, and hydration of limestone. A $Ca(OH)_2$ solution from limestone was prepared in a 15 L reactor, and CO_2 gas was sent through the reactor by an injection pipe. After the production of nano calcites, they made a handmade paper and cover these papers with obtained calcite particles. Then, they analyzed the effects of $CaCO_3$ particles on the paper's printability (ink gloss, ink set-off, dry pick, wet pick) physical/optical properties (internal tearing strength, brightness, roughness, whiteness, opacity, gloss, tensile strength, stiffness, bursting strength) (Johannsen, 1999). Generally, limestone contains not only CaO and CO_2 but also silicon dioxide, aluminum oxide, magnesium oxide and so on as impurities which have unwanted effects on the properties of the synthesized calcium carbonate. So, using calcium hydroxide with very low impurity would be a better way to produce fine particles.

2.3   Effects of Flow Rates of Raw Materials

In a carbonization process of $CaCO_3$, some operating conditions such as the initial concentration of $Ca(OH)_2$, the gas flow rate, and the slurry flow rate would influence the batch processing time of crystallization when the volume remained the same. The change in the carbonation time can affect the quality of the products. If the carbonation time is too fast, controlling the diffusion and nucleation of the first $CaCO_3$ particles will be difficult. An increase in the gas flow rate will lead to an increase in the rate of mass transfer between two phases. So, by increasing the gas flow rate, the carbonation time decreases. For the same reason, the increase in the $Ca(OH)_2$ solution flow rate will cause a decrease in the carbonation time (J. F. W. Chen, Y. H., 2000). It can be said that, the most important stage for controlling the carbonation rate is the CO_2 absorption on the liquid surface which is affected by the flow rates of starting materials (Gupta, 2004).

Injecting the CO_2 gas into the system so fast will cause an excess ions of $CO_3^=$ in the reaction chamber, so, due to the adsorption of excess ion on the particle surface is proportional to the excess species concentration in solution, and the morphology of the particles would change and the particle size would decrease until the equilibrium adsorption is reached. Then, particle size and crystal structures become insensitive to the excess ions in the system (Jung, 2000). Also, the enhancement factor which is a condition that makes particles structure and size as covetable, plays a major role as a significant operating parameter in the synthesis of nano calcite particles. The enhancement factor is related to the flow rates of $Ca(OH)_2$ and CO_2 flow rates. As the ratio of flow rates of CO_2 and $Ca(OH)_2$ decreases, the enhancement factor decreases, too (Jung, 2000).

Basic calcium carbonate (BCC) synthesis was studied by Ji-Whan Ahn et. al, and they predicted that the formation of BCC depended on the temperature and concentration of the initial solution and also, CO_2 gas flow rate. It was obtained that in the case of a low concentration of the $Ca(OH)_2$ solution, basic calcium carbonate particles were synthesized at a lower flow rate of CO_2 gas in proportion to the relative concentration (Ahn et al., 2003).

Flow rates of raw materials can be adjusted with respect to the desired properties of the products, but the enhancement factor, carbonation time and carbonation rate should be considered and then, optimum values of flow rates should be chosen. Flow rates of $Ca(OH)_2$ and CO_2 will actually affect adsorption rate directly. So, controlling the injection conditions is also important as much as flow rate to improve the adsorption of raw materials in the system (Wu, Wang, Zhu, & Wang, 2007).

2.4 Effects of Supersaturation of Ca(OH)$_2$ Solution

$CaCO_3$ synthesis with carbonization method is a widespread production technique in the industry. The shape and size of $CaCO_3$ is controlled by the change of reaction conditions such as reaction temperature, flow rate of CO_2 gas, absorption rate and also initial calcium hydroxide concentration (Ahn et al., 2003). As mentioned earlier, in both the liquid-liquid and gas-liquid reaction systems of the calcium carbonate precipitation, it was clear that the concentrations in solution are as important

as the temperature in determining the nucleation rate, growth rate, and morphology of calcium carbonate particles.

Basically, there are three stages of crystallization; these are dissolution of $Ca(OH)_2$, CO_2 diffusion through the liquid phase, and the $CaCO_3$ crystallization. If the amount of $Ca(OH)_2$ that is fed to the reactor is so high, undissolved $Ca(OH)_2$ will remain in the solution, which is called a $Ca(OH)_2$ slurry. The excess $Ca(OH)_2$ particles can cause a growth on these particles. The ionic equilibrium was first mentioned in a report by Nehrke et al, they asserted that, at a constant degree of supersaturation, the growth rate of $CaCO_3$ particles was highest when the ion ratio in the solution, $r=[Ca^{++}]/[CO_3^{=}]$ was equal to 1 as illustrated at Figure 2.5. The growth rate was decreased symmetrically with increasing or decreasing of the ion ratio.
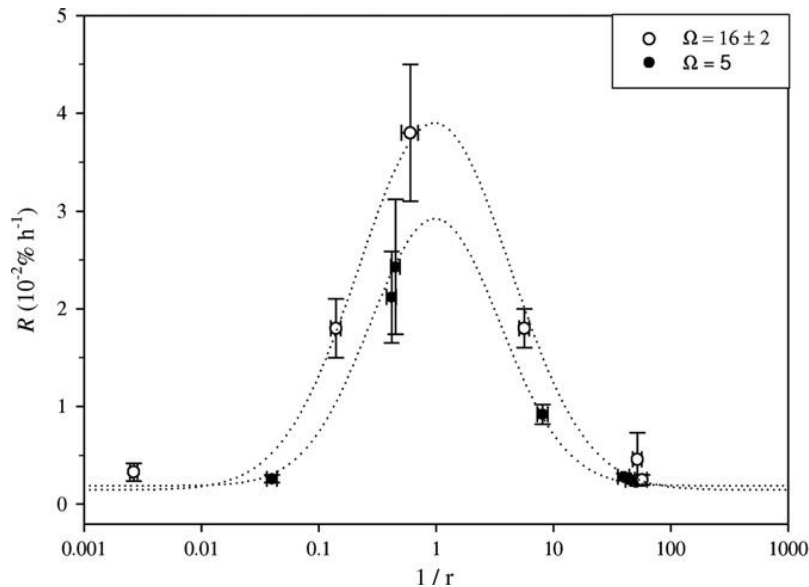
Figure 2.5. Growth rate (R) versus the inverse of the solution $[Ca^{++}]/[CO_3^{=}]$ ratio, r, for two different degrees of supersaturation (Source : Nehrke, Reichart, Vancappellen, Meile, & Bijma, 2007)

In the literature, some studies about the concentration of the initial $Ca(OH)_2$ solution were done. One of these researcher groups was Jung and co-workers, and their results showed that, morphology and size of the particles were caused mainly by the excess species of the reactants in the solution. When the relative enhancement factor (E_r) containing the operation variables was equal to 1, for which stoichiometric reaction condition persisted, the largest mean particle size and cubic shaped particles were

obtained. If the E_r shifted from 1, morphological structures of particles changed from cubic shape to a spindle shape. At the same time, as the excess ions of Ca^{++} concentration in the solution was increased, the mean particle size was decreased (Jung, 2000). But, in this article, the considered concentration values were below the saturation limit of $Ca(OH)_2$. Above the saturation concentration, the obtained particles start to grow as the concentration of the $Ca(OH)_2$ solution was increased.

Kim et al studied the inhibition mechanism of carbonation reaction between $Ca(OH)_2$ and CO_2 by magnesium ion. They investigated the effects of $Ca(OH)_2$ concentration, CO_2 flow rate and temperature effects on the particle size and morphology. Magnesium chloride ($MgCl_2$) was added into the system as an additive. During the precipitation of $CaCO_3$ in the solution, using Mg^{2+} ions enhanced aragonite formation and hindered the calcite growth. According to their experimental results, increasing the magnesium ions concentration caused an increase in the formation yield of aragonite prominently. Furthermore, aspect ratio and particle size were increased due to the increase in the $Ca(OH)_2$ concentration (J. H. Kim, Ahn, Ko, Park, & Han, 2006).

In another study done by Sonawane et al, three different concentration was studied and concentration effects were investigated by using a hydrodynamic cavitation reactor with different sized orifices (Sonawane & Gumfekar, 2010). They used carbonation method and circulated the $Ca(OH)_2$ solution through the system with the help of an orifice, so, reaction and stabilization partitions of the process were split off. At higher $Ca(OH)_2$ concentration, decrease in conductivity took longer time in comparison to lower $Ca(OH)_2$ slurry concentration. This situation denoted that, there was shorter induction time for low $Ca(OH)_2$ slurry concentration, and longer induction time for higher $Ca(OH)_2$. By increasing the molarity of the slurry, they observed that the crystallite size had started to grow (Sonawane & Gumfekar, 2010).

2.5 Effects of Temperature

BCC synthesizing process is a temperature sensitive process due to the raw materials. Calcium hydroxide's solubility decreases with temperature (Johannsen, 1999). But, there is a complex situation about the solubility of CO_2 and $Ca(OH)_2$ materials due to the temperature. It can be said that, the temperature decreases the dissolution rate of $Ca(OH)_2$ (Johannsen, 1999) and also negatively influences the CO_2

solubility in water (Domingo et al., 2006), and so on, solubility of solid product $CaCO_3$ (G. a. Carmona, 2003). It's known that, for homogeneous calcium carbonate precipitation, the necessary conditions are low temperature and supersaturation, and also and weak water hardness.

It's reported almost all sources that the structure of $CaCO_3$ was influenced by temperature. It is possible to say that calcite form was obtained at low temperatures. Otherwise, at higher temperatures, aragonite and vaterite forms can be produced (Beck, 2010). Calcite has the lowest solubility value and amorphous calcium carbonate has the highest solubility value. So, it is possible to say that the solubility of the product increases with decreasing temperature. At the pressure of 1 bar, the calcite polymorphs have the lowest solubility product, which is illustrated at Figure 2.7.

It can be seen from Figure 2.6, in chemical method, a number of polymorphs of calcium carbonate can precipitate simultaneously at diverse conditions. Vaterite seems to be formed between 10 and 70 ºC firstly; on the other hand, aragonite is not formed at low temperatures. It is kinetically stabilized at higher temperatures. At the temperature of nearly 30ºC, spherulites (vaterite structure) with a higher degree of branching than that was observed at 90ºC are formed. This distinctly means that out of the supersaturation ratio, the temperature ratio has a substantial effect on the growth of $CaCO_3$ particles. To obtain vaterite and aragonite, temperature must be higher (J. Carmona, 2004). Vaterite formation is generally known as the result of the aggregation of small nano particles. Calcite, which is the most stable polymorph of calcium carbonate, occurs at lowest temperatures. As a conclusion, all forms of calcium carbonates, both aragonite and vaterite, transform to stable calcite (Beck, 2010).
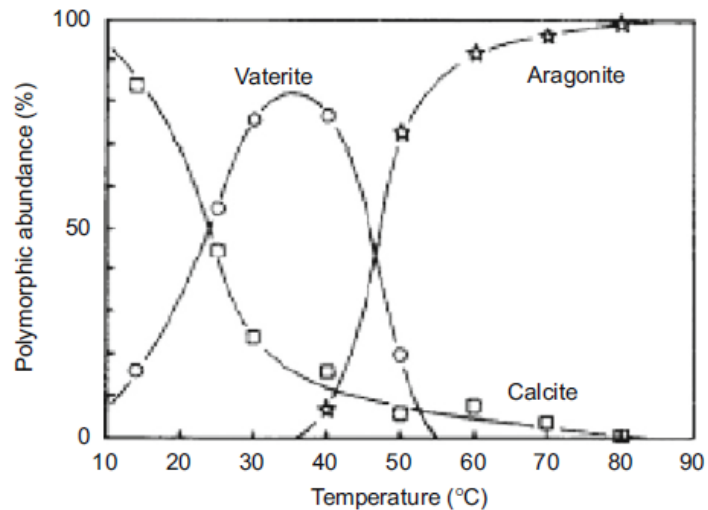
Figure 2.6. Initial polymorphic composition of CaCO$_3$ in dependence of the temperature (Source : Ogino, 1987)

In carbonization method, calcite formation was observed the first time at temperatures lower than 25ºC (García-Carmona et al., 2003). They denoted that it was possible to synthesize calcite with varied morphologies and sizes without any additive materials by adjusting the temperature during carbonation process. It was observed that the temperature affected the carbonation time and dissolution of ions; and as the temperature was increased, the sizes of products were getting larger and morphologies were changed from cubic to amorphous structures (García-Carmona et al., 2003). So, in carbonization method, temperature should be low (< 25 ºC) due to the solubility of Ca(OH)$_2$, for synthesizing nano calcite particles. Because it is well known that as the temperature was decreased, solubility of Ca(OH)$_2$ was increased (Johannsen, 1999).
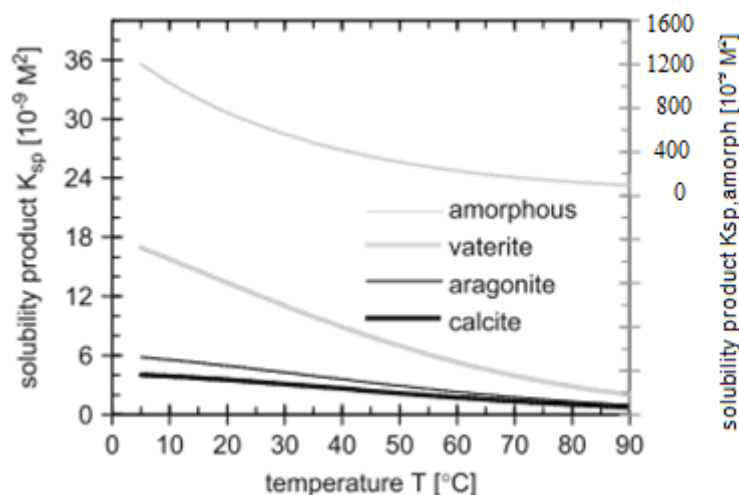
Figure 2.7. Solubility product of amorphous CaCO$_3$ and the three anhydrous crystalline polymorphs at 1 bar (Source : Beck, 2010)

2.6   Effects of Stirring Conditions

The stirring effect of the solution on the crystallization behavior was reported in literature (J. F. Z. Chen, C.; Chen, G. T. , 1996; J. F. W. Chen, Y. H., 2000; Ibrahim et al., 2012; Jung et al., 2010; M. K. H. Konno, 2002). Stirring methods, agitation rates, and types of stirring reactors generally affect significantly the particle size and morphology of CaCO$_3$ (K. N. Kim, Shin, Son, & Kim, 2005). The conventional precipitation process is often carried out in a stirred tank or column reactor, because stirring is a leading part of the process. Stirring mode, the speed and type of stirrer substantially affect the interphase diffusion. For example, Chen and Jung studied the mixing types and effects of these types on the produced calcium carbonate particles' quality (Jung, 2000; Jung et al., 2010). High gravity reaction precipitation was introduced as a novel technology and the key part of this system was a packed rotator. A stirring reactor was filled up with the prepared calcium hydroxide solution already, but also, this solution was pumped through a packed rotator and it was contacted with carbon dioxide gas. A packed rotator ensured a micromixing (mixing on the molecular scale) of the initial materials in each other and this micromixing had a significant effect on the particle size distribution (J. F. W. Chen, Y. H., 2000).

In the study by Jung et al, a stirring tank and Couette-Taylor (CT) reactors were compared. They reported that, the Taylor vortex in CT reactor promoted more homogeneous mixing conditions, resulting in the production of smaller particles with a

uniform shape throughout the reactor. On the other hand, the local non-homogeneity of the mixing intensity causes the synthesis of both scalenohedral and rhombohedral shaped particles at a high concentration, in the stirred tank reactor. At a high calcium hydroxide concentration, in the CT reactor, particles obtained were all spindle-like shaped particles and, in the stirred tank, these particles had a complex structure which contained both spindle-like and rhombic shaped calcium carbonates. So, it can be clearly said that, the difference in the mixing conditions between the stirred tank and CT reactors was more obvious at high slurry concentrations (Jung et al., 2010).

The agitation is one of the indispensable parts of the calcium carbonate precipitation process. Dissolution of $Ca(OH)_2$ can take place either chemically or diffusion controlled as a function of the stirring efficiency (Domingo et al., 2006). The reasons are minimizing the effects of dense calcium carbonate protective layer, enhancing the mass transfer between the phases and increasing the penetration of carbon dioxide to the calcium hydroxide slurry for considerable conversions (Ibrahim et al., 2012).

Agitation speed is also as important as agitation method in the precipitation processes. Xu et al tried to obtain carbonate ions from the sodium carbonate solution and they used distillated water and formed calcium hydroxide solution. Their study included the agitation speed effects on the consumption of carbonate in sodium carbonate ions and they observed that the increase in the agitation speed had caused an increase in the carbonate consumption (Figure 2.8) (Xu, 1998). On the other hand, Kanakis and Dalas reported that, stirring rate (between 60 and 350 rpm) had no significant effect on the crystallization and nucleation parts of the precipitation process (Kanakis, 2000).

Stirring speed and conditions are as important as reaction temperature, CO_2 gas dispersion, addition of additives etc. in the process of calcium carbonate precipitation. Therefore, considerable amount of concerns should be focused on developing the process equipment and investigating the relation between the morphologies of products and conditions (Ye & Chen, 2011).
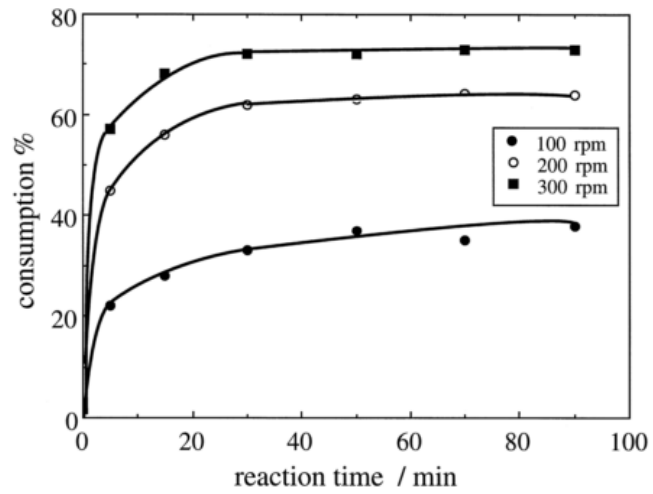
Figure 2.8. Effect of agitation speed on the consumption of carbonate in sodium carbonate solution (Source : Xu, 1998)

CHAPTER 3

MATERIALS AND METHODS

3.1 Materials

The main chemicals used in nano calcite production in large scale studies were $Ca(OH)_2$ powders and CO_2 gas. $Ca(OH)_2$ was purchased from Merck Chemicals with 96% chemical purity (3% $CaCO_3$ and 1% other impurities). Carbon dioxide gas (CO_2) was purchased from Karbogaz A.Ş. with 99.999 % purity. Acetone, that had been used as an auxiliary agent for the drying process was provided from Merck Chemicals. The other equipment used in the experiments were: Water Purification System (Millipore Elix-s/mill) for obtaining ultra-pure distillated water; Hettich-Zentrifugen Universal 320 for centrifuge processes; Thermo Scientific Orion 5-Star Plus for pH measurements; Orion 013605MD Electrode Conductivity Cell for conductivity measurements; Star Navigator program for recording the pH and conductivity measurements; SDPROC Controller Panel; AALBORG Command Module for the regulator of CO_2 flow rate; Nüve FN 500 Drying Oven and Nüve EV018 vacuum oven for drying process; Malvern Zetasizer Nano Series for the particle size and zeta potential analysis; FEI Quanta250 FEG SEM for scanning electron microscope; Phillips X'Pert Pro for XRD measurements; Micromeritics-Gemini V for BET surface area measurements and Perkin Elmer-Diomand TG/DTA devices for thermogravimetric analysis.

3.2 Methods

The carbonization reaction was carried out in a semi batch reactor with a new developed method. Crystallization reactors set ups that we organized for the carbonization experiments were illustrated in Figure 3.1 and Figure 3.2. The crystallization systems consist of a reactor with a mechanical stirrer, an industrial pump, gas and liquid rotameters, a liquid rotameter, a control unit, and a computer to record data. The diameter of pipe that had been used in the circulation system was 12 mm. The

inner diameter of carbon dioxide injection cable was 4 mm. the length of the reaction chamber, that the carbon dioxide distribution had been provided and diffusion of two materials had been actualized within it, was 29 cm and diameter of this chamber was 8.5 cm. The length and diameter of the mechanical stirrer were 50 cm and 4.5 cm, respectively. The reactor was first filled with deionized water from Water Purification System (Millipore Elix-s/mill) calcium hydroxide powder added to prepare $Ca(OH)_2$ solution. Then, the solution was circulated through the reaction chamber by a pump. The solution was stirred for about 30 minutes for a complete dissolution. Afterwards, CO_2 gas was allowed to diffuse within the liquid phase in the reaction chamber. Electrical conductivity and pH values in the solution tank were measured and recorded continuously. Also, during the reaction, the temperature of the solution has been kept by using a cooling coil. Samples were withdrawn at certain intervals during crystallization. Measured conductivity and pH values provided information about the consumption of either Ca^{++} or $OH^{=}$ ions in the stabilization tank. When the conductivity value approached to 0 or pH value decreased to 7, the crystallization was stopped by terminating the CO_2 flow and the $Ca(OH)_2$ circulation was ended. Samples were withdrawn and separated by centrifugation at 6000 rpm for 20 min, dried for characterization. Products were taken from the stabilization tank during crystallization, and particle size distribution and zeta potential measurements were obtained by the dynamic light scattering (DLS) method using Malvern Zeta Sizer instrument.

Parametric studies were conducted for the production of $CaCO_3$ particles in nano size, homogeneous distribution, and different morphologies. The effects of flow rate of calcium hydroxide, flow rate of carbon dioxide gas, pipe diameter and volume of stabilization tank were studied by adjusting other parameters unchanged. In addition, effects of concentration of calcium hydroxide solution, volume and length of the reaction chamber, stirring rate and temperature were conducted by using a shower in flow system in the reaction chamber (Figure 3.2).
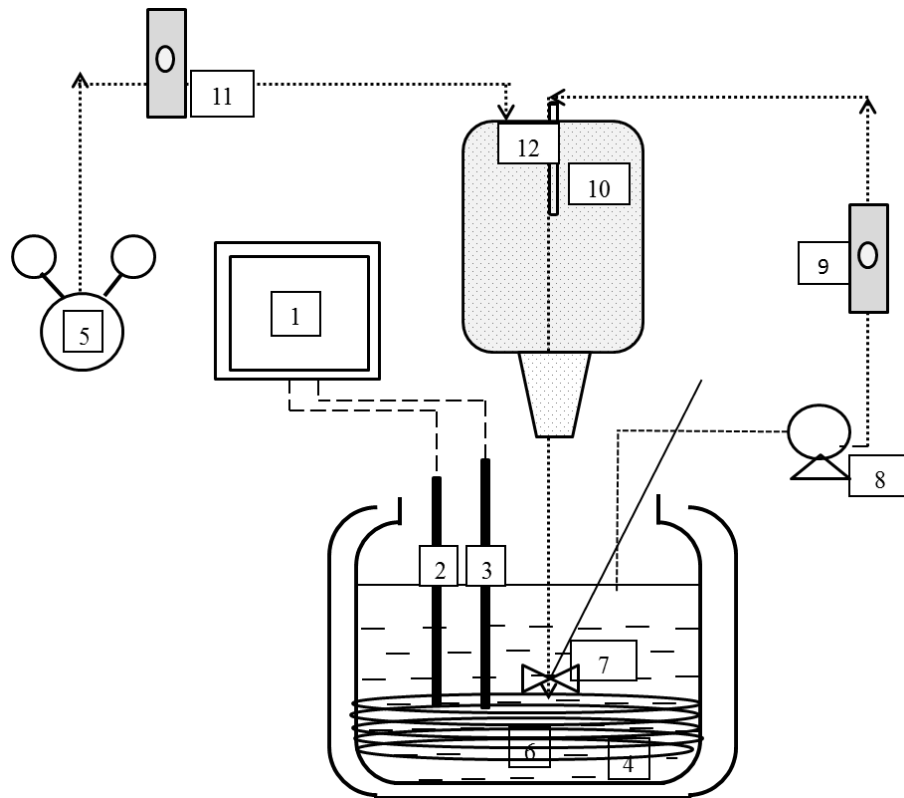
Figure 3.1. The experimental set up with circular flow : (1) Star Navigator computer program, (2) DuraProbe 4- Electrode conductivity probe, (3) pH probe, (4) $Ca(OH)_2$ solution, (5) CO_2 tank, (6) cooling coil, (7) mechanical stirrer, (8) centrifuge pomp, (9) rotameter for $Ca(OH)_2$ flow, (10) reaction chamber, (11) rotameter for CO_2 gas flow, (12) pipe used in the circulation
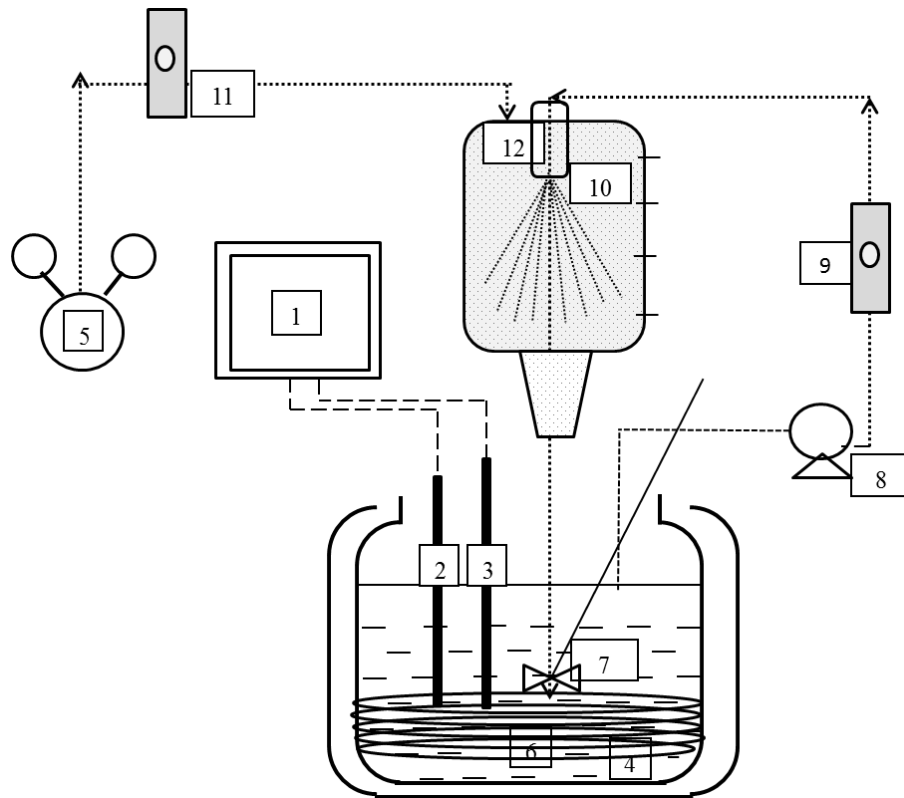
Figure 3.2.The experimental set up with a shower : (1) Star Navigator computer program, (2) DuraProbe 4- Electrode conductivity probe, (3) pH probe, (4) $Ca(OH)_2$ solution, (5) CO_2 tank, (6) cooling coil, (7) mechanical stirrer, (8) centrifuge pomp, (9) rotameter for $Ca(OH)_2$ flow, (10) reaction chamber, (11) rotameter for CO_2 gas flow, (12) shower

3.3   Product Characterization

3.3.1 Average Size and Size Distribution Measurements

Average size and size distribution of the $Ca(OH)_2$ and precipitated $CaCO_3$ slurries during the crystallization process were obtained by using Dynamic Light Scattering (DLS) technique by Malvern Nano ZS. 2 ml of sample were injected into a disposable cuvet and automatic measurement program was chosen. Size distribution by mean intensity and mean number, also average particle diameters can be graphed by this technique.

3.3.2 Zeta Potential Measurements

Zeta potential of the $Ca(OH)_2$ and $CaCO_3$ suspensions was determined by a Malvern Zeta Sizer - Nano ZS instrument with several individual measurements. The reason to measure zeta potential more than one was to obtain an average zeta potential value. Arithmetic mean of the individual measurements was calculated and particle interactions and the colloidal stability of the precipitation system were determined by evaluating the magnitudes.

3.3.3 SEM Analyses

Synthesized $CaCO_3$ crystals' morphologies were analyzed visually by scanning electron microscope which was fitted with a field emission source (FEI Quanta250 FEG), operating at high vacuum mode. The produced $CaCO_3$ powders must be quite dry to analyze efficiently and obtain high-quality images. Small amount of sample were put on a carbon tape and coated with gold in order to increase the conductance of the crystals for SEM viewing.

3.3.4 XRD Analyses

The crystal structure of the produced $CaCO_3$ particles was determined by the X-ray powder diffraction (XRD) method. These measurements were carried out by a modified computer-controlled Phillips X'Pert Pro X-ray diffractometer. Small amount of sample was put into a zero background sample holder and introduced to detector as received. The diffraction pattern was recorded for 2θ from $5°$ to $80°$ and a 2θ step scan of $0.033°$ was used. Obtained XRD patterns were used to determine the crystal structure, but also, crystal size calculations could be done by using Scherrer formula which was given below:

$$\tau = \frac{K\lambda}{\beta cos\theta} \qquad (3.1)$$

Where, τ is the mean size of the ordered (crystalline) domains. K is a dimensionless shape factor, λ is the X-ray wavelength, β is the line broadening at half the maximum intensity, and θ is the Bragg angle. XRD peaks for various forms of $CaCO_3$ crystals and amorphous $CaCO_3$ were given in Figure 3.3 as a reference.
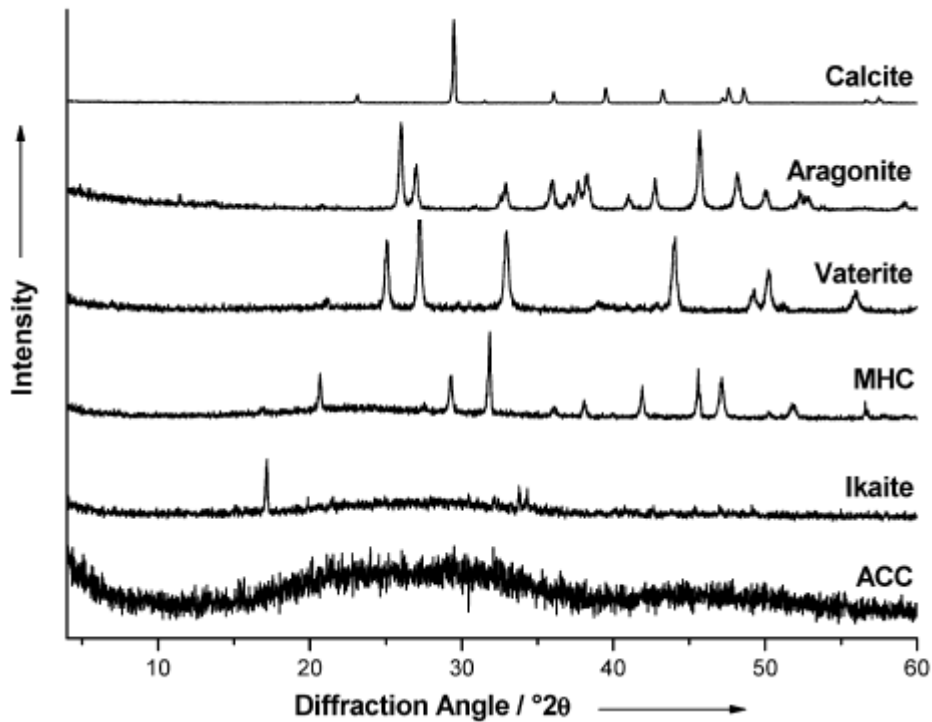
Figure 3.3. X-Ray powder diffraction patterns for all forms of calcium carbonate
(Source : Nebel 2008).

3.3.5 BET Analyses

The surface area of the crystals was determined using Brunauer, Emmett and Teller (BET) theory by BET Micromeritics Gemini V instrument. Precise specific surface area evaluation of $CaCO_3$ crystals was provided with this technique by using nitrogen gas. Small amount of sample were heated up to 100ºC for 24 hours. Then, sample's surface was coated by a nitrogen monolayer. Monolayer formation of gas molecules on the surface was used to determine the specific surface area, while the principle of capillary condensation could be applied to assess the presence of pores, pore volume and pore size distribution.

3.3.6 TGA Analyses

The amount and rate of change in the weight of $CaCO_3$ powders as a function of temperature in a controlled manner were measured with thermogravimetric analysis (TGA) technique by Perkin Elmer-Diomand TG/DTA instrument. The samples were periodically heated to 900ºC and changes in the weight were determined based on decomposition, oxidation, or dehydration. With this technique, crystallization temperatures of the products were detected. TGA analysis of calcite particles were given in Figure 3.4 as a reference (Oniyama, 1995).
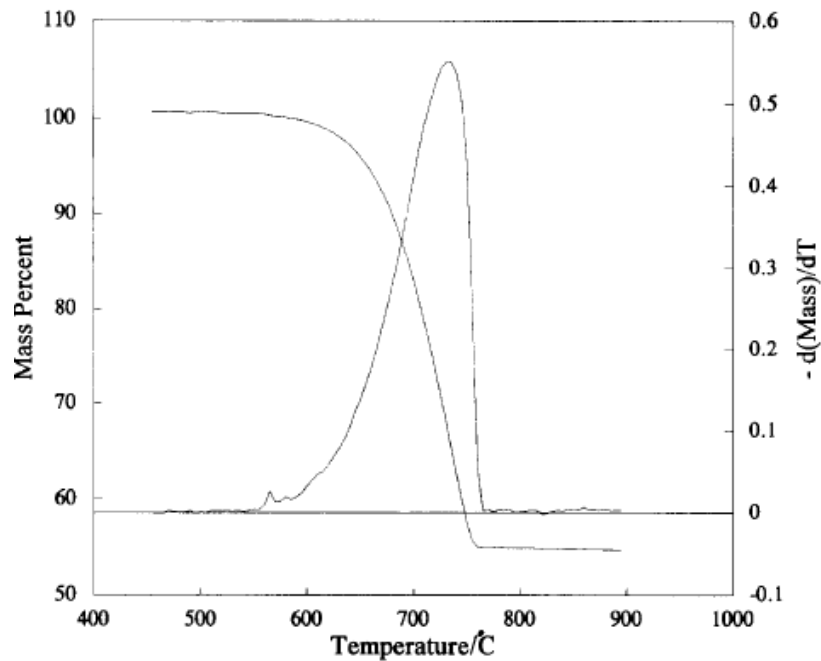
Figure 3.4. Typical TGA data showing mass and (-dm/dt) vs. temperature of the calcite sample (Source : Oniyama, 1995)

CHAPTER 4

RESULTS AND DISCUSSIONS

4.1 Effect of Carbon Dioxide Flow Rate

Calcium carbonate ($CaCO_3$) is produced in industrial scale generally by the carbonation method (Jian-Feng Chen 2000). The morphology and size distribution of the $CaCO_3$ particles were generally depended on temperature, the degree of the saturation, and the operating conditions.

In this thesis, effects of various parameters were investigated on the production of $CaCO_3$ particles in nano size, homogeneous size distribution and different morphologies by employing the newly developed method by keeping other parameters constant. Effects of CO_2 gas flow rate on the production of $CaCO_3$ particles in large scale by carbonization method. The circulation flow rate of calcium hydroxide solution was 0.2 m^3/h. The experiments were performed at room temperature, and the CO_2 flow rates were 5, 20, 40, 60, 80 and 100 ml/s by keeping all of the other operating conditions constant. During the process, stirring rate was 800 rpm, reaction chamber length was 29 cm, concentration of $Ca(OH)_2$ solution was 15 mM, inner diameter of circulation pipes was 12 mm, stabilization tank volume was 12 L, and reaction chamber volume was 1.5 L. It was foreseen that the CO_2 flow rate would directly affect the diffusion and consequently, the reaction times and particle sizes would be affected, too. As the flow rate of CO_2 increases, the carbonization time decreases (J. F. W. Chen, Y. H., 2000).

At the time of the 15 mM $Ca(OH)_2$ solutions were started to dissolve at each set, pH value of the solution reached to 12, and as the amount of produced $CaCO_3$ particles increased, it started to drop slowly until the pH value of 7, and then reaction was stopped. At the same time, while $Ca(OH)_2$ was completely dissolving in the water, the conductivity reached to a constant value, and subsequently the CO_2 gas was injected into the system. During the reaction, the conductivity reduced linearly and then it reached a value of 0 mS/cm. After that, it rose a little until the pH value of the solution decrease to 7. These changes can be seen clearly at Figure 4.1 for all of the experiments.

The time depended conductivity and pH values changes can be seen in Figure 4.1. According to the graph, the increase in the CO_2 gas flow rate caused a decrease in the reaction times. The reasons of this situation were about the contact time of the $Ca(OH)_2$ solution and CO_2 gas, and dissolution ratio of these two raw materials in each other. When the CO_2 gas was injected through the reaction chamber with a very slow flow rate (5 ml/s, e.g.), the distribution time of the CO_2 gas in the reaction chamber would be slower than the others and the diffusion of the gas through the liquid phase would take more time. Also, giving CO_2 gas to the system so fast caused an excess ions of $CO_3^=$ in the reaction chamber, so, which is why the morphology of the particles changed and particle size was decreased until the equilibrium of the adsorption. The adsorption of excess ions on the particle surface was proportional to the excess species concentration in solution. Correspondingly, particle size and crystal structures became insensitive to the excess ions in the system (Jung, 2000).
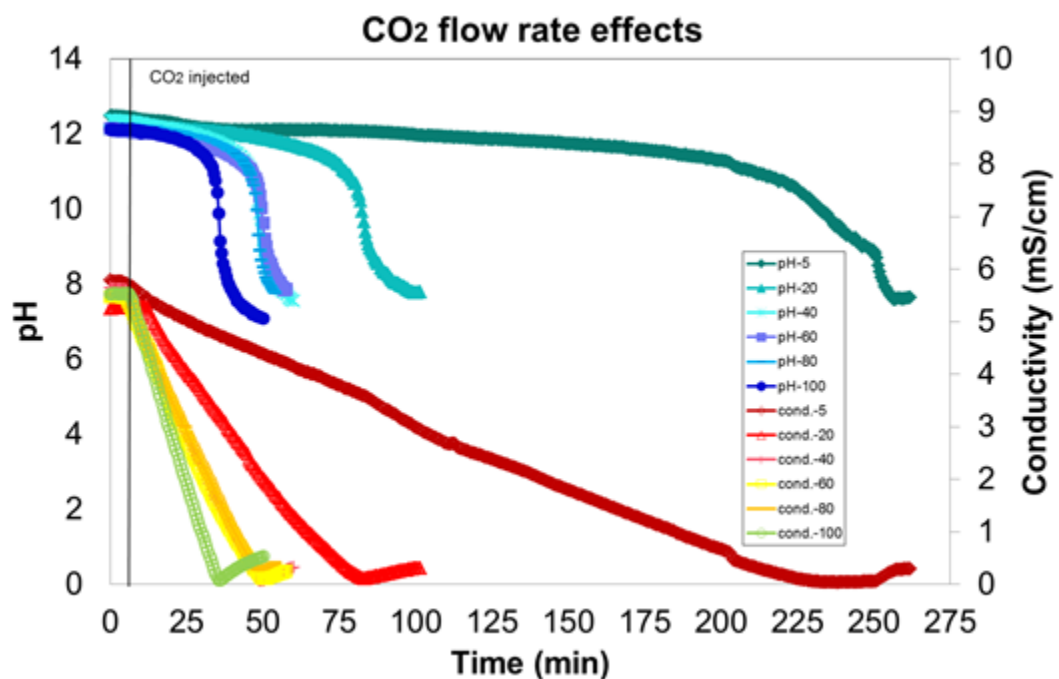
Figure 4.1. Effects of CO_2 gas flow rate on the pH-conductivity values of the experiments

An increase in the gas flow rate would lead to an increment in the rate of mass transfer amid two phases. So, by increasing the gas flow rate, the carbonation time decreased. For the same reason, the increase in the $Ca(OH)_2$ solution flow rate caused a

decrease in the carbonation time (J. F. W. Chen, Y. H., 2000). It can be said that, the most important stage for controlling the carbonation rate is the CO_2 absorption on the liquid surface which is affected by the flow rates of starting materials (Gupta, 2004).

In all experiments, 7 different samples taken from the beginning of the reaction to the end were analyzed using DLS device to evaluate the particle size, and size distribution with respect to number and intensity of the particles for the lowest, the highest and average flow rates (Figure 4.2, Figure 4.3).
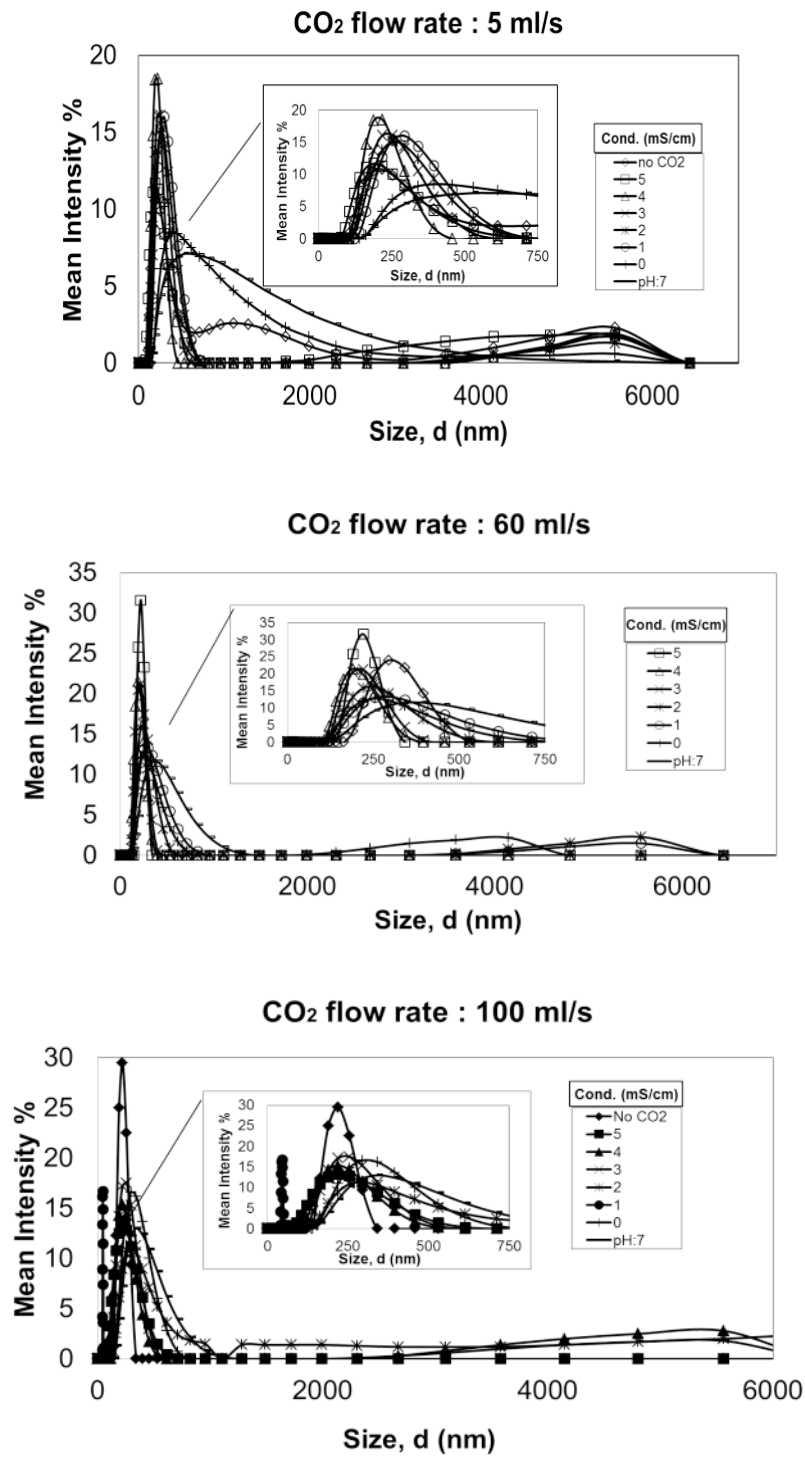
Figure 4.2. The particle size distributions by mean intensity of the samples were taken at different conductivity values.
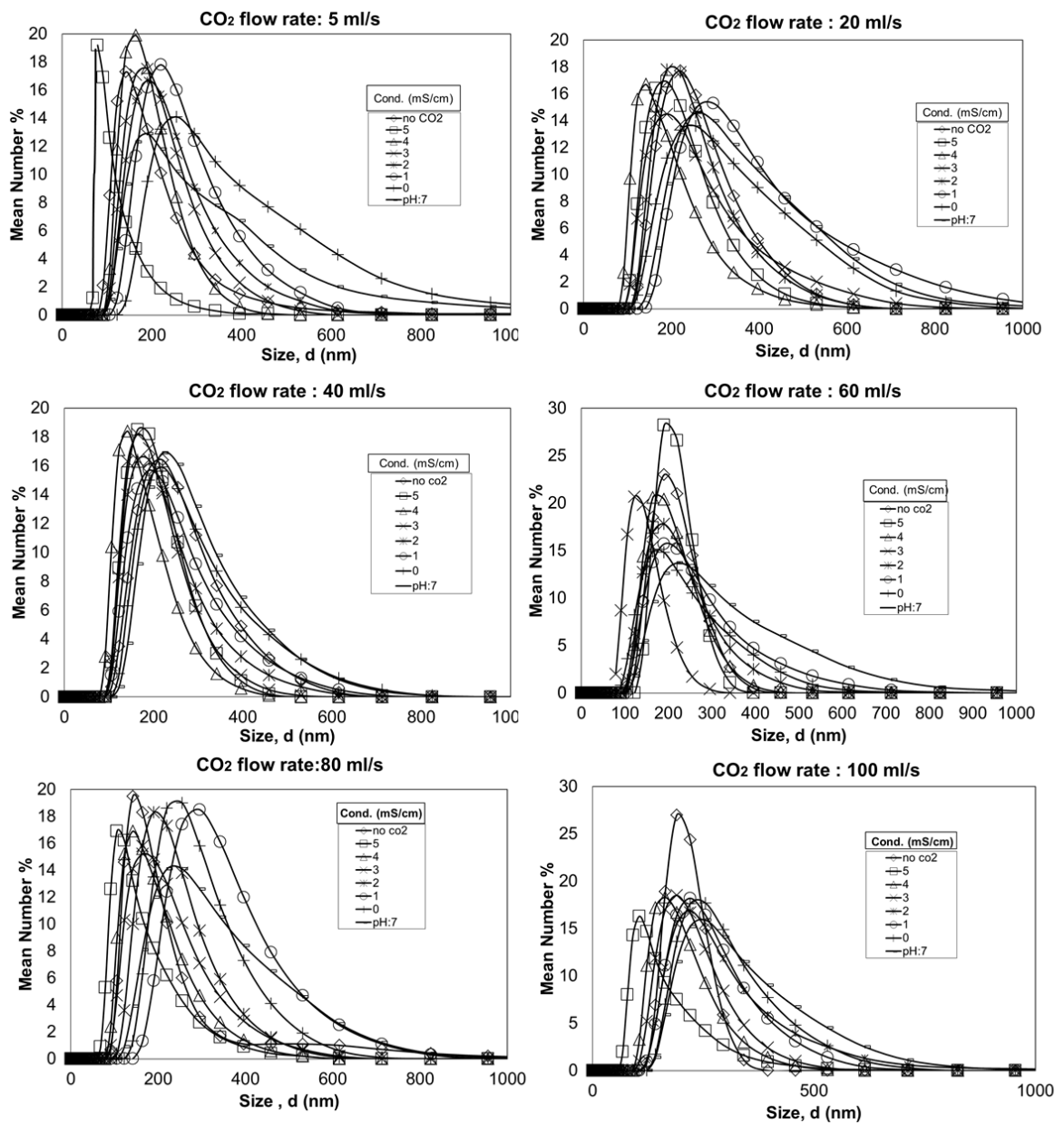
Figure 4.3.The particle size distributions by mean number of the samples were taken at different conductivity values

During the reaction, samples were taken at the conductivity values of 5, 4, 3, 2, 1, 0 mS/cm and the last sample was taken when the pH value dropped to 7. It can be seen from the mean intensity and size graphs at Figure 4.2, the particle sizes were distributed in the range of 200 nm and 300 nm. In this figure, mean intensity graph of the 5 ml/s flow rate of CO_2 gas experiment was the remarkable point. In this graph, while the reaction was coming to the end, an increase was observed in the hydrodynamic diameter of the particles. Generally, size distribution of nano calcite particles were decreased due to the increasing flow rate of CO_2 gas (Jung, 2000).

The changes of particle sizes and $Ca^{++}/CO_3^{=}$ ions ratios depend on the changes of $Ca(OH)_2$ solution's concentration, temperature and flow rate of CO_2 gas and also an increase in the CO_2 gas flow rate can cause an increase in the nucleation rate (J. H. Kim et al., 2006). At the initial stages of the reaction, the particles were more intensive and close to each other, and also clustered; but, as the reaction proceeded, more individuality started and monodisperse structured particles formed. Size distribution showed a variety between 150 nm and 1 μm with the effect of impurity in the used $Ca(OH)_2$ powders.

On the other hand, size distribution by mean number for each experiment was calculated using DLS analysis method (Figure 4.3). Here, with these analyses, it was seen that size of the particles were changed between around 100 nm and 500 nm, but generally the dimensions of 200 nm particles were obtained.

Zeta potential of the produced particles is substantial because of its values are related with the stability of colloidal dispersions. The zeta potential indicates the degree of repulsion force between the particles and the next adjacent, just as the charged particles' repulsion forces in a dispersion. A high degree of zeta potential value provides the stability for the molecules and sufficiently small particles, and also, generates a resistance to aggregation in the solutions or dispersions. But, when the zeta potential value is small, attraction force exceeds repulsion force, so dispersion deteriorates and clusters occur.

The graphs of average size and zeta potential values depended on time for all CO_2 flow rate experiments were given in Figure 4.4. Zeta potentials changed between the values of 35 and 55 mV. Especially, the increase of the zeta potential away from the 30 mV, indicated an increment in the repulsion force among the particles, and produced structures of calcite particles became more monodisperse.

In the first graph, zeta potential value increased from nearly 30 mV, and then it decreased again when the reaction reached to the end. This situation meant that, the particles here were more agglomerated than others. Because, the lowest average values of zeta potential were obtained in the CO_2 flow rate of 5 ml/s. In all of the other flow rates, zeta potential values started at values greater than 30 mV and agglomerations were actually lower. Nevertheless, because of the impurities and pollution caused by the environment, it can be wrong to make a sentence such as an increase in the flow rate of CO_2 gas significantly affects the zeta potential values.
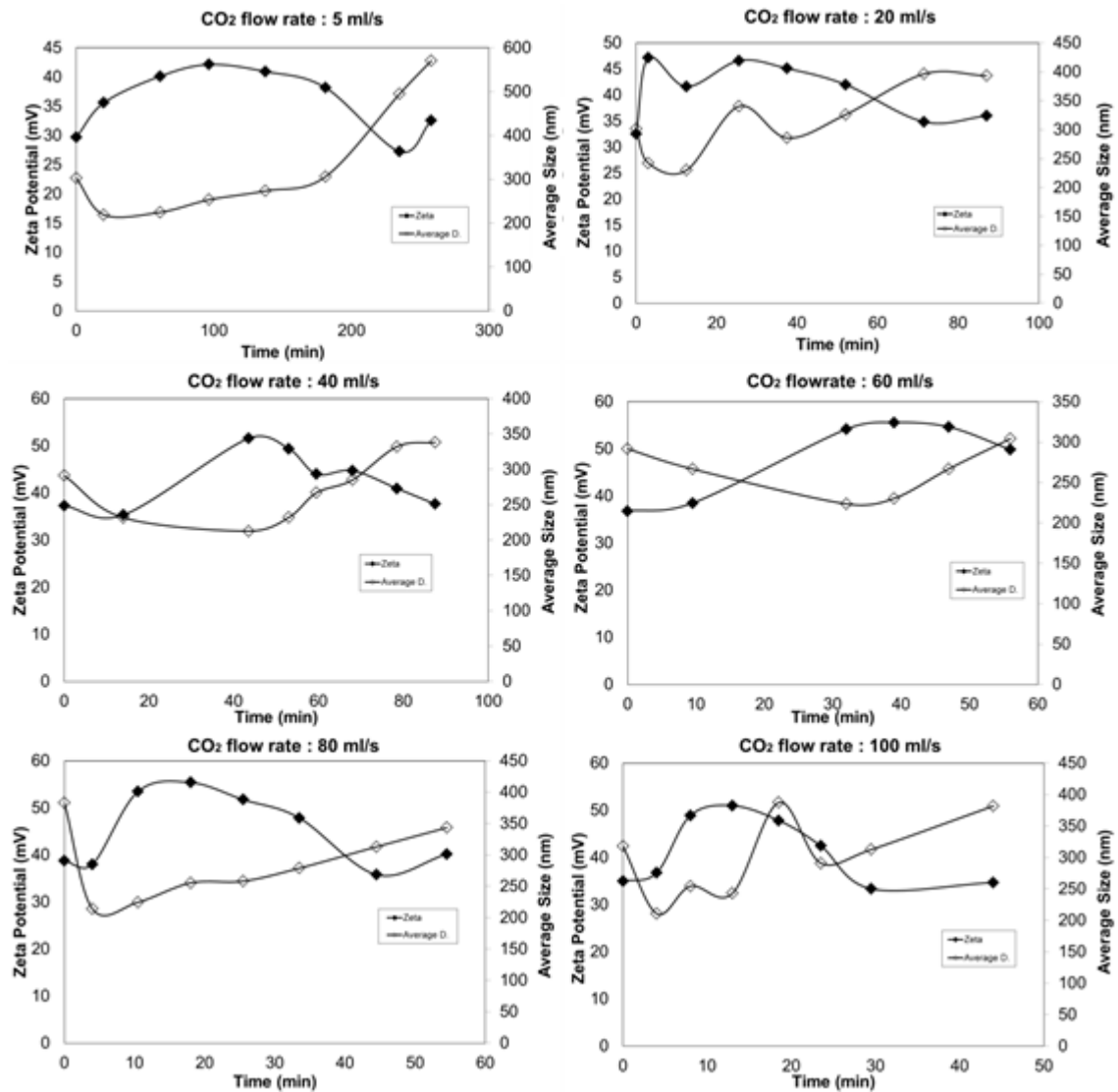
Figure 4.4. Zeta potential and average particle size graphs for all CO_2 flow rate experiments.

A decrease in the average particle sizes at the early parts of the reaction could be seen in all graphs, but then, these average particle size values increased again (Figure 4.4). Zeta potential values of the particles varied due to the $Ca^{++}/CO_3^{=}$ ions ratio in the solution. If there were excess amounts of Ca^{++} ions in the media, zeta potential increased towards a positive way. On the other, an excessive amount of $CO_3^{=}$ ions in solution was resolved, zeta potential value increased showing a negative tendency (Chibowski, Hotysz, & Szcześ, 2003). It's known that, zeta potential influences the attractive and repulsive forces between the particles, thus it causes an agglomeration or grown by merging of the particles. Thereby, it can be said that zeta potential is inversely proportional to the average size of particles. As the zeta potential increases, charges of

the particles apply repulsive force to each other, so smaller and individual particles can be produced. On the other hand, a fall in the zeta potential shows the attraction forces between the nano calcite particles, thus these particles collide and clusters occur in the solution.

Samples were taken at specific conductivity values in order to figure out the evolution of the reaction, and SEM images of these samples were taken. In general, to observe the formation of the nano calcium carbonate particles during the process, SEM images of the 5 ml/s CO2 flow rate experiment were given in Figure 4.5. SEM images of the samples which were taken at the beginning of the reaction (5, 4 mS/cm), it was seen that the size distribution was not homogeneous. Both large and small particles, and also different morphologies were observed. Until the electrical conductivity value of 2 mS/cm, large clusters were formed by the particles clinging on to each other. As the reaction progressed, agglomerated structures started to disperse and monodisperse structures were composed, at the same time, scalenorhombohedral and rhomboscalenohedral crystal structures were evolved into forms of cubic rhombohedral structures. When the samples were taken from the end of the reaction (conductivity values of 1, 0 ms/cm and pH:7), SEM images represented that, mainly morphologically rhombohedral structured particles have been formed. Frequently, these particles were hollow shaped calcite particles and size distributions were quite homogeneous. A reason for these porous structures may be the sudden decrease in the pH of the solution towards the end of the process.

The SEM images of the samples were taken from the experiments which had been done with different CO_2 gas flow rates in large scale, were given above (Figure 4.6). In all experiments, samples were collected at specific electrical conductivity values until the end of the reactions to figure out the formation mechanism of the particles. Homogeneous size distributions were observed in all of the experiments. But, the smallest particles were synthesized when the CO_2 flow rate was the lowest (5 ml/s).

Here, it can not be said that the particle size and size distribution are evolved linearly with increasing CO_2 gas flow rate. When the carbon dioxide gas is injected through the system in a controlled manner, a more desirable level of calcite particles are examined. The most important point we observed here is the time of the adsorption of CO_2 gas through the calcium hydroxide solution.
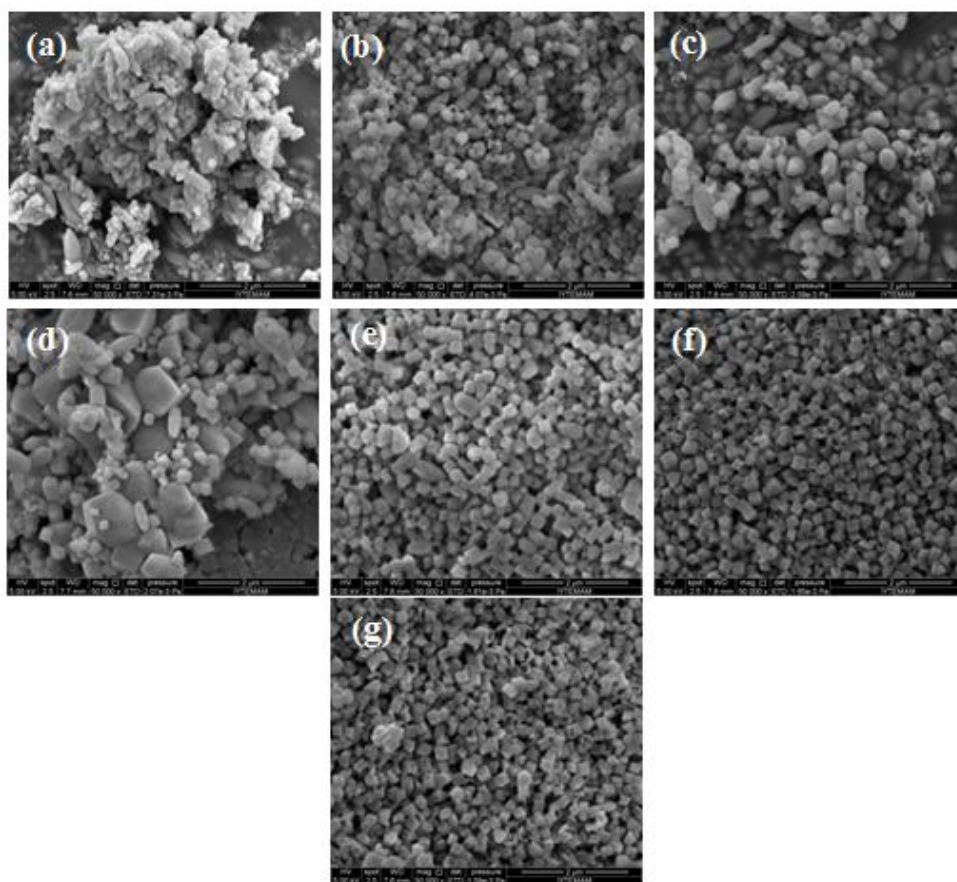
Figure 4.5. SEM images of the experiment of 5 ml/s CO_2 gas flow rate. Conductivity values: (a) 5 mS/cm, (b) 4 mS/cm, (c) 3 mS/cm, (d) 2 mS/cm, (e) 1 mS/cm, (f) 0 mS/cm and (g) after the reaction completed pH:7 (at 50000 magnifications)
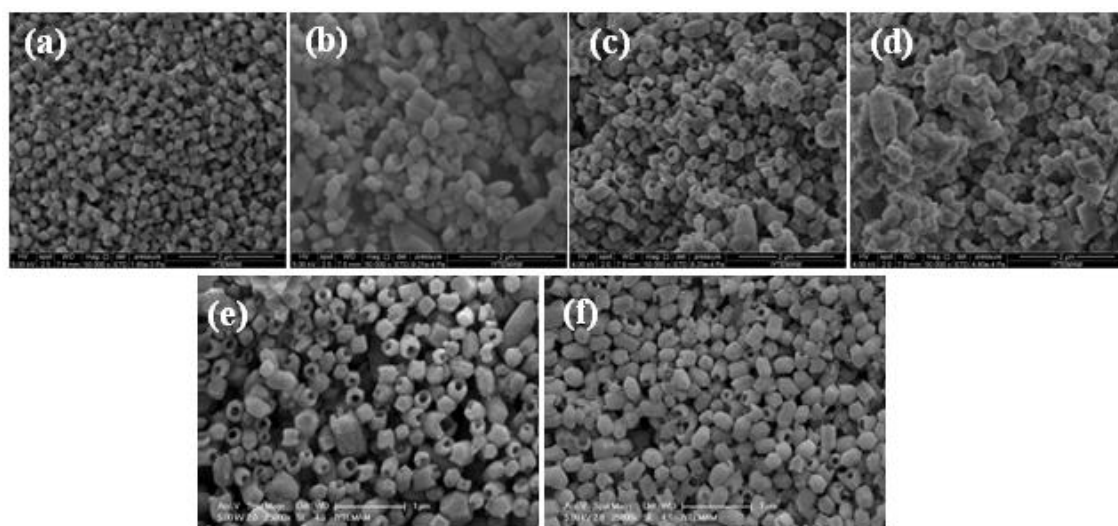
Figure 4.6. SEM images of the produced calcium carbonate particles by using different CO_2 flow rates : (a) 5 ml/s, (b) 20 ml/s, (c) 40 ml/s, (d) 60 ml/s, (e) 80 ml/s, (f) 100 ml/s (at 50000 magnifications)

Polymorphism of calcium carbonate had been formed in different ways due to the different adsorption times of carbon dioxide through the calcium hydroxide particles' surfaces. By looking at the experimental data we collected, it can be said that, the large particles that were seen in the beginning of the reactions, were crumbled to small ones and smaller particles were synthesized. When the carbon dioxide flow rate was investigated parametrically, it was seen that the most optimum results were observed with the lowest flow rate (5 ml/s). Nucleation rate is increased with the increasing flow rate, for this reason, larger particles may occur as a result of uncontrolled and rapid reactions. As a result of the experiments, rhombohedral and hollow shaped nano $CaCO_3$ particles were produced in large scale. Hollow shaped structures increase the surface areas, so, they can cause a better mechanically performance in the application areas.

BET results of the produced $CaCO_3$ particles showed that the surface area of the particles firstly increased and then it decreased again (Figure 4.7). The reason of this increase may be the formation of the hollow shaped nano calcite particles. As the holes began to form on the surface of the particles, an increase in the surface area was expected. The surface area started to decrease when these holes started to fill with Ca^{++} and $CO_3^=$ ions. On the other hand, TGA analysis result of these particles was illustrated in Figure 4.8. Generally, it can be said that, as the decomposition temperature of the product increased, an increase in the size of the particles could be observed. Here, it was seen in this TGA result that, the produced nano $CaCO_3$ particles' decomposition temperature was lower than the commercial $CaCO_3$ decomposition temperature. That means, produced particles' sizes were smaller than the commercial ones. SEM images also supported this conclusion. The first slope of the produced nano $CaCO_3$ particles in the TGA graph showed that the decomposition was slow and started at lower temperatures.
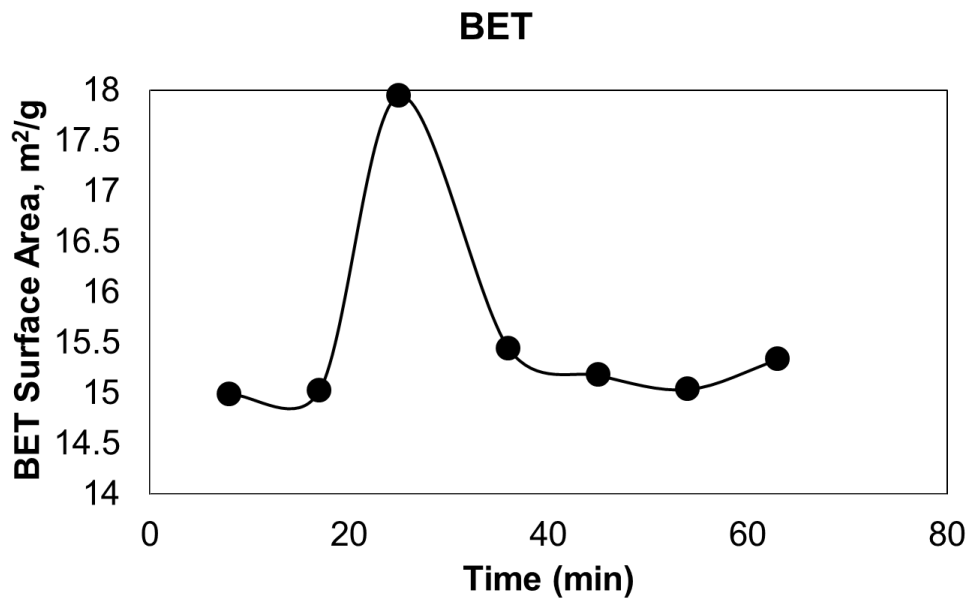
Figure 4.7. BET results of produced nano CaCO$_3$ particles
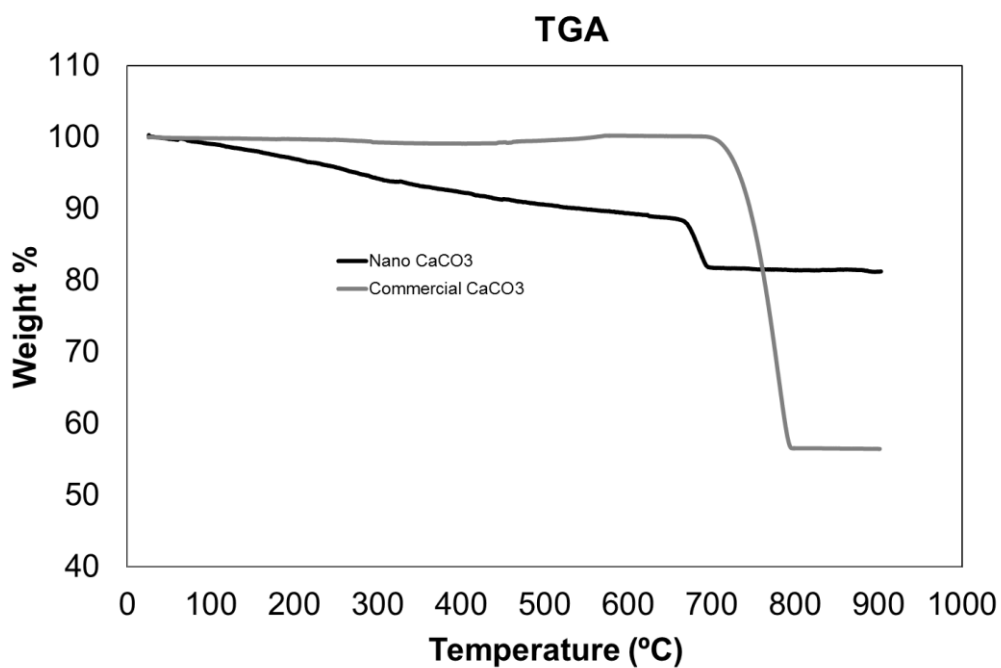
Figure 4.8. Thermogravimetric analysis results of produced nano CaCO$_3$ particles

4.2 The Effect of Calcium Hydroxide Flow Rate

Under normal conditions, a small amount of $Ca(OH)_2$ powders dissolve in aqueous solution. The equation given below shows the solubility of calcium hydroxide in water at the temperature of 298 K (Elfil & Roquesb, 2001). The dissolution of calcium hydroxide powders in water was defined to proceed through two steps: Firstly, calcium hydroxide particles were chemically dissolved on the surface (4.1); and secondly, ions of Ca^{++} diffused away from the surface (4.2) (Domingo et al., 2006). Diffusion rates of particles to the media and diffusion rate of CO_2 gas in the reaction chamber were affected by the flow rate of $Ca(OH)_2$ solution.

$$Ca(OH)_2 \leftrightarrow Ca^{2+} + 2\ OH^- \text{ (solid surface)} \quad Kps = 10^{-5.3} \qquad (4.1)$$
$$Ca^{2+} + 2\ OH^- \text{(surface)} \leftrightarrow Ca^{2+} + 2\ OH^- \text{ (bulk solution)} \qquad (4.2)$$
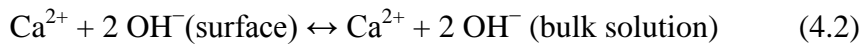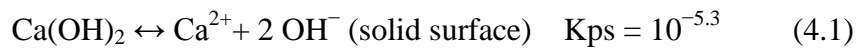
The effects of $Ca(OH)_2$ solution's flow rate on the size and structure of the synthesized $CaCO_3$ particles are substantial in our system which basically uses a carbonization method that ensures recirculation of CO_2 gas through a reaction chamber. Thus, different $Ca(OH)_2$ flow rates experiments were investigated to observe these effects. All experiments were done at room temperature. For these experiments, the concentration of calcium hydroxide was set to 15 mM, because, the saturation concentration at room temperature is nearly 18 mM and the studied molarity should be lower but close to this value to obtain fine particles. This solution was fed to a 12 L batch reactor and dissolved with the help of a mechanical stirrer. The studied calcium hydroxide flow rate values were 0.2, 0.4, 0.6, 0.8 and 1.0 m^3/h with a constant gas flow rate of 20 ml/s.

Electrical conductivity and pH values of experiments which were done with different solution flow rates were illustrated in Figure 4.9. It can be seen that the reaction times decreased with increasing $Ca(OH)_2$ flow rates. The reason can be shown as the contact time. The contact times of liquid and gas phases in the reaction chamber were rised with increasing $Ca(OH)_2$ flow rate.
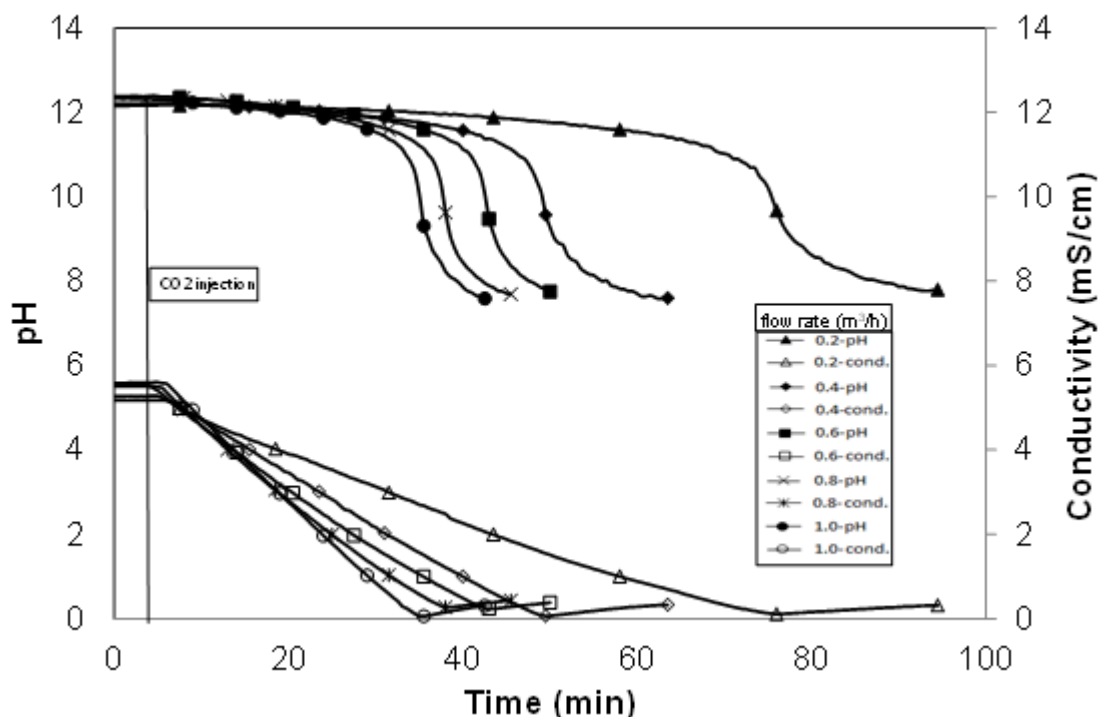
Figure 4.9. Conductivity and pH values of all Ca(OH)$_2$ flow rate experiments

In all experiments, 7 different samples taken from the beginning until the end of the reaction were analyzed using DLS device to evaluate the particle size, and size distribution with respect to mean intensity and number of particles (Figure 4.10, Figure 4.11). During the process, samples were taken at the conductivity values of 5, 4, 3, 2, 1, 0 mS/cm and finally when pH of the solution dropped to 7. Generally, graphics showed the same measurement results. Particles sizes by mean intensity have been varied between the dimensions of 200 nm and 500 nm. The reason for the peaks that had represented the large particles was the impurities in the Ca(OH)$_2$ powders. By interpreting the SEM images obtained (Figure 4.13), there were not any large particles larger than 2 μm in the synthesized products.
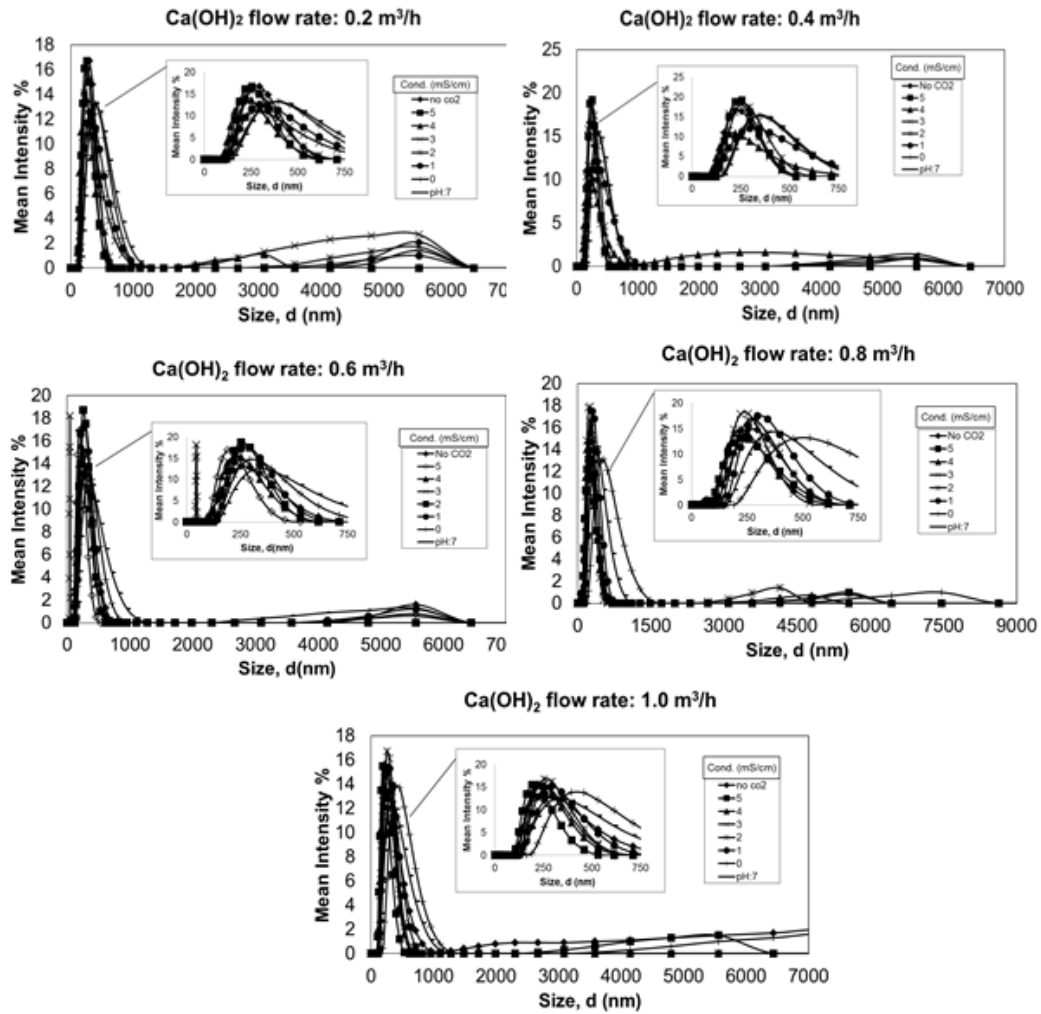
Figure 4.10. The particle size distributions by mean intensity of the samples were taken at different conductivity values from different experiments of calcium hydroxide flow rates.

Dynamic light scattering (DLS) device's operating principle is based on the measurement of the hydrodynamic diameter of the particles formed by the surrounding ions. Emergence of smaller sized particles at the beginning of the reaction is due to the measurements of very small hydrodynamic diameters of these particles. As the reaction progress, release and adhesion of ions increase and hydrodynamic diameter of particles can be affected. Thus, as the electrical conductivity values decrease, size of the particles get smaller but hydrodynamic diameters get larger. Also, the morphological structures of the particles affect the size distribution significantly. It was seen from the SEM images of the samples taken from the system during the reaction, the diameters of the calcite granules began to shrink (Figure 4.13).
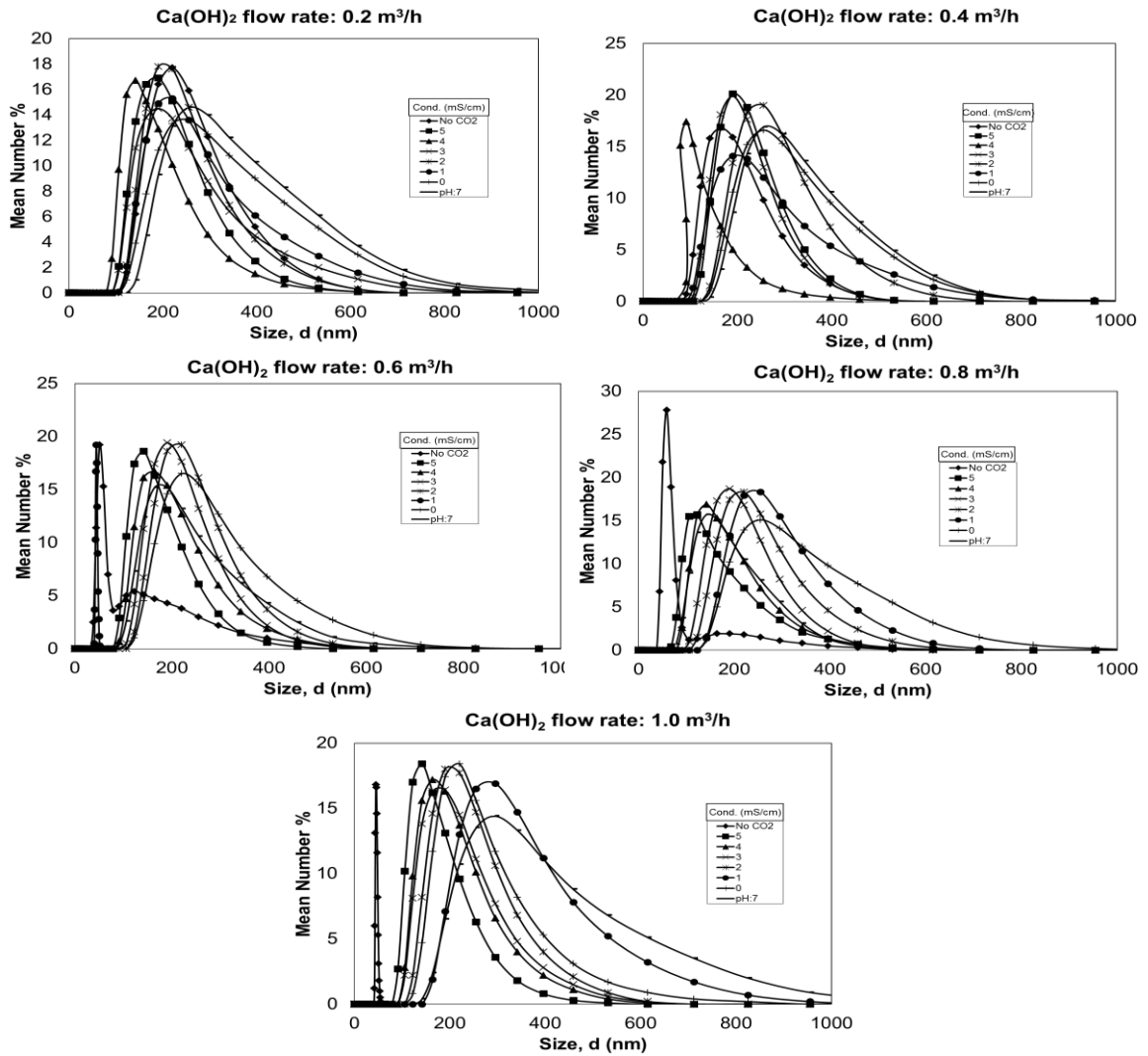
Figure 4.11. The particle size distributions by mean number of the samples were taken at different conductivity values from different experiments of calcium hydroxide flow rates.

Size distributions by mean number for all of the liquid flow rate experiments were given in Figure 4.11. Generally, graphics showed the same measurement results. Particles sizes by mean number have been varied between the dimensions of 100 nm and 300 nm. As the flow rate of calcium hydroxide increased, number of small particles in the calcium carbonate solution at the end of the process decreased.

Zeta potential can be defined as a particle's resistance applied through the other particles that try to merge with it. If these particles had negative charges, they applied repulsive force to each other and a high resistance occurred not to be agglomerated; thus the general zeta potential of this solution would be so high. The calcium carbonate precipitation starts with the injection of CO_2 gas through the reaction chamber, so, with

the dissolution of the gas, number of negative charged $CO_3^=$ ions increased the zeta potential of the solution in the stabilization chamber. This increment was seen in all of the experiments at Figure 4.12. As the positively charged materials in the fluid increased, zeta potential of the particles decreased. This process gave rise to the expansion of the diameter of the particle, because, positively charged materials started to attach on the surface of the particles. After a while, the number of Ca^{++} ions was increased, therefore, a decline in the zeta potential occurred. When the zeta potential is outside of the range of +30 and -30 mV that means, agglomeration between the particles starts to decrease. As the zeta potential moves away from this range, the particles applied more repulsive force to each other; hence it is expected to be comprised monodisperse structures. In the graphs given in Figure 4.12, it was observed that the zeta potential of the samples started from +30 mV, and then they were increased, so more individual particles synthesized. On the same graphs, average particle sizes of $CaCO_3$ particles were seen. As the reaction progressed, average particle sizes were increased in all experiments. On average, particles in the size range of 200 nm and 350 nm were produced.
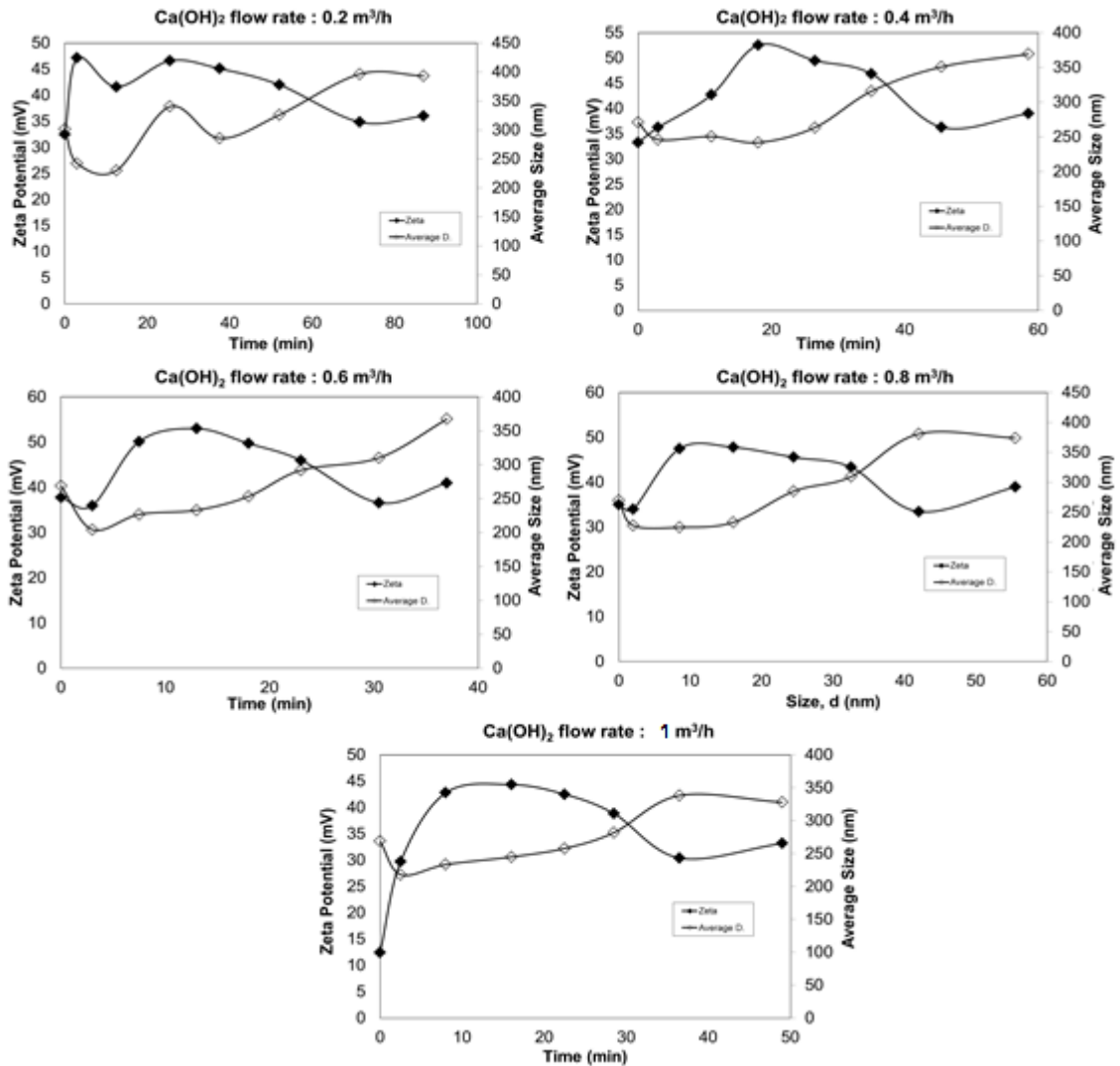
Figure 4.12. Zeta potential and average particle size graphs for all Ca(OH)$_2$ flow rate experiments.

The SEM images of the nano produced calcium carbonate by changing the flow rates of calcium hydroxide were given in Figure 4.13. Homogeneous size distributions were obtained in almost all experiments. But, the smallest particles were viewed in the experiments of calcium hydroxide flow rate of 0.8 and 1.0 m^3/h. by looking at the lower flow rate experiments; we can say that, synthesized particles were larger and more agglomerated. Also, it can be said, particle sizes and size distributions changes linearly with increasing liquid flow rates. Here, in higher flow rate experiments, it was proved that the adsorption of the gas through the liquid phase was better. But, in the experiment done with 1.0 m^3/h, obtained nano calcite particles' morphologies were different and

42

hollow-shaped. Sizes of these particles were changed in the range of $100 - 200$ nm, generally.
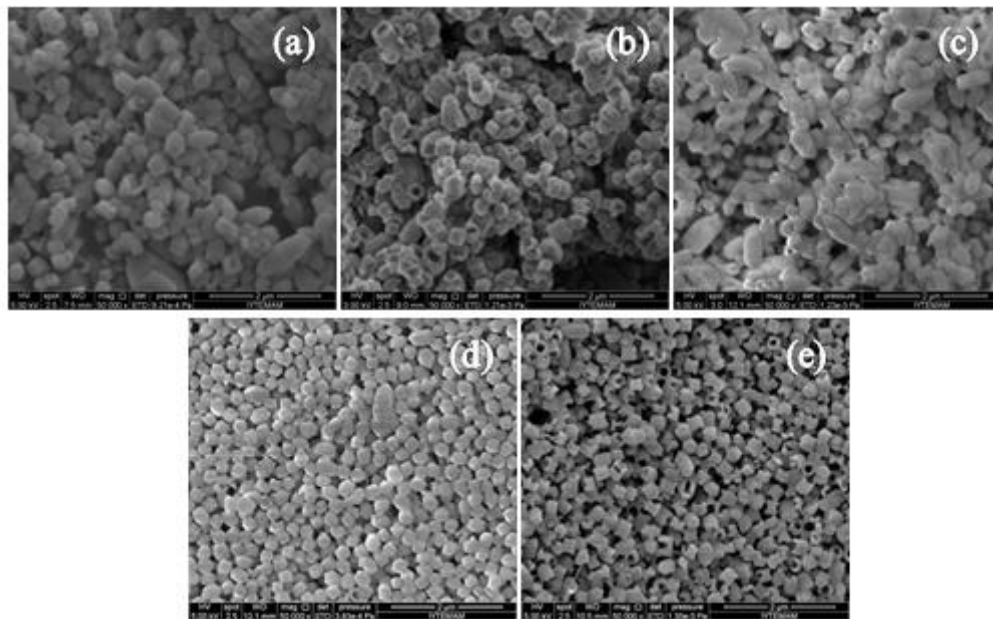
Figure 4.13. The SEM images of the calcite particles produced by different flow rate of calcium hydroxide experiments. Flow rates of $Ca(OH)_2$: (a) 0.2 m^3/h, (b) 0.4 m^3/h, (c) 0.6 m^3/h, (d) 0.8 m^3/h and (e) 1.0 m^3/h (at 50000 magnifications)

Calcium carbonate polymorphisms were formed in different formats due to different flow rates of calcium hydroxide. Especially with higher flow rates, calcite particles with hollow-shaped rhombohedral morphology were produced. By looking at all data, it has been observed that optimum calcium hydroxide flow rates were 0.8 and 1.0 m^3/h. With the studies done with these flow rate values, produced calcium carbonate's size distributions were homogeneous and their sizes were nearly 150 nm. Zeta potential values of samples from all experiments were close to each other and they were higher than 30 mV, hence, agglomeration or clusters were not seen in these products. However, particles with more monodisperse structures were observed from the optimum flow rate experiments.

4.3   The Effects of Calcium Hydroxide Concentration

Morphology and sizes of the calcium carbonate particles depend on the temperature of the system and the degree of the supersaturation concentration of the solution which depends on this temperature. A supersaturated calcium hydroxide solution caused a change in the crystal structure of calcium carbonate particles from unstable vaterite structure to stable calcite structure. Morphological structures of these particles can be controlled by the pH of the solution in a well-organized crystallization process (Jung, 2000).

During the nano calcium carbonate process, the temperature of the solution in the stabilization tank and the concentration of this solution which depends on the temperature are quite important. It was observed that produced particles' sizes were thrived from nano sizes to micron sizes when the molarity of initial calcium hydroxide solution was above or below the saturation point. Expression of saturation is different for the easy-soluble and hard-soluble systems. The species' concentration, that are required to calculate the ionic activity and so supersaturation, were defined by using a computer program based on the algorithm of a successive approximation of the ionic strength (Tai, 2001). By using the graph given in Figure 4.14, it was seen that the saturation concentration of calcium hydroxide solution was 18 mM approximately at the room temperature.
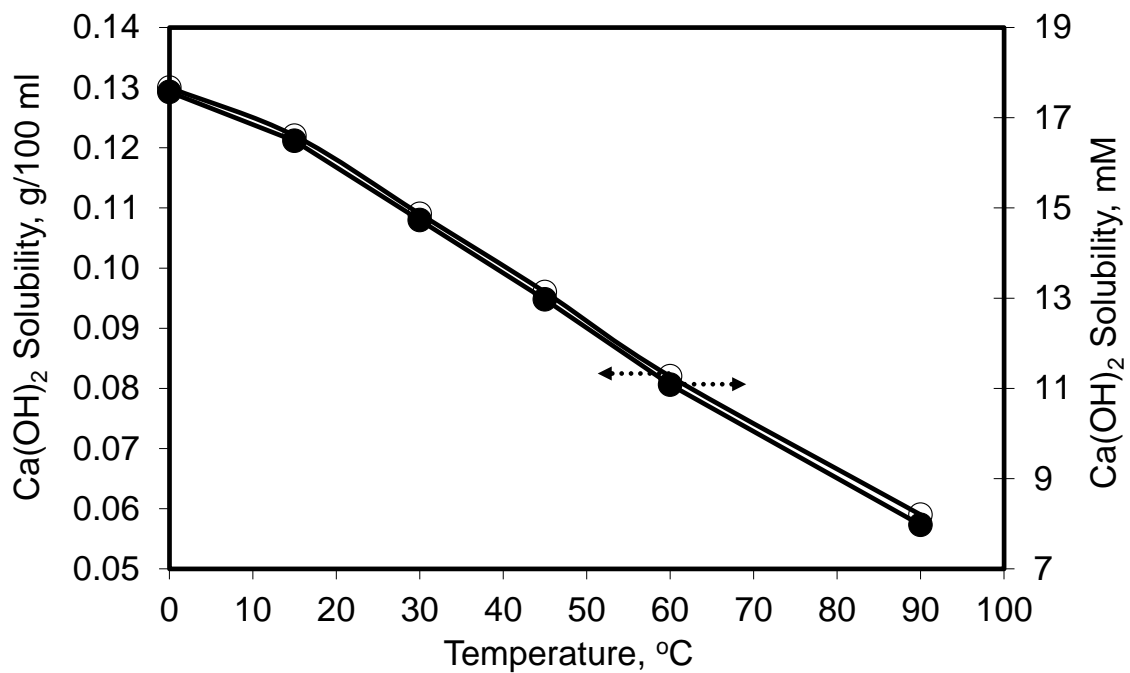
Figure 4.14. Graph of calcium hydroxide solubility in water with respect to the temperature (Source : Lieth, 1930)

The solution supersaturation should be controlled within the metastable region to examine the crystallization process and growth of crystals; otherwise, nucleation would occur at higher supersaturation and mess up the operation.

Experiments were done by keeping constant some parameters of the experimental system and only changing the molarities of calcium hydroxide solution in the large scale production of nano $CaCO_3$ particles to observe the effects of the feed solution concentrations. The parameters that kept constant were temperature, flow rates of calcium hydroxide and carbon dioxide, diameter of pipes, volumes of reaction chamber and stabilization chamber, and also stirring rate. The experimental set up was given in Figure 4.14. The studied $Ca(OH)_2$ concentrations were 1, 5, 10, 15, 20, 30 and 50 mM.

The changes in the pH and electrical conductivity values in the processes which started with different initial calcium hydroxide concentrations with respect to the time were given in Figure 4.15. As the molarity of the initial calcium hydroxide solution was increased, it was observed that the reaction completion times were increased, too. First electrical conductivity values of the feed solutions changed due to the amount of the calcium hydroxide powders dissolved in the water; at low concentrations, electrical

conductivity values started at nearly 0 mS/cm, on the other hand, at high concentrations, this value increased to about 8 mS/cm. In general, in all of the studies, electrical conductivity values have begun to fall from the moment of CO_2 gas injected to the reaction chamber. The experiments with low concentrations (1, 5 and 10 mM), conductivity graphs had only one slope; however, with the concentrations of higher than saturation point (20, 30 and 50 mM), the conductivity graphs had two different slopes. Two different slopes meant the excess amount of the Ca^{++} ions was dissolved in the solution.

After obtaining a homogeneous calcium hydroxide solution (constant conductivity values) with the help of a mechanical stirring, reaction started with the injection of the gas and crystallization occurred in the reaction chamber. Ca^{++} and $CO_3^{=}$ ions were pulled towards to each other and number of Ca^{++} ions started to decrease; due to this situation, conductivity of the solution stated to decrease suddenly. This decrease can be seen easily in the experiments done with low concentrations. But, in the experiments done with supersaturated solution, a second slope in the conductivity charts occurred with respect to the excess Ca^{++} ions. The conductivity and pH charts of the solutions with the lowest and the highest concentrations were given in Figure 4.15 to observe this situation more clearly. The markers on the lines represent the points when the samples taken from the solution. The diameters, size distributions and crystal structures of the particles from these samples were analyzed by SEM, XRD and DLS.
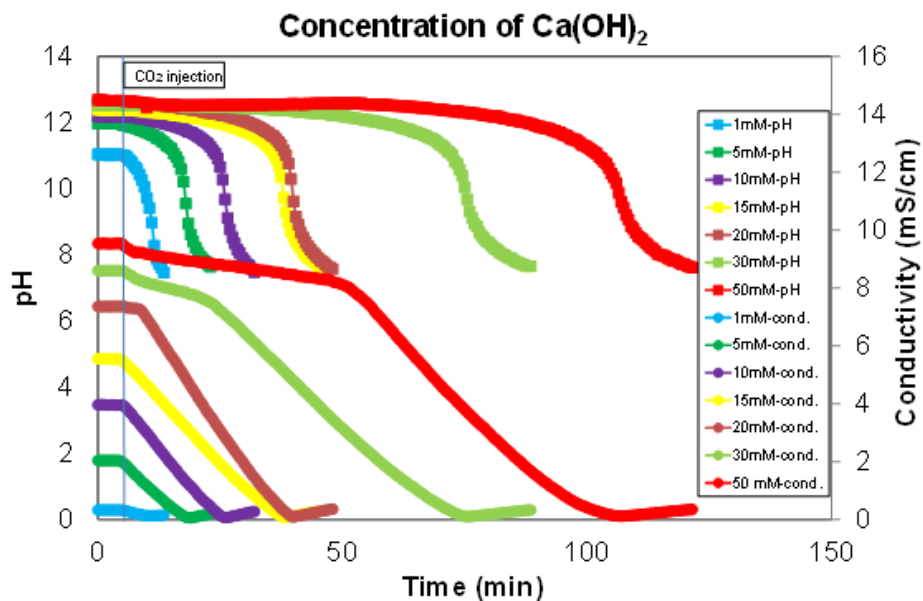
Figure 4.15. The graph of pH and electrical conductivity changes of the experiments which were done with different initial $Ca(OH)_2$ molarities
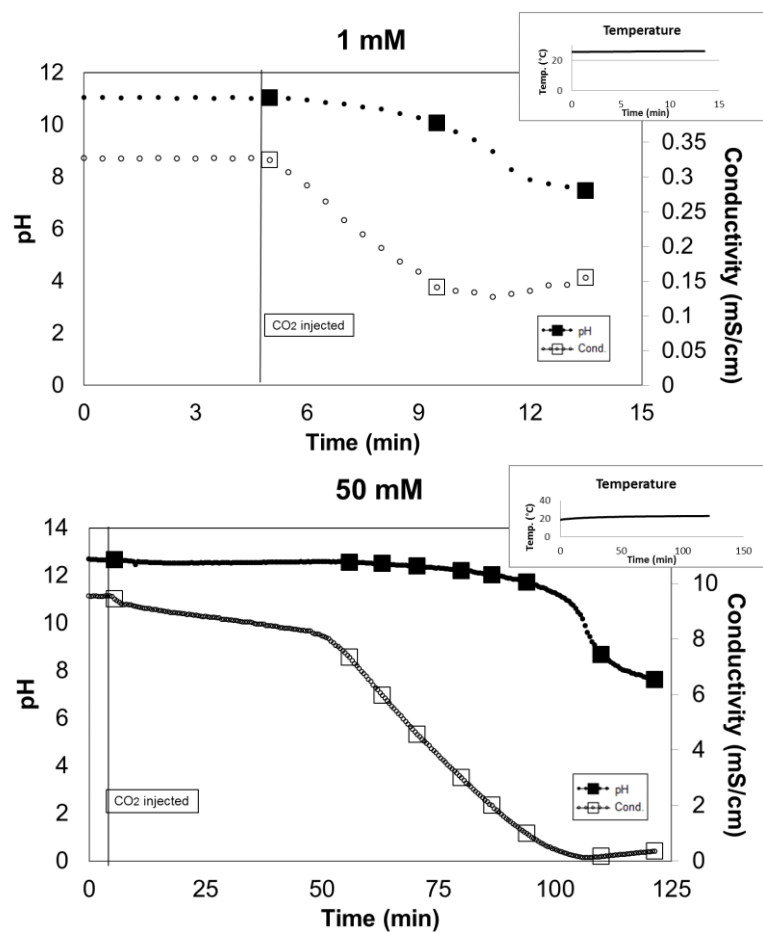
Figure 4.16. Electrical conductivity and pH values of the experiments which were done with the lowest and the highest concentrations of calcium hydroxide solution

The DLS results of all experiments were shown in Figure 4.17. In these charts, it was observed that as the molarity of the initial calcium hydroxide solution was increased, the diameter of the particles increased after the supersaturation point. Especially, after the supersaturation concentration, growth of the diameter of the particles was uncontrolled. Before the supersaturation concentration (18 mM), as the concentration was decreased, the particle size increased, too. Thus, it was realized obviously that, the finest particles were synthesized at the saturation concentration.
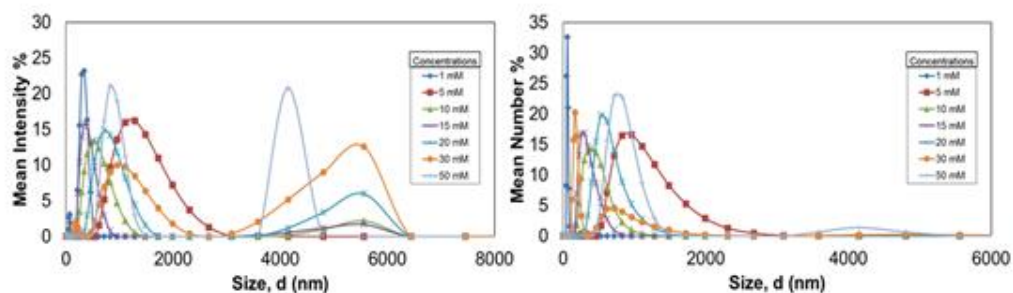
Figure 4.17. Size distributions by mean intensity and number for all of the experiments

Lower than saturation level and supersaturation concentrations were examined in lots of studies up till today, and effects of them on the morphologies of nano particles were discussed (G. a. Carmona, 2003; Tai, 2001). By looking at the charts in Figure 4.17, in the concentrations higher than supersaturation point, both small and large particles were produced. SEM images of these samples (Figure 4.20) showed not the same results as DLS graphs. There were no particles which had dimensions of 6-7 μm. In this instance, the large particles in the DLS graphs could be the clusters which were formed by the merger of the small particles. Likewise, large particle formation was observed in the lower concentration studies (1, 5 mM).

DLS (Dynamic Light Scattering) analysis gave the charts which showed the size distributions by mean number as well as by mean intensity (Figure 4.17). In these charts, the effects of the saturation concentrations were easily understood. Especially in the 15 mM study which was the closest to the saturation point, large number of particles, which were small in size were observed. An increase in the number of large particles was observed with respect to the distance from the point of saturation in the other studies. Formation of larger particles and size distributions in the lower suspension concentrations has been one of the subjects discussed in literature. The reason was explained as; at the higher concentrations which were close to the supersaturation point, nucleation on the crystals, was dominant on the growth of the particles has caused a decrease in the diameter of the particles (Wei, 1997). Therefore, they defended that the smaller particles would be obtained with the calcium hydroxide concentrations close to saturation point. However, in these articles, the formation of the particles by using higher initial concentrations was not mentioned.

The mean sizes of the particles during the reaction were changed (Figure 4.17). The average sizes of the formed calcium carbonate particles started to drop as the concentration of the suspension increased to 15 mM. But, the excess amount of Ca^{++} ions in the media held on the surface of the calcite crystals and they caused the formation of larger particles; thus, particle diameters started to enlarge with the concentrations higher than 15 mM. The finest particles were produced with the experiment of 15 mM which was just below the saturation point (Figure 4.20).

Zeta potential and average size values of these experiments were given in Figure 4.18. The zeta potential is proportional to the particles' demands of pushing, pulling and forming clusters. Zeta potential on the sub-micro calcite surface is a sensitive function of salt concentration of the suspension, calcite content, and pH of the suspension (Yuan, Cheng, Zhou, Yuan, & Semiat, 2008)

The significant zeta potential range for calcium carbonate particles is between -30 mV and +30 mV. The zeta potential value in this range represents flocculation and agglomeration between the particles. Because of the attraction potential of the particles is so high. In cases outside this range, formed particles are individual and have homogeneous size distributions. By examining the charts below (Figure 4.18), it can be said that as the concentration of the initial calcium hydroxide solution increased, zeta potential values started at a value of close to 30 mV. At low concentrations, especially at the studies of 1 and 5 mM, zeta potential values were within this mentioned important range; hence, here there were lots of formations of agglomerated particles. The most individual particles were synthesized with the experiments that were closest to the level of saturation.
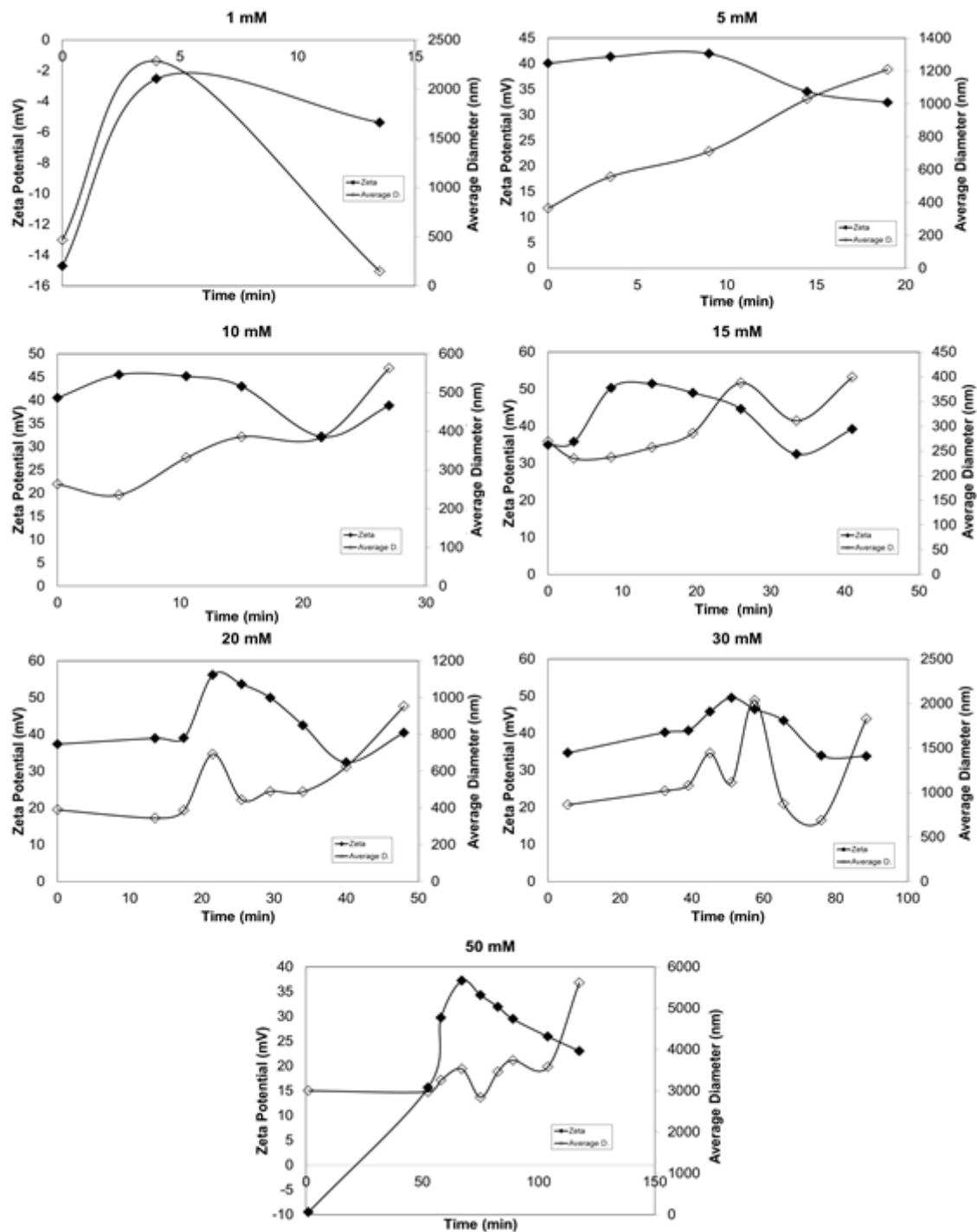
Figure 4.18. Zeta Potential and average diameters of the particles produced with different Ca(OH)$_2$ concentrations

SEM images of the calcium carbonate particles were presented in Figure 4.20. At low concentrations such as 1 and 5 mM, produced particles' structures were obviously cubic-shaped. As the concentration of the suspension increased to 10 or 15 mM, calcite particles protected their rhombohedral structures, but, they showed a sharp

decline in their sizes. As the concentration values exceeded the level of supersaturation, the morphologies of the particles showed a transformation from cubic-like structures to needle-like structures. Finally, at the end of the experiment of 50 mM, particles with non-homogeneous size distribution and scalenorhombohedral structures were produced.

In addition to all these analyzes, XRD patterns of these produced powders were shown in Figure 4.19. These XRD results represented that until the saturation concentration (5, 10 and 15 mM), all of the produced powders completely contained calcite particles, on the other hand, after the saturation point (20, 30 and 50 mM), synthesized powders contained calcite and also calcium hydroxide particles due to the excess amounts of Ca^{++} ions.
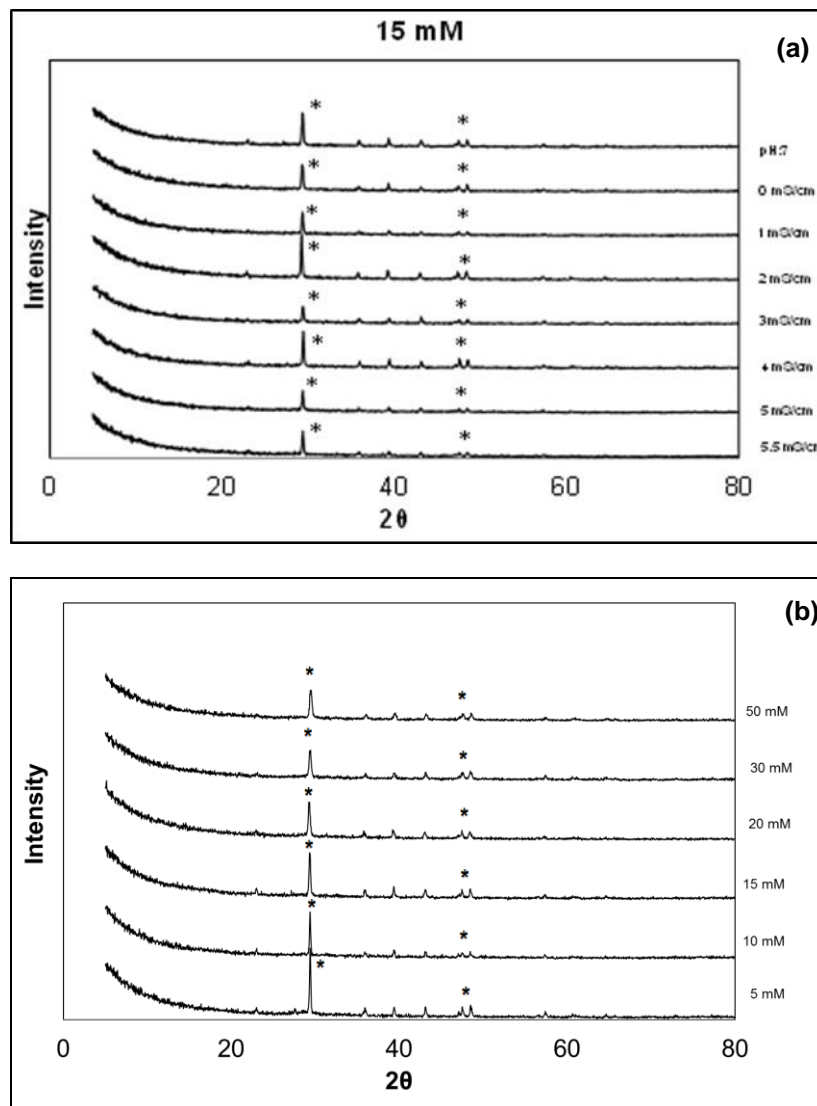
Figure 4.19. XRD patterns of the produced particles: (a) for 15 mM, (b) for all experiments (* calcite peaks)
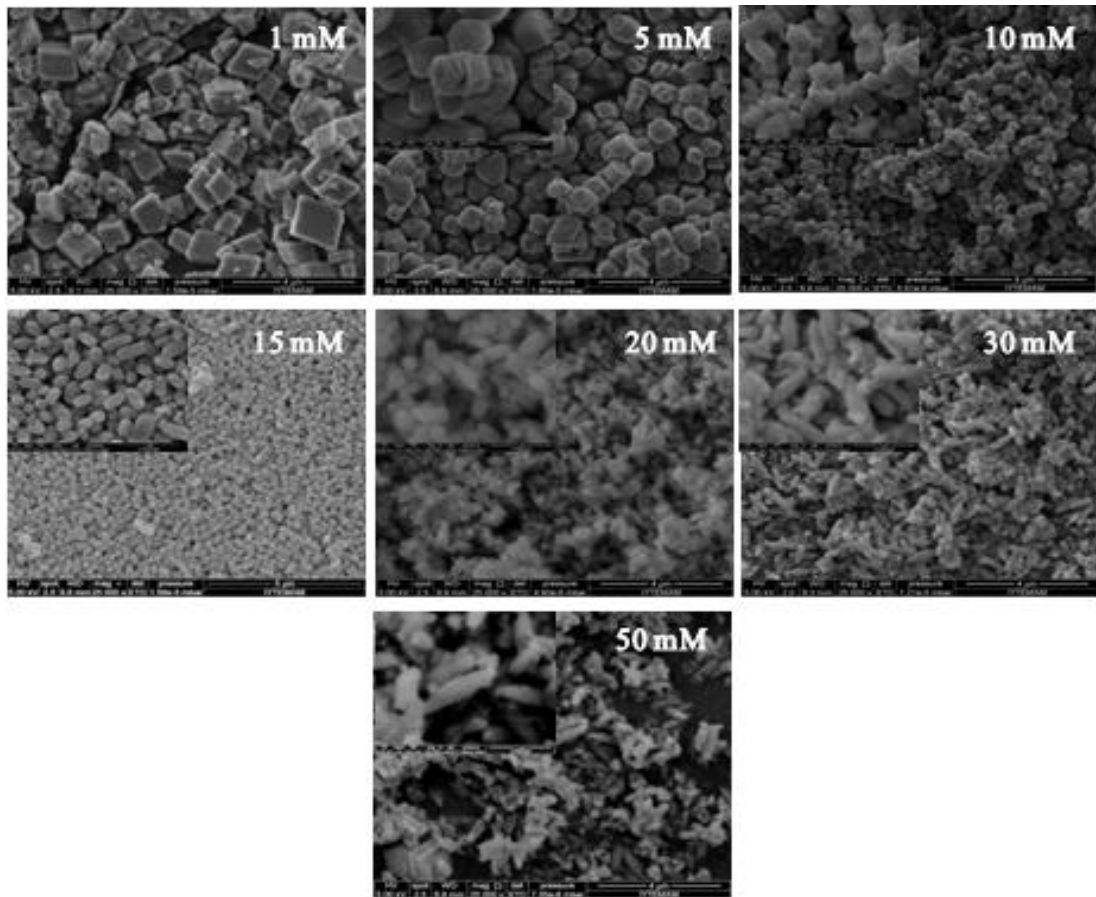
Figure 4.20. SEM images of the produced CaCO$_3$ particles with different Ca(OH)$_2$ concentrations (25000 magnifications)

Generally, with these experiments, it was examined that the initial calcium hydroxide concentration affected the crystal structures, sizes and size distributions of the resulting calcium carbonate particles. The key point of the concentration studies was the saturation level. Effect of key point was seen clearly on the chart of average diameters of particles in Figure 4.21. It can easily be understood from this graph that, the smallest particles were produced with the experiment whose concentration was close to this critical saturation level. The diameter of particles increased as the initial concentration increased or decreased from this saturation level.
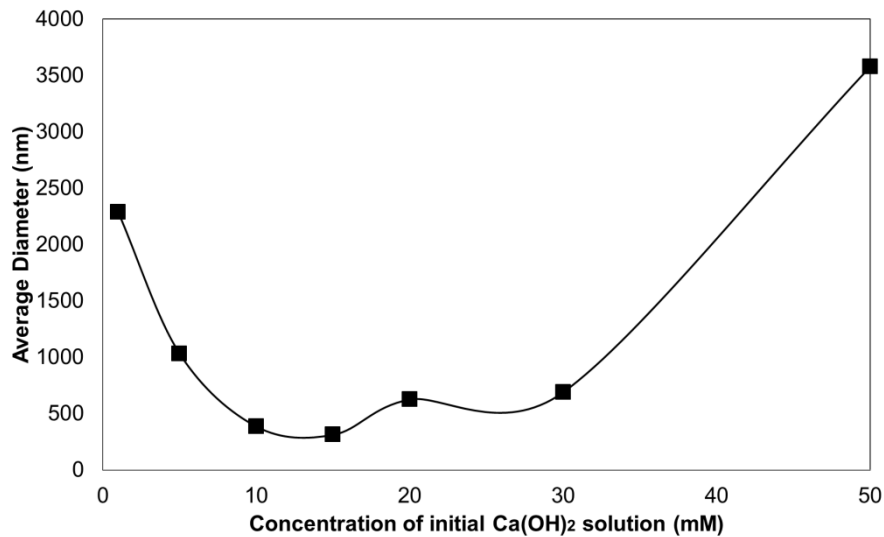
Figure 4.21. Average Diameters of the particles with respect to the concentration of calcium hydroxide solution

After exceeding the critical point, produced particles lost their rhombohedral structures and they started to have scalenohedral structures. Their size distributions started to be non-homogeneous. Also, before this critical point, morphologies of the particles were obviously cubic shaped, but their diameters were larger. XRD patterns of these experiments proved that all of these synthesized particles were calcite.

4.4 The Effects of Diameter of Pipes

The effects of the diameters of recirculation pipes on the produced calcite particles' size and structures were investigated with the experimental set up shown in Figure 3.1. Pipes with 5 different diameters were used and these pipes' inner and outer diameters were given in

Table 1. The inner and outer diameters of pipes used in the experiments. During the experiments, temperature, volumes of stabilization and reaction chambers, stirring rate, concentration and flow rates of raw materials were kept constant.

The mass transfer of a gas phase (CO_2) through a liquid phase ($Ca(OH)_2$ solution) occurs by the surface area. This cross-sectional area of the fluid flown downwardly is proportional to the volumetric flow rate of this fluid, videlicet; diffusion has a major role within this process. Diffusion can be optimized by changing the

diameters of pipe, in other words, by narrowing or expanding the cross-sectional area of the fluid phase (Figure 4.22). In this part of the studies, the influences of this optimization process on the calcite particles' size distributions within a crystallization reactor.

Table 1. The inner and outer diameters of pipes used in the experiments

	Inner Diameter (mm)	Outer Diameter (mm)
A	12	16
B	9	12
C	7	10
D	5	8
E	4	6
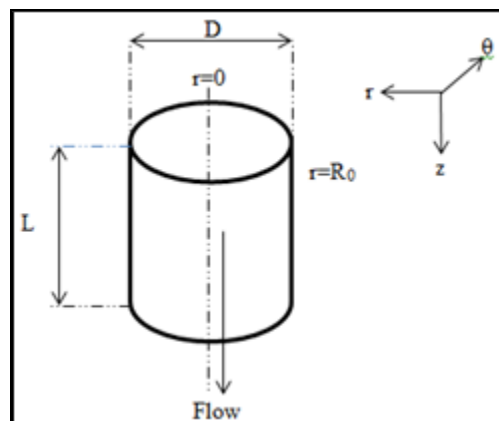
Figure 4.22. The cross-sectional area of a pipe used in the system

Figure 4.22 showed a cross section of a pipe, L was the length, D was the diameter of the pipe which was variable in these studies. Also, the schematic model of the flow was seen in Figure 4.23. The equation of the volumetric flow rate was written as:

$$Q = v \times A \tag{4.3}$$

Here, Q was the volumetric flow rate, v was the velocity of the fluid and A was the area. Equation given in (4.4) represented the cross-sectional area of a cylindrical pipe:

$$A = (\pi D^2)/4 \qquad\qquad (4.4)$$

Considering the equations, when the diameters of the pipes were changed, volumetric flow rate and cross-sectional area would be changed. Thus, diffusion of a gas phase to a liquid phase and the contact time of these phases would be changed, too.
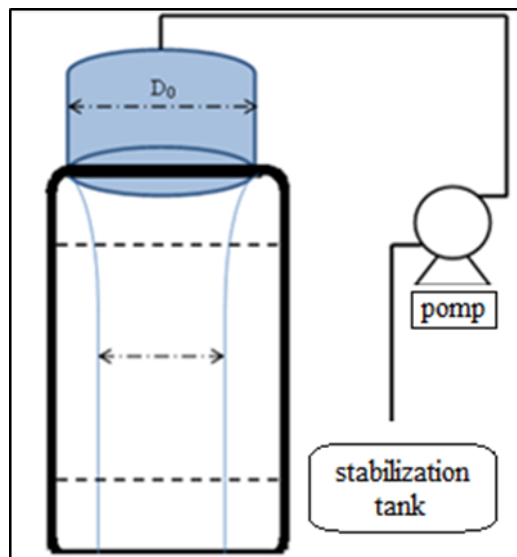
Figure 4.23. The schematic model of the flow

Figure 4.24 illustrated the consumptions of the OH^- and Ca^{++} ions of all experiments. It was clear that, as the diameter of the pipes decreased, conversion time of the calcium hydroxide solution was elongated. It can be said that the crystallization time was lower for the small diameter pipes.

The growth of the particles during the process was illustrated in a graph given in Figure 4.25. Here, the reaction parts were divided and numbered. The expressions of these numbered parts were given in Table 2. It can be said by looking at this chart, the particles' average sizes were increased with respect to the time. However, in SEM images (Figure 4.5), it was observed that the particles were getting smaller as the

reaction proceeded. Thus, the graph given in Figure 4.25 explained us that the "hydrodynamic diameters" of the particles have begun to expand.
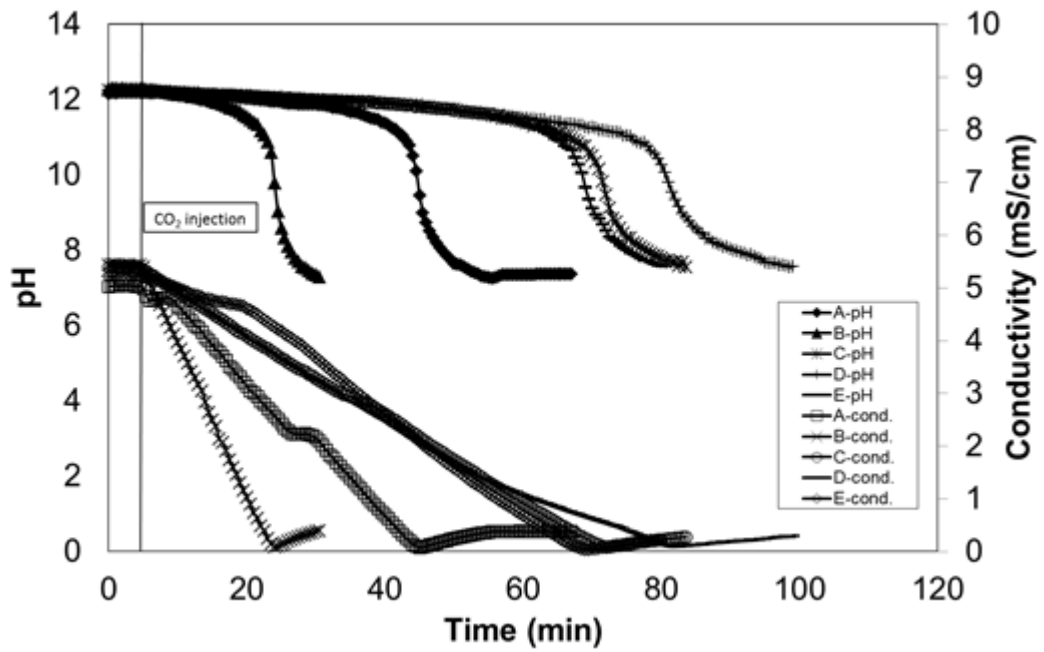
Figure 4.24. Electrical conductivity and pH values of the experiments done with different pipes

Table 2. Reaction parts and conductivity and pH values of these parts

Reaction Parts	Conductivity (mS/cm)	pH
0	5	12.2
1	4	12
2	3	11.9
3	2	11.8
4	1	11.5
5	0	9.3
6	0.3	7
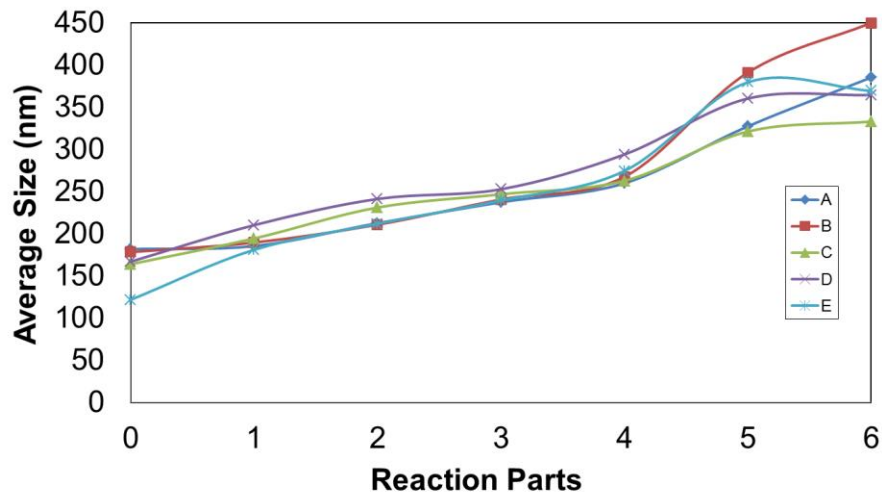
Figure 4.25. Changing average diameters of the calcite particles during the process

For all of the pipe diameter experiments, size distribution graphs by mean intensity and mean number from DLS analysis were given in Figure 4.26. Produced nano calcium carbonate particles' mean sizes were about 200-250 nm due to the graphs. Homogeneous size distributions were obtained for all of the experiments. In the middle of the processes, average particle sizes were increased (Figure 4.27). The reason for this situation was that, in the middle of the precipitation processes, zeta potentials of the particles were suddenly decreased. This sudden decrease in the zeta potential pointed out the agglomeration and formation of flocculates between the particles. These agglomerated particles would be perceived as large particles by DLS device. Also, by looking at these graphs, it can be said that the sizes of the particles were changing between 150 nm and 350 nm (Figure 4.26-b). Particles larger than 1 μm were not synthesized, because it was proved by the SEM images (Figure 4.28), the larger particles seen in the Figure 4.26-a were the impurities or flocculated particles.
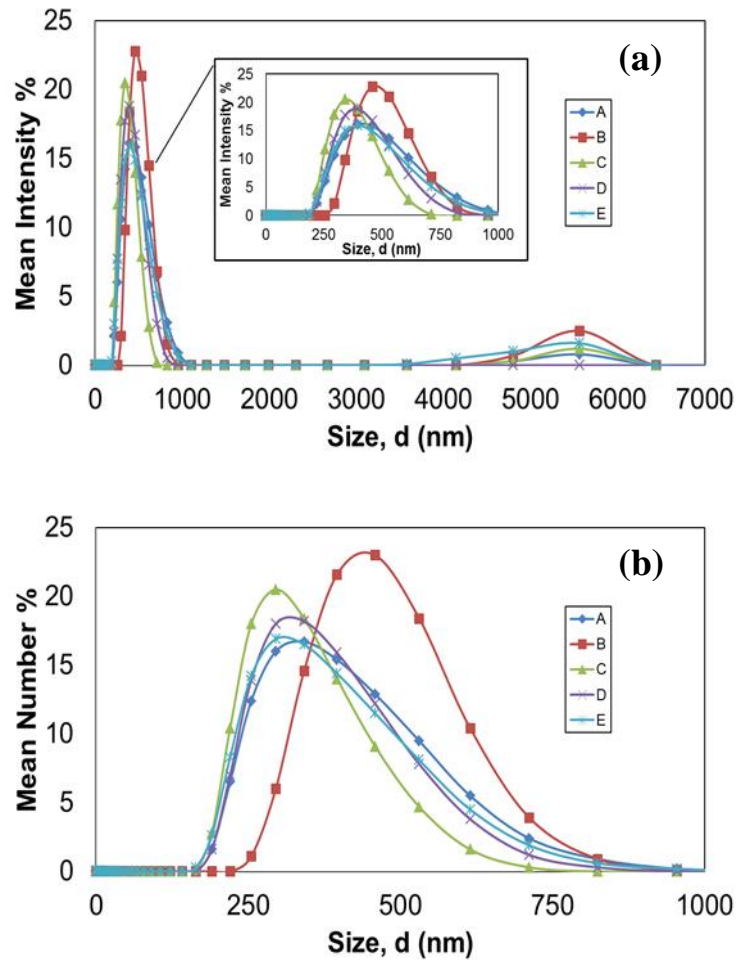
Figure 4.26. Size distributions by mean intensity and number for all pipe diameter experiments: (a) mean intensity graph, (b) mean number graph

Zeta potential and average size values of the samples taken at different conductivity values of the pipe diameter experiments were illustrated in Figure 4.27. As the reaction proceeded, the mean sizes of the particles were increased. Moreover, it can be said that, the zeta potential increased until the electrical conductivity value was decreased to 3 or 2 mS/cm, then it decreased a little during the reactions, and after all, with the last sample (at low pH values), it increased again. This situation meant that, at the end of the reactions, in solutions whose pH were low, the agglomerated granules started to be individual particles.
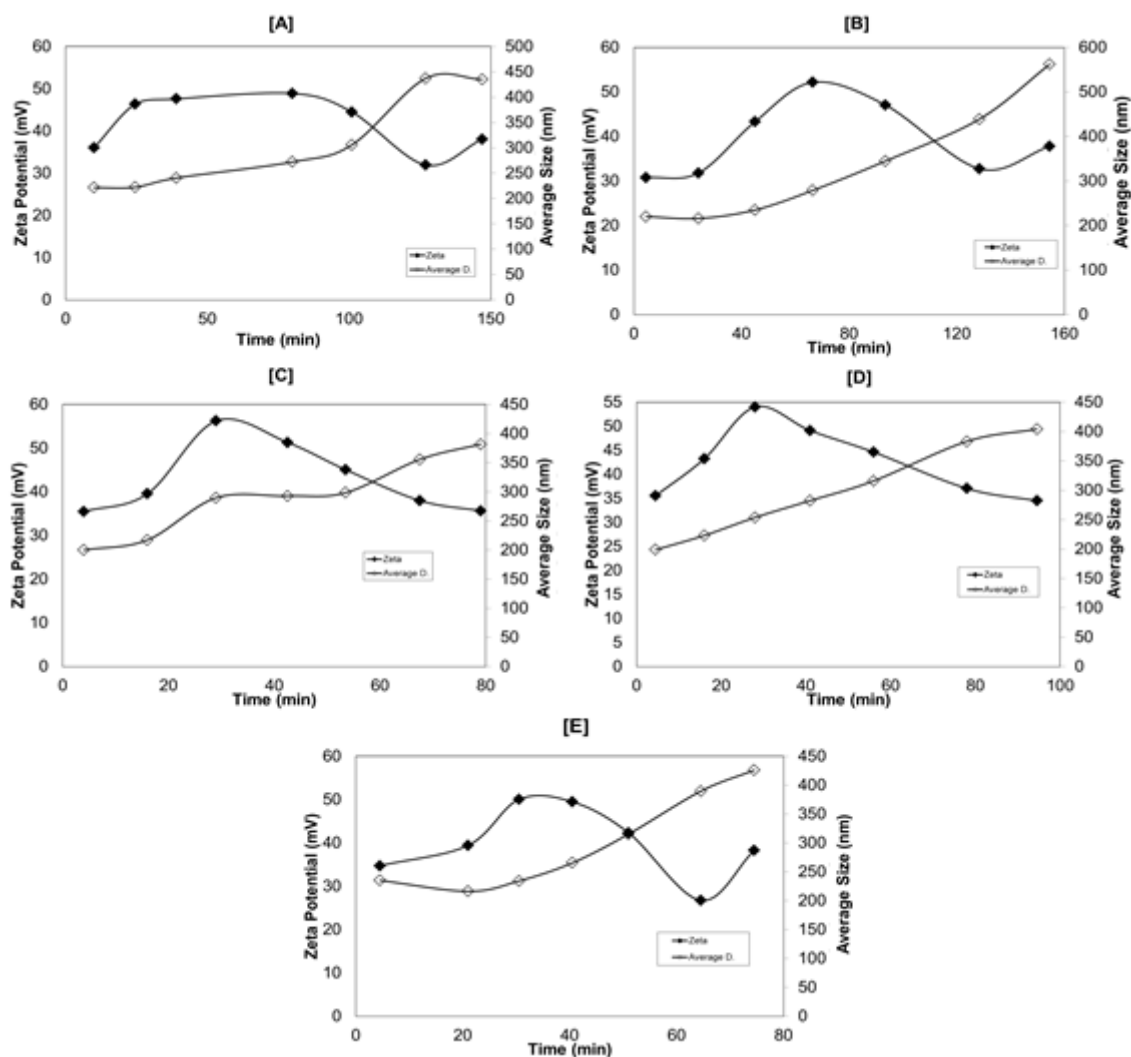
Figure 4.27. Zeta Potential and average diameters of the particles produced with different pipe diameters experiments

By looking at the SEM images obtained from the experiments done by all pipes which had different inner diameters, all the synthesized products were in nano sizes and had homogeneous size distributions. All of them had cubical morphologies similar to the circular ones (Figure 4.28).

It was possible to see the formation stages and mechanisms of the $CaCO_3$ particles during the reactions via SEM images of the samples taken at regular intervals from beginning until the end of the reactions. The images of the samples taken at the beginning of the reaction, the particles were agglomerated and had heterogeneous size distributions (Figure 4.5). As the reaction proceeded, these particles' morphologies transformed from needle-like shaped scalenorhombohedral structures to cubic-shaped rhombohedral structures. The conversion mechanism of particles was same for all of the

experiments, and also, all of the produced calcite particles' sizes were seen nearly same and about 150-200 nm.
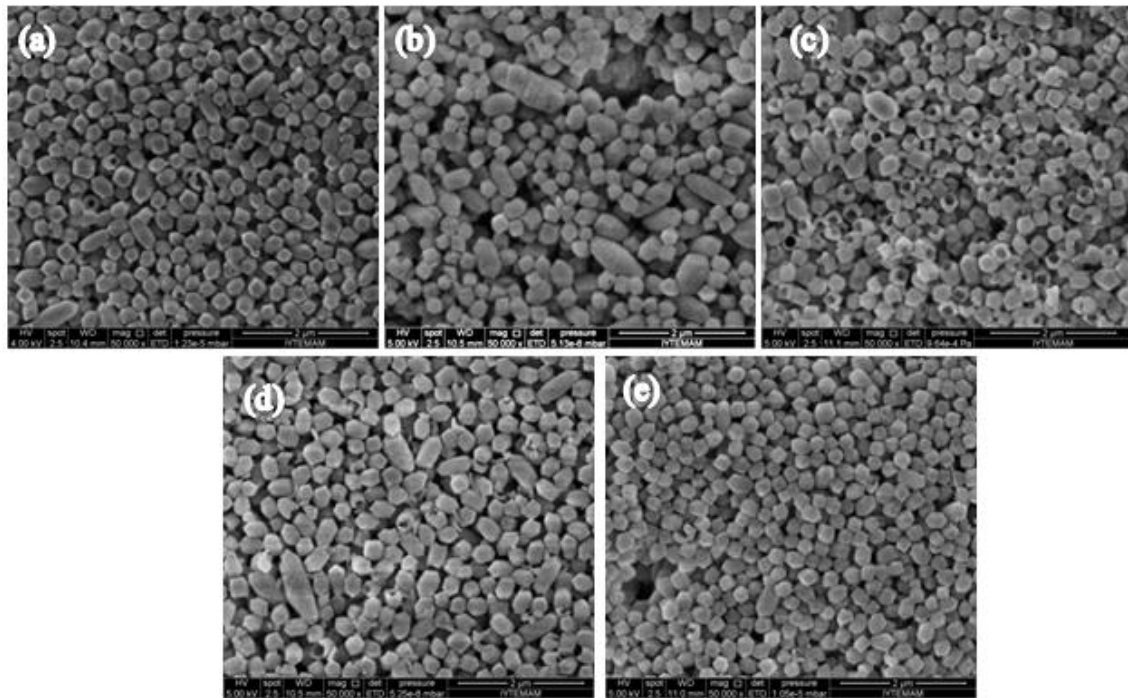
Figure 4.28. The SEM images of the produced $CaCO_3$ particles by different pipes. Inner pipe diameters were : (a) 12 mm, (b) 9 mm, (c) 7 mm, (d) 5 mm, (e) 4 mm (at 50000 magnifications)

Because of the crystallization was an ionic reaction, it was difficult to control the crystallization rate and crystal sizes and size distributions in the solution especially in large scale production. Therefore, one of the parameters for controlling the crystallization rate was the diameter of circulation pipes. Our results were not very changeable. Produced nano calcite particles were seemed almost same; however, the graphs obtained from the DLS analyses showed that larger particles were obtained with the 9 mm in diameter pipe. That means, pipe diameters did not affect the diffusion or absorption rate of CO_2 through the $Ca(OH)_2$ solution linearly. An optimum choice about the circulation pipes should be done for the industrial scale productions of nano calcite.

4.5　The Effects of Volume of Stabilization Tank

In the experimental set up given in Figure 3.2, it was possible to control and separate the nucleation and crystallization parts of the reaction by separating the stabilization tank and reaction chamber from each other. Because, the sizes of the nanometric particles depend on not only the growth rate of the nucleates, but also, the nucleation rate (Lin, 2002). In the production process, the liquid and gas phases were not diffused into each other in a solution. The reaction was carried out with the absorption of the gas, which was distributed homogeneously in the chamber, through the surface of the liquid phase. The $Ca(OH)_2$ solution accumulated in the stabilization tank was recirculated to the reaction chamber until the reaction completed. The effects of volume of the stabilization chamber on the process and synthesized product was investigated by changing the reactor's volumes.

The graph below (Figure 4.29) illustrated the changes in the pH and conductivity values of the $Ca(OH)_2$ solutions in the experiments done with three different stabilization tanks. These pH and conductivity values showed the consumptions of OH^- and Ca^{++} ions in the system. As the volume of the solution was rose, reaction time was also increased. Because of the concentration is same and 15 mM in all the experiments, pH and conductivity values started at the same points. Increase in the reaction time ensured more controllable process of nano calcite production. The consumption time in the tank and the completion time of the reaction were increased linearly due to the increasing volume of stabilization tank. Consequently, more stable and individual particles could be produced by injecting the CO_2 gas to the system in a controlled manner. As the reaction time decreased, the morphological structures and sizes of the synthesized particles were changed.
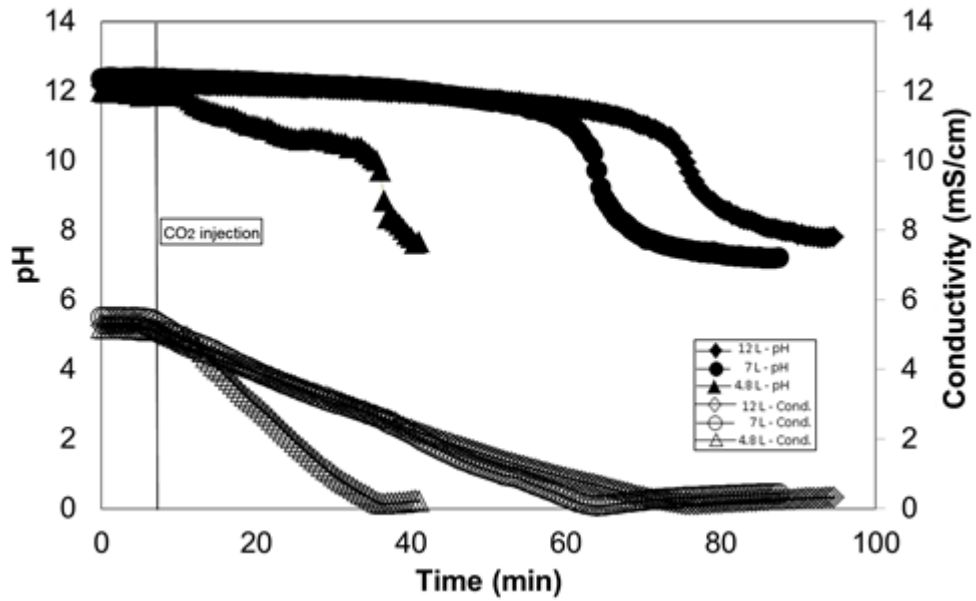
Figure 4.29. Changes in the pH and conductivity values of the Ca(OH)$_2$ solution in all of the stabilization tank volume experiments

By looking at all three experiments' DLS graphs, almost the same size distribution results were observed. The sizes of the particles were about 150 – 350 nm and the number of large particles were very low (Figure 4.30). Zeta potential values were out of the ±30 mV, thus, it can be said that the attraction between the calcite particles was very low (Figure 4.31). Especially in the experiment done with 12 L stabilization tank, the diameters of the particles were calculated by DLS method, smaller than the others (Figure 4.30).
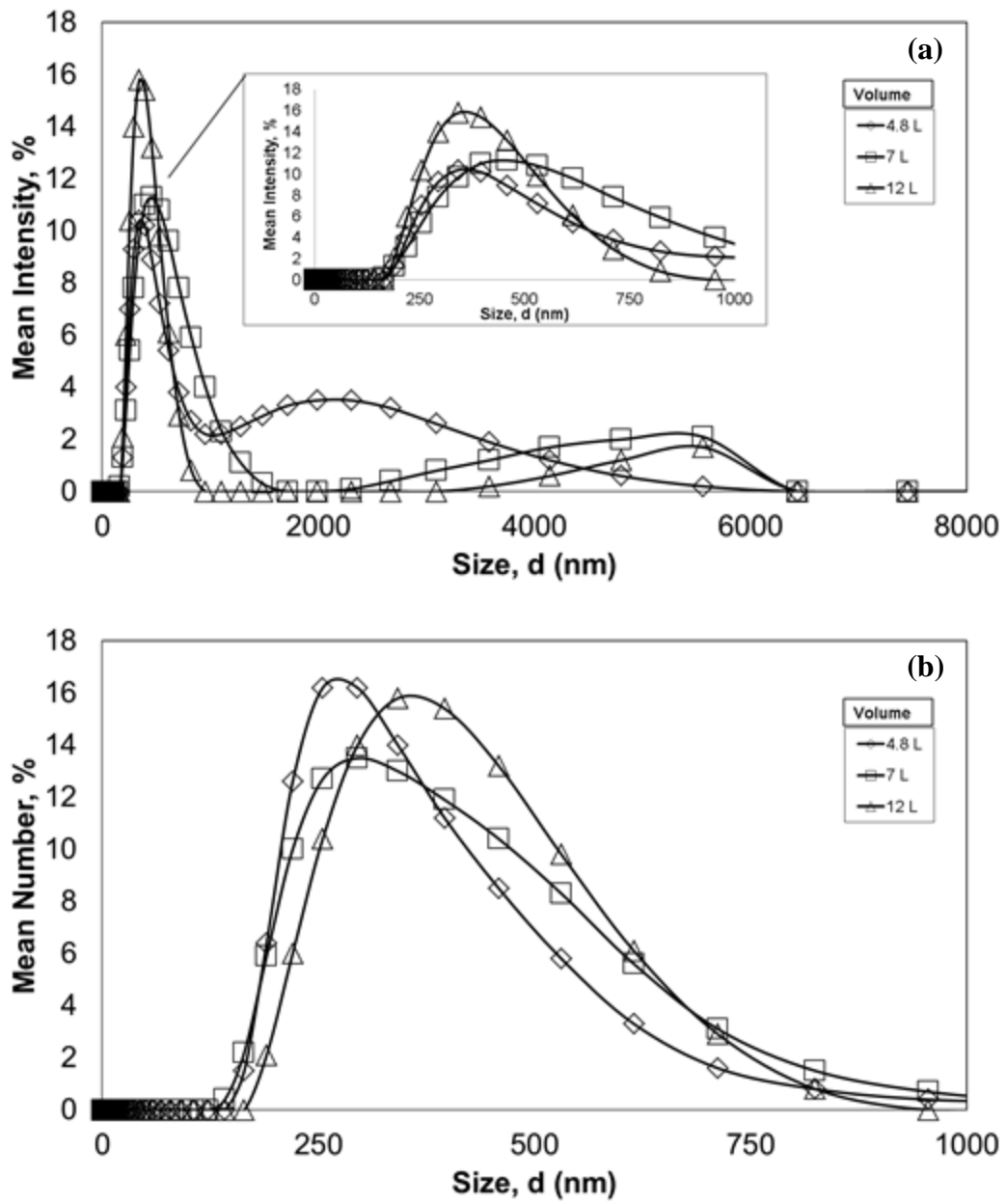
Figure 4.30. Size distributions by mean intensity and number for stabilization tank volume experiments: (a) mean intensity graph, (b) mean number graph
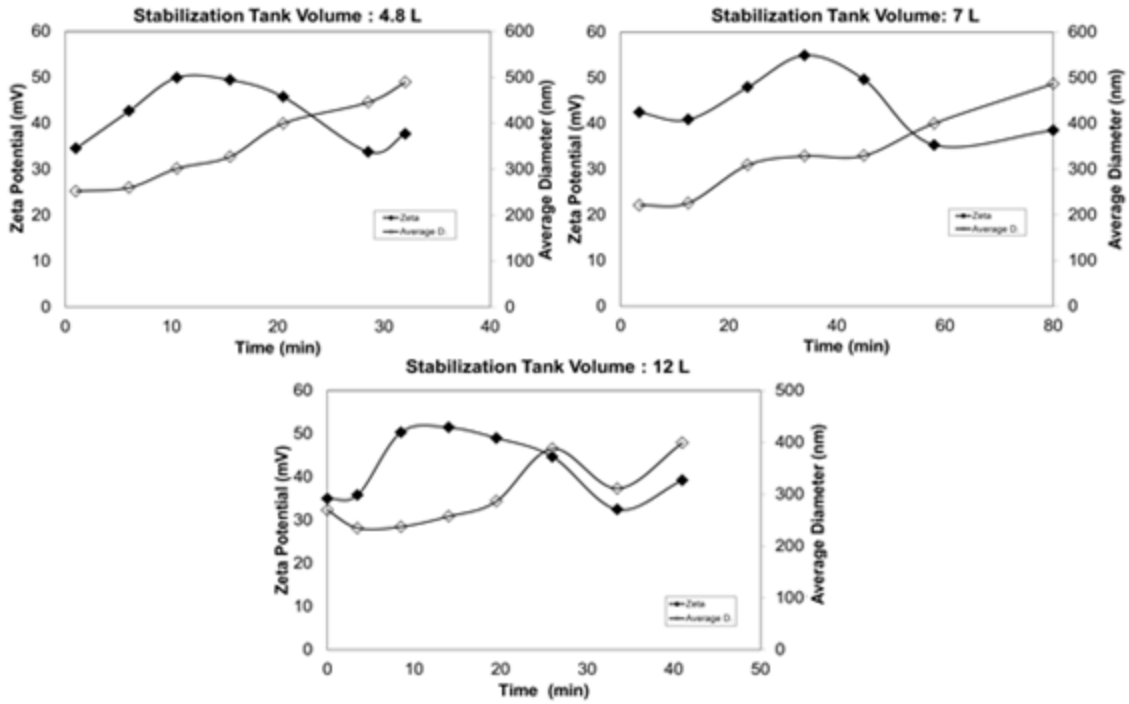
Figure 4.31. Zeta Potential and average diameters of the particles produced with volumes of stabilization tanks experiments

The obtained SEM images (Figure 4.32) has shown that, although different volumes of stabilization tanks were studied, calcite particles in nano sizes and homogeneous size distributions were synthesized again in all of the experiments. Particles larger than the others were produced in the smaller tanks. The reason of it was the uncontrolled diffusion of the carbon dioxide gas into the calcium hydroxide solution in the small-volume experiments. The reaction time was decreased with the decrease in the stabilization tank volume; therefore, absorption of the gas phase on the surface of the liquid phase did not occur homogeneously. The change in the stabilization tank volume did not affect the morphologies of the products. The nano particles obtained in all of the experiments had rhomboscalenohedral crystal structures.
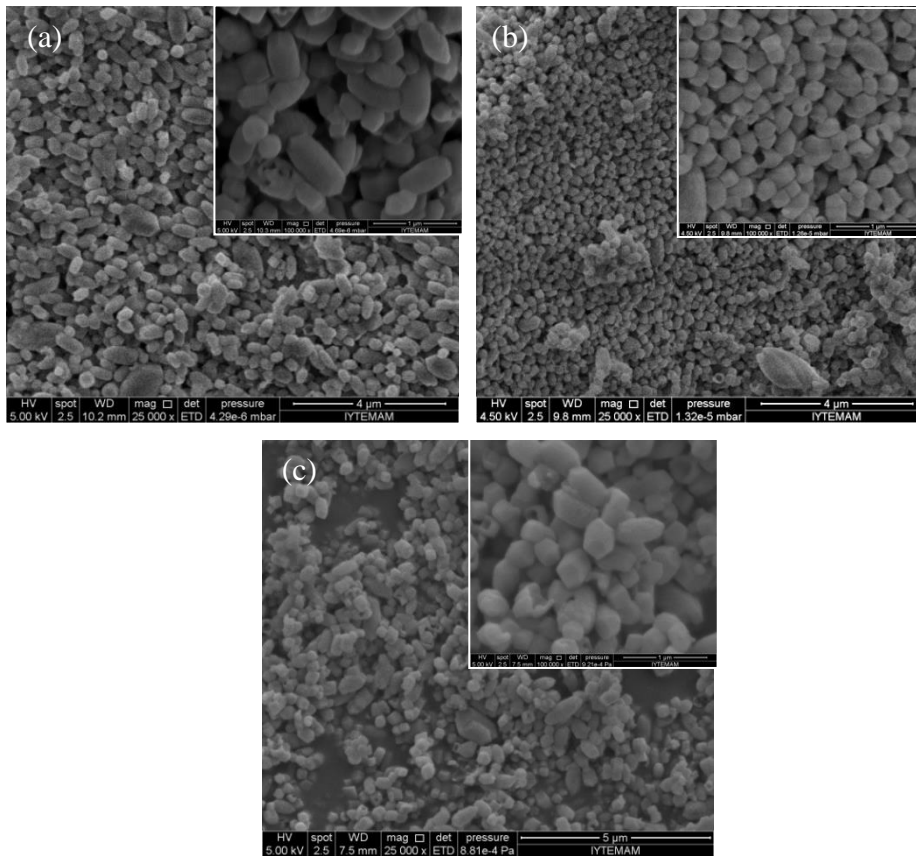
Figure 4.32. SEM images of the calcite particles produced by the experiments with different stabilization tank volumes: (a) 4.8 L, (b) 7 L, and (c) 12 L (at 25000 magnifications)

4.6 The Effects of Length of Reaction Chamber

The reaction chamber length was directly proportional to the contact time of the calcium hydroxide solution flowing into the reaction chamber and the carbon dioxide that was distributed homogeneously in the medium. In the studies, the reaction chamber volume was 5 L and the calcium hydroxide solution was given to the system with 0.2 m^3/h flow rate by a sprayer (Figure 3.2). The sprayer was fixed at the top, bottom and middle points of the reaction chamber. Hereby, the residence time of the calcium hydroxide solution that was recirculated, in the reaction chamber (Figure 3.2).The distance of the sprayer from the exit of the chamber was proportional to the contact time, and as the contact time was increased, the particles were expected smaller and to be more homogeneous structured.

For every experiment, the graphs which illustrated the pH, conductivity values and OH- consumption of the system were given in Figure 4.33. The concentrations of the solutions were 15 mM in all three experiments. Thus, the solution at the beginning of the reaction was expected to be contained 15 mM Ca^{++} and 30 mM OH^- ions theoretically. But in practice, these values were lower in the experiments (Figure 4.33). The reason can be explained as; the calcium hydroxide powders were not dissolved in water completely. Nearly 24 % of the calcium hydroxide was not dissolved in the solvent due to its solubility properties (Burns & Jachuck, 2005). The reason of the differences between these theoretical and experimental results could be explained as the incomplete dissolution of the $Ca(OH)_2$ solution in higher concentrations which were close to the supersaturation concentration.

Mean intensity and mean numbers graphs showed that the sizes of produced nano calcite particles were changed between about 150-300 nm (Figure 4.34). It was expected that as the contact time of the gas and liquid phases was increased, the reaction became more controllable. If the distance of sprayer header from the exit of the reaction chamber increased, the diffusion of the carbon dioxide gas into the surface of the calcium hydroxide solution was occurred more homogeneously. Due to the agglomerated particles had been occurred in the medium, the micro-sized particles were seen in the intensity graph. However, SEM images illustrated that, particles larger than 300 nm were not synthesized with our systems (Figure 4.36). The zeta potentials of the solutions changed in the range of 30 and 45 mV (Figure 4.35). It was known that the Ca^{++} and OH^- ions started to apply attraction forces through each other in cases where the reduction occurred in the zeta potential values of the solutions. The increase in the diameters of the formed calcite particles could be observed with the zeta potential values approached to 30 mV.
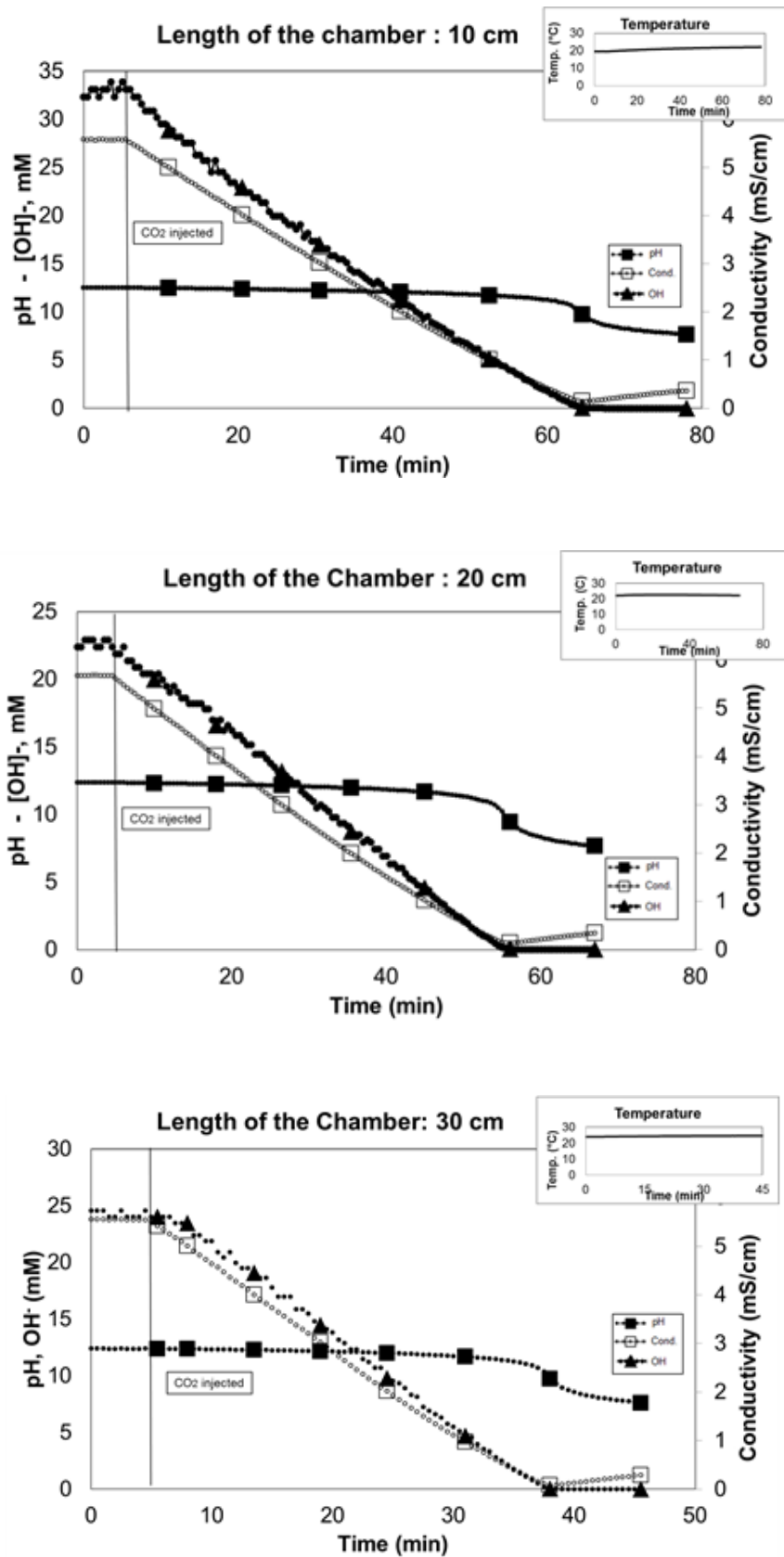
Figure 4.33. Changes in the pH, OH⁻ and conductivity values in the experiments done with different chamber lengths
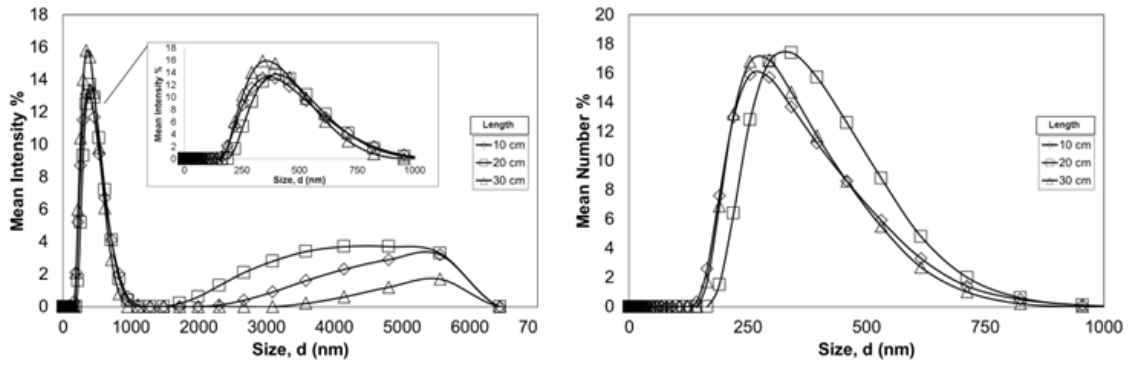
Figure 4.34. Size distributions by mean intensity and number for length of reaction chamber experiments
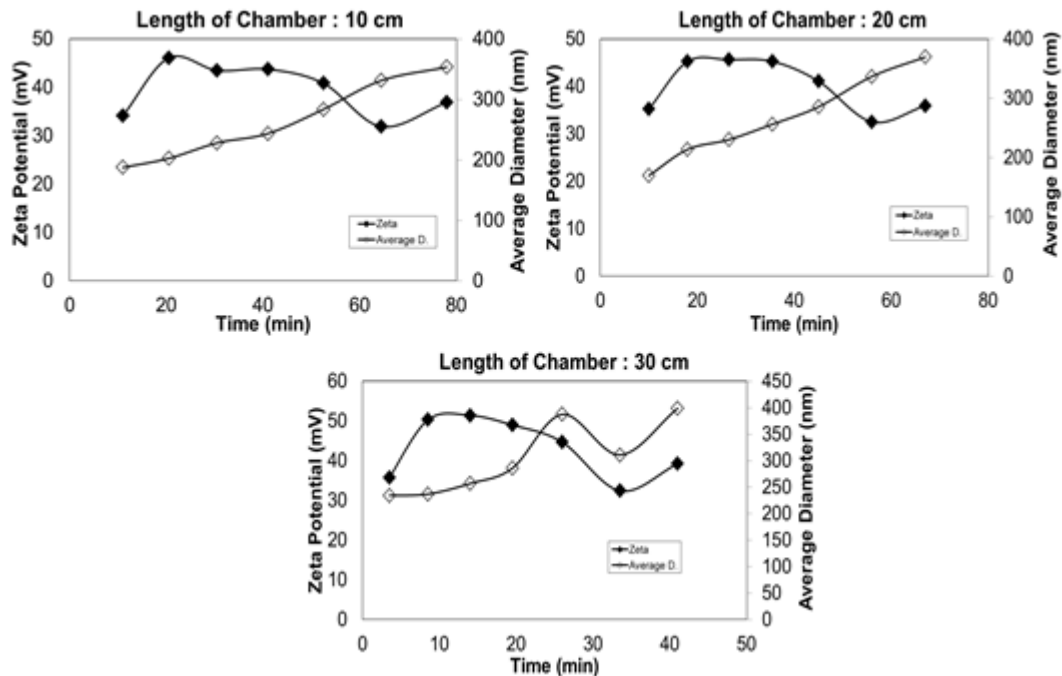
Figure 4.35. Zeta Potential and average diameters of the particles produced with different reaction chamber lengths experiments

An increase in the residence time of the calcium hydroxide solution in the reaction chamber, caused more controllable reaction had been carried out. The rate of diffusion affected the sizes and size distributions of the calcite particles (J. F. W. Chen, Y. H., 2000). Nano calcite particles were produced in smaller sizes and more homogeneous size distribution as the distance of the shower from the exit of the chamber was increased. As the distance was getting longer, namely, as the contact time of the carbon dioxide and calcium hydroxide solution was increased, the production

became to be more uncontrolled and the synthesized particles were a little larger than the others. It was seen that the particles' structures were monodisperse and scalenorhombohedral shaped. Varying contact times did not induce any changes in the crystal structures of the particles. Due to the concentrations of the initial solutions were 15 mM, XRD spectrums of these powders attested that these products were all calcite (Figure 4.19).
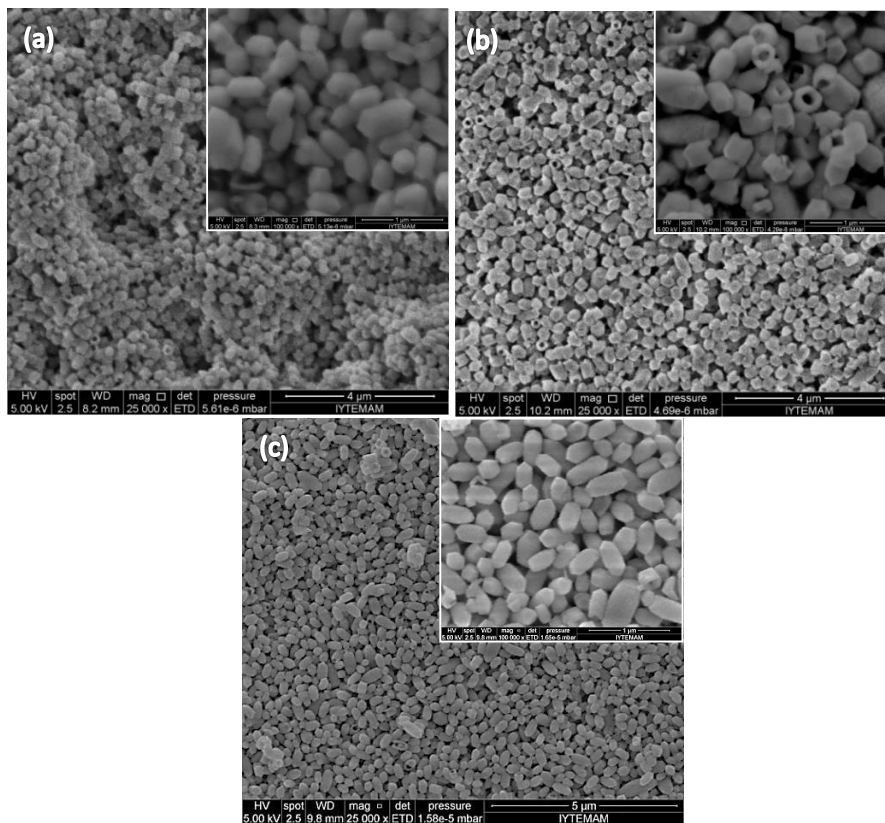
Figure 4.36. SEM images of the produced calcite particles by all length of chamber experiments : (a) 10 cm, (b) 20 cm, (c) 30 cm (at 25000 magnifications)

4.7 The Effects of Volume of Reaction Chamber

Stabilization tank and reaction chamber were separated from each other to get the process of nano calcium carbonate process under control. The most important factor here was the requirement of the separation of the nucleation and crystallization stages from each other. The reaction chamber was supposed to be the region that the carbon dioxide gas had been distributed homogeneously within it and calcium hydroxide

solution was spread into this gas media. In this media, the volume of the reaction chamber was as important as the flow rates of calcium hydroxide and carbon dioxide. The denseness of the carbon dioxide gas in this chamber had an influence upon the diffusion rate and so the morphologies of the particles. In this instance, two different experiments with reaction chamber volumes of 1.5 L and 5 L were done to observe these effects. All of the other parameters of the system were kept constant (Figure 3.2).
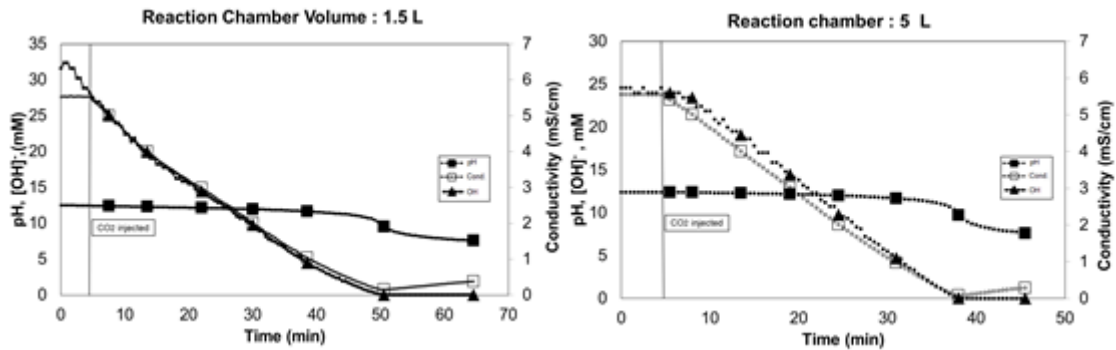
Figure 4.37. Changes in the pH, OH⁻ and conductivity values in the experiments done with different chamber volumes

The changes in the values of pH, [OH]⁻ and conductivity of two different reaction chamber volume experiments were illustrated in the graphs above (Figure 4.37). The concentrations of calcium hydroxide solution were set as 15 mM. Due to this concentration, theoretical amounts of Ca^{++} and OH⁻ ions in the solution must be 15 and 30 mM, respectively. In the experiment with the chamber volume of 1.5 L, OH⁻ ions were achieved to this theoretical value, but, in the study with the chamber volume of 5 L, this OH⁻ ions concentration started from about 25 mM. The reason for this was that the calcium hydroxide particulates had not been dissolved completely in the water. From the moment that the CO_2 injected into the system, declines in the conductivity and concentration of [OH]⁻ ions which showed that the reaction begun to occur were seen. After all the Ca^{++} ions were consumed, along with the conductivity value decreased to zero, a reduction in the pH value occurred and it decreased from nearly 12 to 7. Electrical conductivity decreased to zero meant the reaction had been completed and all individual Ca^{++} ions were consumed. The reason for the reduction in pH values was the increment in the HCO_3 ions concentration in the system.

Mean intensity and mean number graphs of particles were obtained from the DLS analyses for both of two experiments (Figure 4.38, Figure 4.39). In both of the experiments, samples which were taken at the specific conductivity values were analyzed. Generally, the particles whose diameters were about $150 - 200$ nm were produced. Because of the flow rate of CO_2 that was injected into the chamber was constant, it can be said that, carbon dioxide concentration was higher in the chamber whose volume was smaller. Based on this, the realization of a controlled reaction had been prevented by carbon dioxide gas that had been diffused more intensely into the surface of calcium hydroxide solution. In the mean intensity graph of experiment done with 1.5 L chamber (Figure 4.38-a), the increment in the sample which was taken at the end of the reaction, verified this hypothesis. In the same experiment which was repeated with 5 L reaction chamber, the smallest size distribution was obtained from the sample that was taken at the end of the reaction.

Average diameters of the particles were increased from about 200 nm to 400 nm. However, it should be noted that, these values which were calculated by the DLS device, showed the hydraulic diameters of the particles. On the other side, zeta potentials of the particles were higher than 30 mV and a decline in zeta potential occurred at the end of the reaction. The consumption of the ions in the solution, completely formation of $CO_3^=$ ions and the attraction between Ca^{++} and $CO_3^=$ ions can be the reason for this situation. After all, a little increment in the zeta potential was seen with the increase in the amount of HCO_3 ions in the solution (Figure 4.40). At the end of the reaction, SEM images of the produced nano calcium carbonate particles were seen in Figure 4.41. As the volume of the reaction chamber increased, the concentration of the carbon dioxide gas in the chamber decreased, and the diffusion took place more slowly. Thus, this allowed occurring of a more controlled reaction. By looking at the SEM images of the experiment done with 5 L chamber, the crystal structures of the particulates were smaller and the size distribution was more homogeneous. The particles had scalenorhombohedral morphological shapes and monodisperse structures (Figure 4.41).
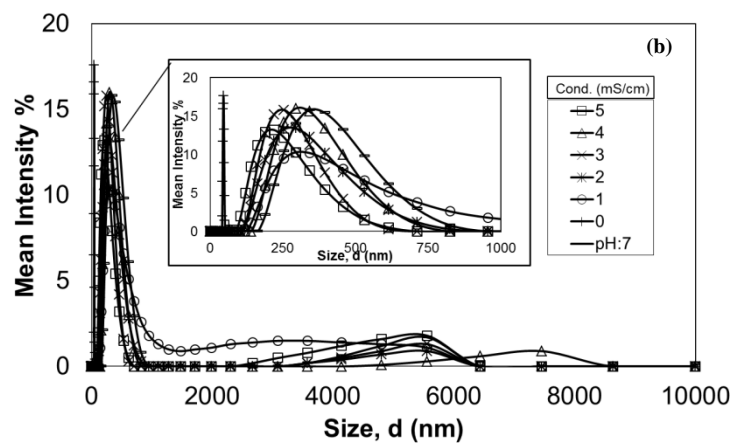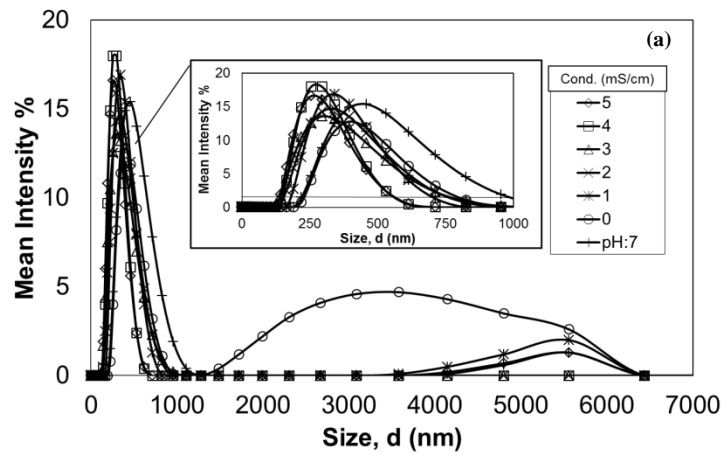
Figure 4.38. Size distributions by mean intensity for different reaction chamber volume experiments : (a) 1.5 L, (b) 5 L
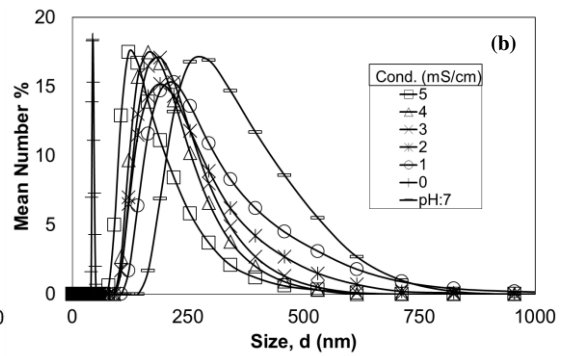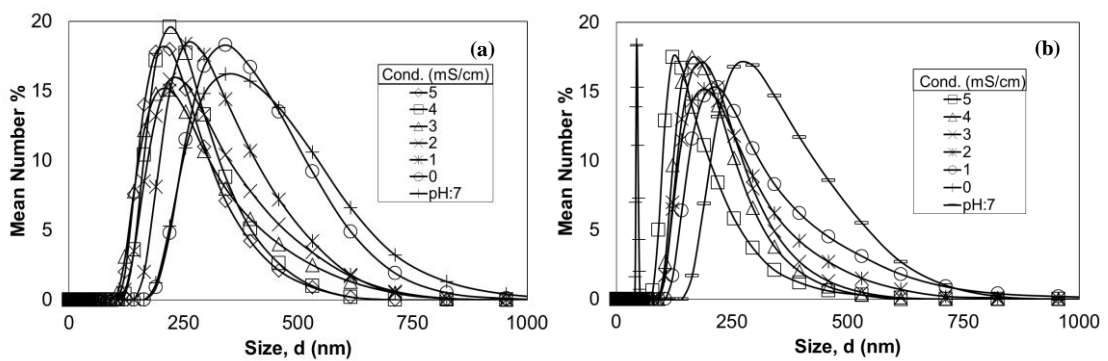
Figure 4.39. Size distributions by mean number for different reaction chamber volume experiments : (a) 1.5 L, (b) 5 L
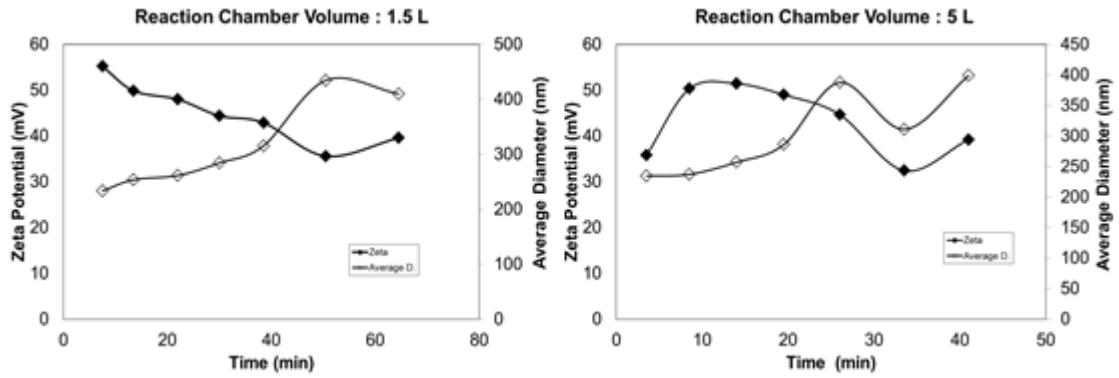
Figure 4.40. Changes in the zeta potential and average diameter for both of the experiments
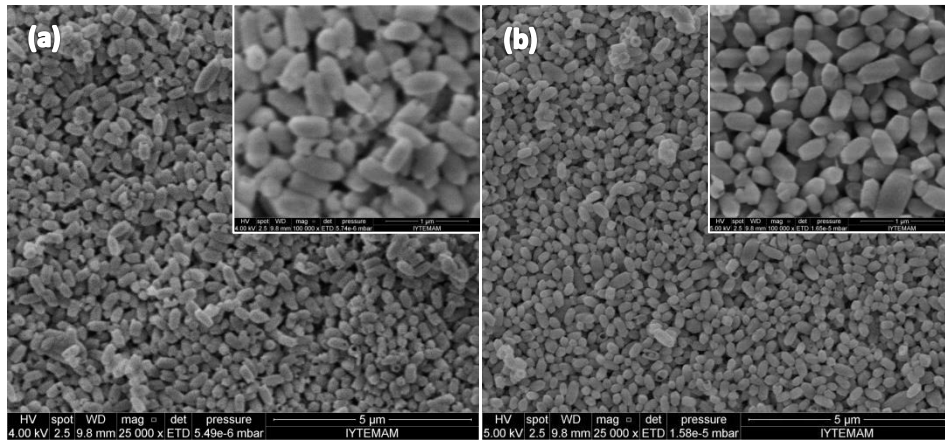
Figure 4.41. SEM images of the produced calcite particles by volume of chamber experiments: (a) 1.5 L, (b) 5 L (at 25000 magnifications)

4.8 The Effects of Stirring Rates

Although the effects of engineering factors are very critical in the scale-up for the calcite production processes, a little attention has been paid to these effects on the particle size and size distribution in the production processes of ultrafine particles in the literature. The studies reported by Chen and Tosun pointed out that macromixing (mixing on the macro scale) and micromixing (mixing on the molecular scale) had a very important effect on the particle size distribution in the chemical processes done with $BaCl_2$ solution and Na_2SO_4 solution (J. F. Z. Chen, C.; Chen, G. T. , 1996; J. F. W. Chen, Y. H., 2000; Tosun, 1988). For instant, in nano calcium carbonate production, when the effects of stirring rate and volume of calcium hydroxide solution on the

73

particle structure were investigated, it was proved that the crystallization rate of aragonite structured calcium carbonate was increased and number of the agglomerated nano calcite particles was decreased with increasing the stirring rate (K. N. Kim et al., 2005).
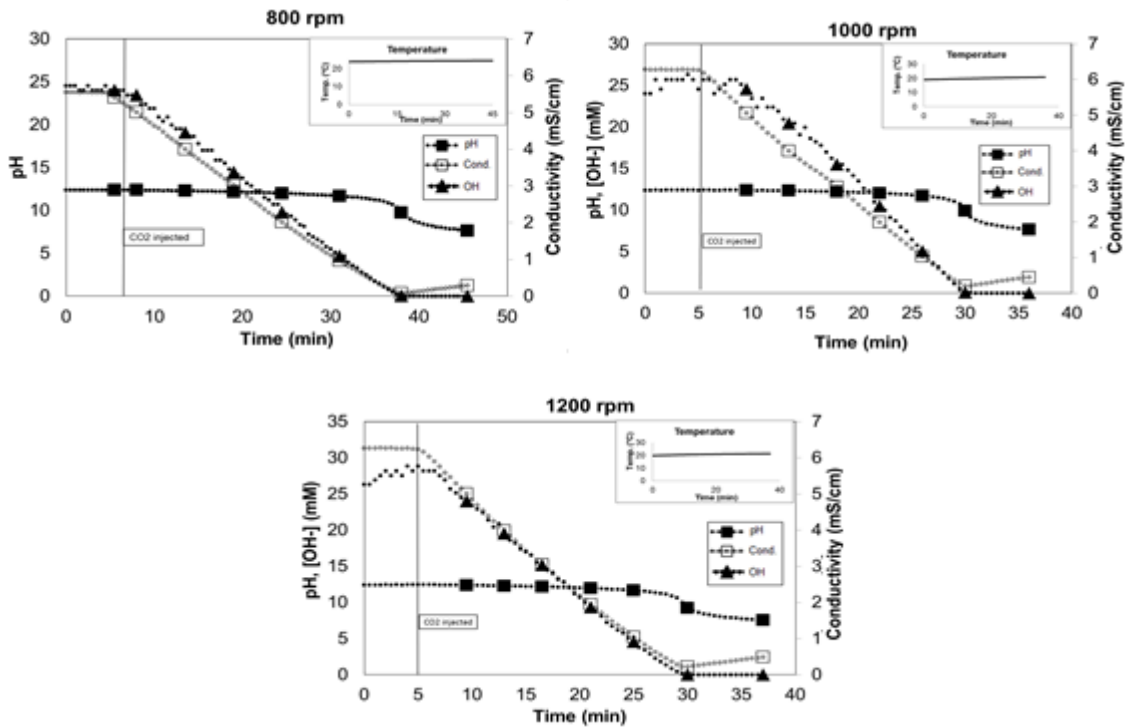
Figure 4.42. Changes in the pH, OH⁻ and conductivity values at the experiments done with different stirring rates

The faster stirring rate has a significant role on the synthesizing calcite systems to enhance mass transfer between the phases, increase the penetration of carbon dioxide to the core of calcium hydroxide for significant conversions and minimize the effects of the dense calcium carbonate protective layer (Ibrahim et al., 2012). With the increment at the mass transfer rate and penetration, the completion time of the reaction was expected to decrease. In the experiments with increasing agitation rate, it was seen that the Ca^{++} ions being exhausted more quickly, so, the reaction was completed more quickly, too (Figure 4.42). When the calcium hydroxide with 15 mM concentration started to be solved in the water, the formation of 15 mM Ca^{++} and 30 mM OH⁻ ions in the media was expected theoretically. Because of the calcium hydroxide was dissolved easier at lower pH values (Coto et al., 2012) and a complete dissolution would not occur

at the pH value of 12, at the beginning of the reaction, nearly 25 mM OH⁻ ions were dissolved in the solution. Thus, the reaction completed as the ions were reacted with each other and consumed, and as the concentration of formed ions (HCO_3^-, $CO_3^=$) increased, pH values started to decrease. The increment in the concentration of bi carbonate ions induced the formation of hollow shaped calcite particles due to these bicarbonate ions severing Ca^{++} ions from the formed calcite particles' surfaces (Figure 4.45).
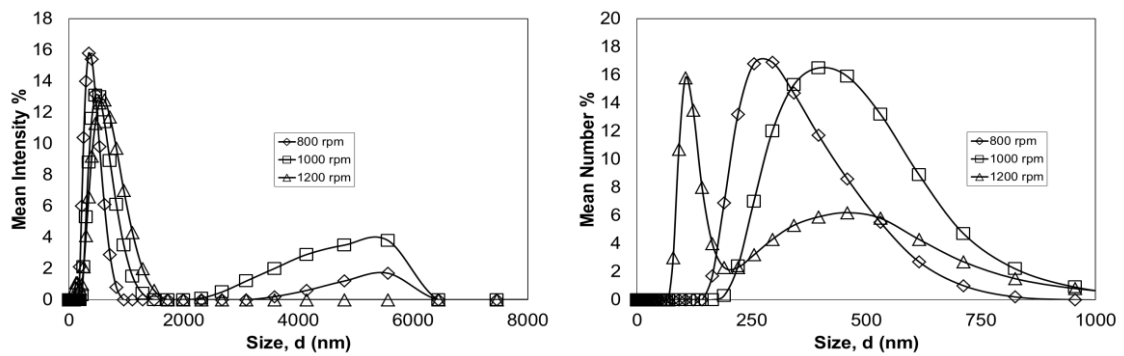
Figure 4.43. Size distribution of particles by mean intensity and mean number

Carmona and Morales claimed that at high stirring speed (>300 rpm), the rate-determining step of the calcium carbonate process is the detachment of Ca^{++} and OH^- ions at the surface (4.5). However, at low stirring speed (<300 rpm) the slow step involves the diffusion of Ca^{++} and OH^- away from the calcium hydroxide surface (4.6) (García-Carmona et al., 2003).

$$Ca(OH)_2 \rightleftharpoons Ca^{++} + 2OH^- \quad (surface) \qquad (4.5)$$

$$Ca^{++} + 2OH^- \ (surface) \rightleftharpoons Ca^{++} + 2OH^- \ (solution) \qquad (4.6)$$
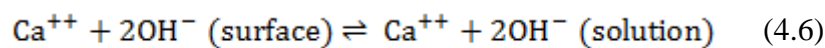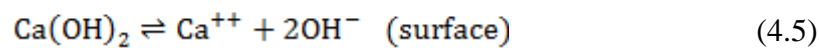
In the literature, various agitation methods, such as acoustic, ultrasonic and in situ grinding, have been already studied for their effectiveness in removing precipitated limiting diffusion layers in processes where the dissolution of the solid reactant and the formation of particles of the solid product proceed simultaneously (Burns & Jachuck, 2005). In another article that calcium carbonate precipitation process was studied with

carbonization method, the stirring methods were the parameters for their experiments (López-Periago, Pacciani, García-González, Vega, & Domingo, 2010). The carbonization method was applied by injecting the CO_2 gas into the solution in the form of bubbles at atmospheric conditions. Their experiments were done without agitation, and with mechanical and ultrasonic agitators. The particles obtained without agitation were in the amorphous structure and clustered, also their sizes were large. On the contrary, with mechanical stirrer, the particles structures were developed and got smaller, with ultrasonic agitation, the smallest and the most stable crystal structures were obtained (López-Periago et al., 2010). So, the stirring methods were as important as stirring rate in the synthesis of nano calcium carbonate particles.
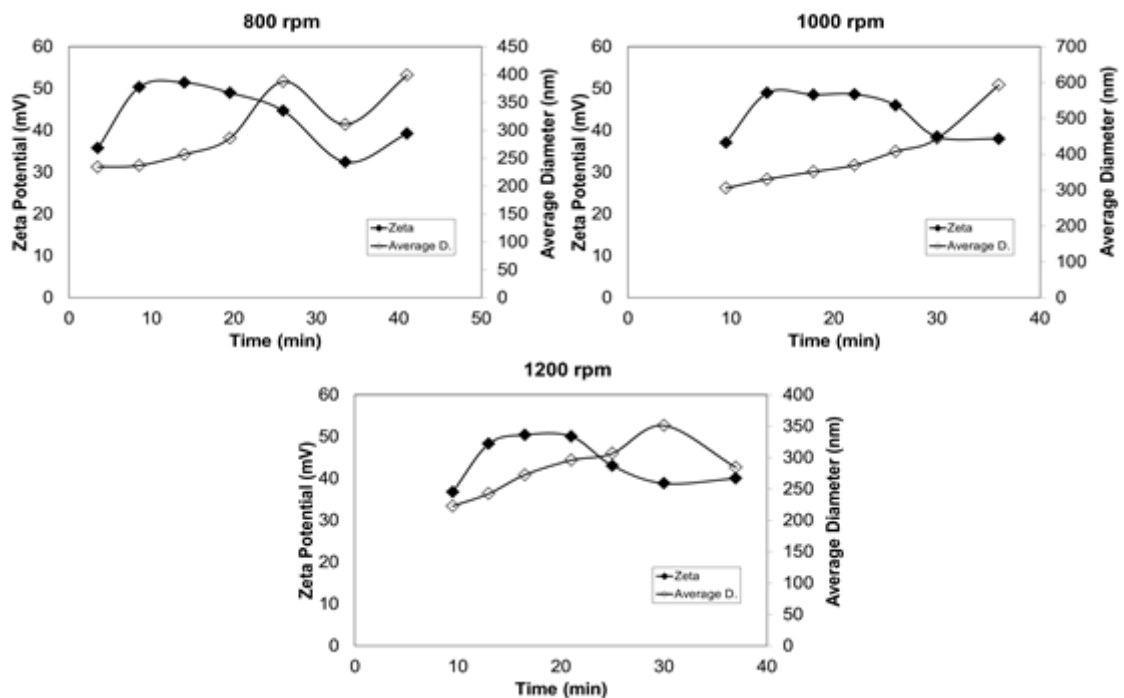
Figure 4.44. Changes in the zeta potential and average diameters of the particles for all stirring rate experiments

Another article was about a reactor which was composed with two coaxial cylinders and stirring was provided with these two different cylinders. They compared the stirring methods by using this reactor with coaxial cylinders and a reactor with mechanical stirrer. They saw that, the particles obtained from the reactor with coaxial cylinders were needle shaped due to the high OH⁻ ion concentration in the solution; on

the other hand the particles obtained from the reactor with mechanical stirrer were cubic-shaped (Jung et al., 2010).

In our system (Figure 3.2), as the stirring rate was increased, the produced calcite particles' sizes were increased, and their morphological structures changed from rhomboscalenohedral to nested hollow scalenorhombohedral structure (Figure 4.45). At low stirring rates, due to the low diffusion rate of carbon dioxide gas through the calcium hydroxide solution, the reaction took place in a more controlled manner. As the stirring rate increased, the mass transfer and diffusion rate would be increased, thus, the reaction occurred more rapidly and uncontrollably. So, it would not be expected that the obtained particles would be in homogeneous size distribution and rhombohedral structure (Figure 4.43). The mean intensity and mean number graphs of the synthesized particles were illustrated in Figure 4.43. By looking at these graphs, the smallest particles were produced with the lowest stirring rate. The SEM images given in Figure 4.45 supported these results. In the SEM images, it was understood that the particles obtained from the experiment done with 800 rpm stirring rate, were smallest and they had the most homogeneous size distributions. A growth in the particle diameters, expansions through the end portions of the particles and agglomeration could be seen as the stirring rate increased in these experiments.
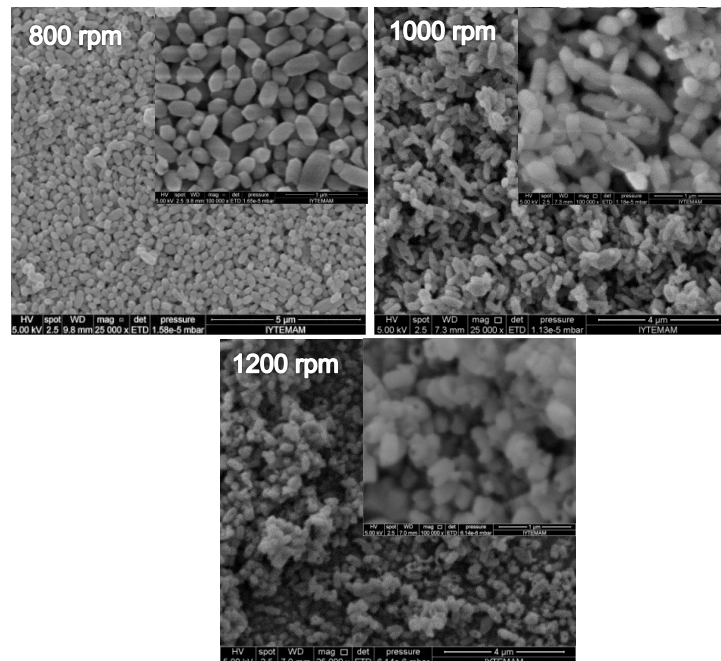
Figure 4.45. SEM images of produced calcite particles by different stirring rate experiments (at 25000 magnifications)

The zeta potential and average particle diameter graphs showed that, the zeta potential values of the particles were changed in the range of +30 and +50 mV (Figure 4.44). A decrease occurred in the zeta potential due to the consumption of the positively charged ions in the solution at the end of the reaction. After this, concentration of bicarbonate ions started to increase and so, zeta potential values started to show an increase again. Also, generally, the average diameters of the particles were increased during the reaction in all of the experiments.

4.9   The Effects of Temperature

As it was explained in the literature survey part, the calcium carbonate production can be done with two different methods. One of these method was chemical method, and the other one was the carbonization method (García-Carmona et al., 2003; H. Konno, 2003). In both of two methods, temperature played a major role due to both the solubility of the reactants with respect to the temperature and crystal structures of the produced particles. In carbonization method, the sizes and morphologies of the crystals can be controlled by some of the reaction conditions such as the concentration of the calcium hydroxide solution, flow rate of carbon dioxide gas and reaction temperature (Ahn et al., 2003). The solubility of the CO_2 gas and $Ca(OH)_2$ solution was sensitive to the temperature, so the raw materials' temperatures should be controlled during the process (Jung, 2000).

In the literature, the articles generally have pointed out that the synthesis of calcite was carried out at a temperature range of 20 and 40ºC. However, higher than 20ºC, the solubility of the calcium hydroxide decreases. So, a complete synthesis can not be occurred at the temperature higher than 20ºC. In the processes done with chemical method, crystal structure of the calcium carbonate particles are changed and aragonite particles are formed at the temperatures higher than 40ºC (H. Konno, 2003). It was known that, amorphous calcium carbonate transformed to vaterite and calcite crystal structures at low temperatures (14-30°C); aragonite and calcite crystal structures at high temperatures (60-80°C). At intermediate temperatures (40- 50°C) the formation of all three varieties were observed (Elfil & Roquesb, 2001). For this reason, our studies were done at the temperatures of 20 and 40°C, and the effects of these temperature changes on the morphologies and sizes of the calcite particles.

Joo and co-workers made a comparison by heating the system at the beginning and in the middle of the reaction, and they investigated the differences of these two methods. If the system was heated from the beginning to end of the reaction until a specific temperature value, it was observed that the larger particles were started to shrink. On the other hand, when the system was heated from the middle of the reaction, it was observed that the smaller particles started to expand, but more individual particles were formed (Ahn et al., 2003). But, such a kind of this system can not be effective and productive in the industrial fields. Thereby, in our system, the feed solution was heated before the reaction started, and until the end of the reaction, the temperature kept constant at a specified value.

When looking at the pH-conductivity graphs of experiments done at different temperatures (Figure 4.46), as the temperature increased, it was seen that the reaction times decreased due to the solubility of calcium hydroxide solution at higher temperatures decreased (Figure 4.14). Although the initial conductivity value was 5 mS/cm at 20°C, at 40°C, this initial conductivity value was started about 6 mS/cm. This situation showed that there were large amounts of undissolved Ca^{++} ions in the solution at 40°C.
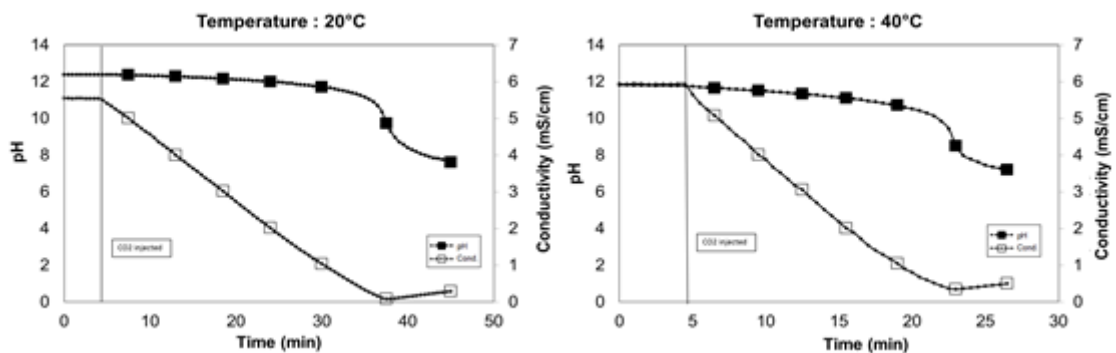
Figure 4.46. Conductivity-pH graphics of experiments done at different temperatures
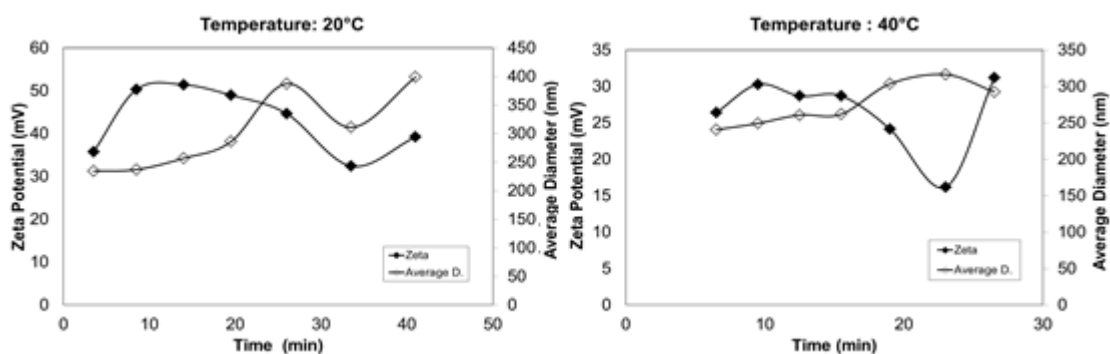
Figure 4.47. Changes in the zeta potential and average diameters of the particles for all temperature experiments

The temperature of the system generally affected the morphologies; also, it caused a growth in the diameter of the formed particles. The increment in the temperature caused a formation of nested and cubic shaped crystals. Hereby, these nested particles came together and formed larger particles, so, an increase occurred in the mean intensity graph of experiment done with 40 ºC (Figure 4.48). Another graphs proved this nested and clustered particles were the zeta potential and average diameter graphs illustrated in Figure 4.44. The zeta potential values of the samples taken from the experiment with the temperature of 40 ºC were in the range of ± 30 mV, and this range showed the potential attraction forces between the particles. In fact, the maximum point of this attraction was also the point that all Ca^{++} ions consumed. At this stage of the reaction, the presence of large amounts of bicarbonate ions made the solution negatively charged.
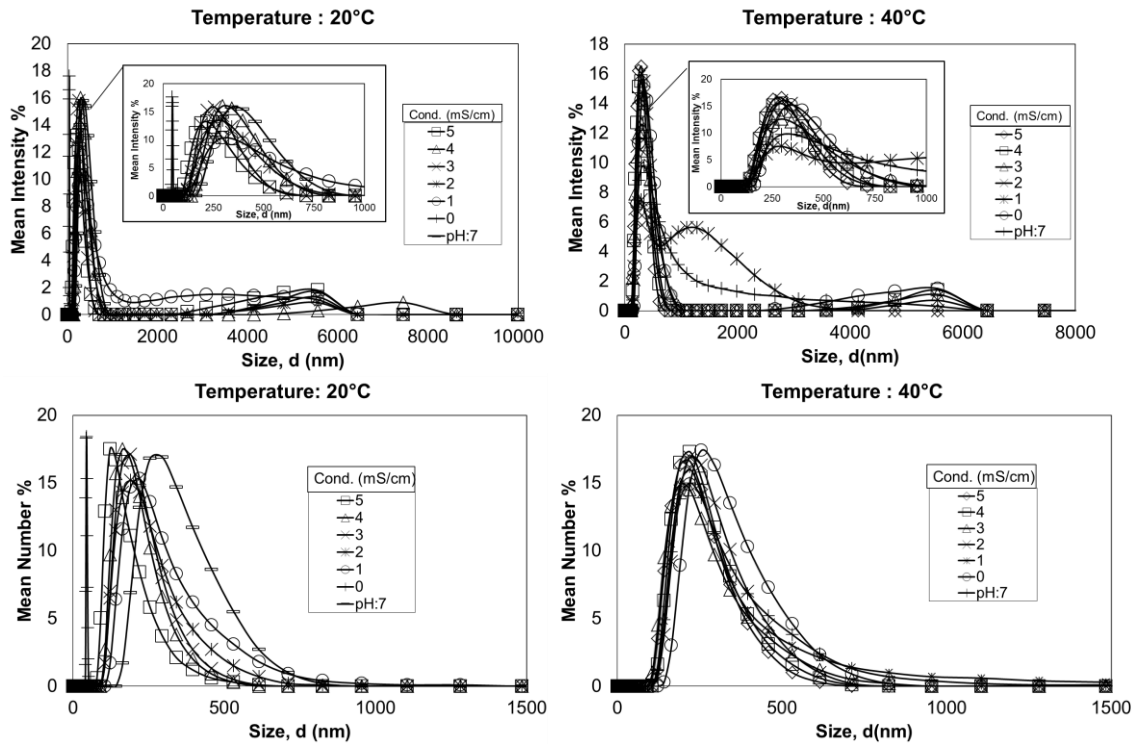
Figure 4.48. Size distributions of particles by mean intensity and mean number for both of the experiments

The obtained SEM images showed the changes in the sizes and crystal structures of synthesized particles with the increase in temperature (Figure 4.49). Although, the produced particles from the experiment done with the temperature of 20 ºC, were absolutely monodisperse and exhibited a homogeneous distribution, on the other hand, at 40 ºC, this situation was completely reversed. Also, an increase in the average particle diameters was observed. It could be shown as a result for this situation that, large amounts of undissolved Ca^{++} ions were adhered on the surfaces of the $CaCO_3$ particles and at the same time, attraction forces of the particles were became stronger due to the charge of the solution was turned to negative way in an uncontrolled manner because of the rapidly consumption of calcium ions.
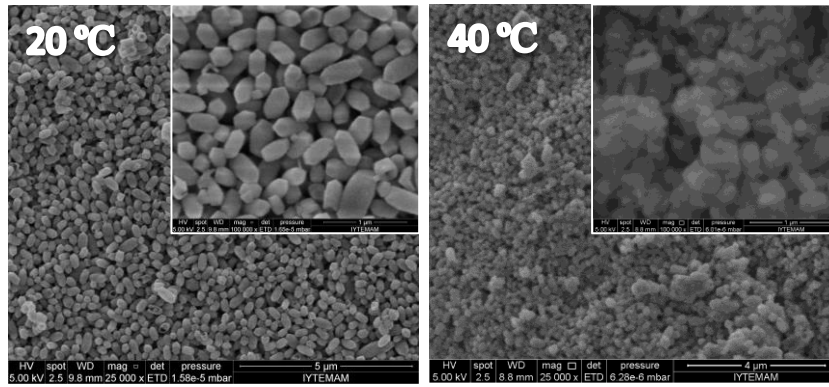
Figure 4.49. SEM images of the produced particles with different temperature experiments (at 25000 magnifications)

CHAPTER 5

CONCLUSION

In this study, nano sized $CaCO_3$ particles were produced in homogeneous size distribution and different morphologies in large scale. Depending on the synthesizing conditions, some parameters which were the flow rates of raw materials, concentration of calcium hydroxide solution, volumes of reaction chamber and stabilization tanks, diameters of pipes used in the circulation, length of reaction chamber, stirring rate and temperature, were investigated with an engineering approach and effects of these parameters on the products were analyzed. After all experiments, observed particles were analyzed using DLS, DSC, TGA, XRD and SEM methods.

One of the most important factors concerning the production conditions and quality or textures of the products was flow rates of raw materials. In our experiments, flow rates of CO_2 and $Ca(OH)_2$ solution were examined. By changing the CO_2 flow rate, it was observed that the particle size and size distributions were not evolved linearly. CO_2 flow rate directly influenced the gas intensity within the reaction chamber, so, adsorption rate and diffusion rate. The results of all analyses have shown that the finest particles were produced with the lowest gas flow rate. The reason was that the nucleation rate was increased with higher flow rates. Thus, larger particles occurred as a result of uncontrolled and rapid reactions at higher gas flow rates. The most optimum condition for CO_2 flow rate was the 5 ml/s. The smallest and rhombohedral particles were synthesized with 5 ml/s gas flow rate experiment, and DLS results and SEM images proved this hypothesis.

On the other hand, increasing the calcium hydroxide flow rate decreased the contact time of liquid and gas phases. Although homogeneous size distributions were obtained in all of the experiments, the finest particles were obtained with the higher flow rates. Also, the yield of adsorption in a short time between two phases was better than other experimental processes in which low flow rate has been used and morphologies of the particles changed from cubic shaped to hollow shaped increasing the flow rate of the liquid. The most appropriate conditions were provided with 0.8 and 1.0 m^3/h liquid flow rates.

Another effective factor in synthesizing nano calcite particles was the concentration of initial suspension. The key point of the concentration studies was the level of the supersaturation and had influenced directly upon the diameter of the nano calcite particles. At the critical point (saturation point), the smallest particles were synthesized. Initial concentration differences changing from 1 mM to 50 mM affected the diameter of particles according to determined stable saturation point respectively. Even though, the lower and higher concentration caused larger particle size, at the saturation point small particle size was obtained. Along with this, structures of the crystals were affected by solution concentrations. As the concentration increased, the particles morphologies changed from cubic shaped to scalenohedral structures. The most individual particles were produced with the 15 mM concentrated solution.

The experimental set-up we have developed possessed a circulation system. Thus, the diameters of pipes used in this circulation system could be a significant parameter for nano calcite synthesis, especially in industrial scale. The results we obtained were not very changeable due to the small diameters of the pipes. All the products at the end of the experiments were in nano sizes and homogeneous size distributions. According to our results, pipe diameters did not affect the diffusion or absorption rate between liquid and gas phases linearly. Smaller diameters of pipes caused faster liquid flow. So, an optimum pipe choice should be done with respect to the production conditions.

Calcite particles in nano sizes and homogeneous distributions were precipitated in all of the experiments, although different volumes of stabilization tanks were studied. But, due to the uncontrolled diffusion of CO_2 gas into the $Ca(OH)_2$ solution in smaller tanks, particles that were larger than others, were produced in the smallest stabilization tanks. Moreover, the reaction time decreased with the smaller stabilization tank volume; therefore, absorption was not occurred homogeneously. Furthermore, stabilization tank volume did not affect the morphologies of the products.

In the same way, contact time of two phases, thus absorption and diffusion rates depended on the length of the reaction chamber, too. Due to the same results mentioned above, the contact time of two phases decreased as the length of reaction chamber decreased. Consequently, an increase in the residence time caused occurrence of more controllable reaction. The distance between the shower and the exit of the chamber was increased, smaller particles were obtained. Besides, in the length of reaction chamber experiments, an increase or decrease in the contact time did not cause any changes in

the crystal structures. Also, as the volume of the reaction chamber increased, the concentration of the CO_2 gas in the chamber decreased, and the diffusion rate became slower. Thus, smaller calcite particles were produced using larger reaction chambers.

Another important factor affecting the structure of the crystals was the stirring rate. In our system, particle sizes became larger as the stirring rate increased. At lower stirring rates, diffusion and mass transfer rates were slower, thus, the reaction carried out in a more controlled manner. So, with higher stirring rates, the morphologies of the particles were changed, because, plucking ions from the crystal surfaces became slower. Also, stirring rate increased the amounts of clusters in the solution. The growth in the particle diameters, expansions through the end portions of the particles and agglomeration could be seen, as the stirring rate increased in these experiments. The finest particles were produced from the experiment in which 800 rpm stirring rate has been used.

It was expected that the increase in the temperature of the calcium hydroxide solution changed the morphology of the crystals. We studied two different temperatures because, the solubility of the $Ca(OH)_2$ decreased with respect to increase in the temperature. We observed that the formation of nested and cubic shaped nano calcite crystals was caused from the increment in the temperature. The attraction forces among the particles were increased due to the temperature, thus, agglomerated particles were produced in 40ºC solution. Consequently, these attractive forces could cause ion exchanges among the particles and they started to grow adhering to each other.

Finally it can be said that, nano calcite particles that had been produced by small penetration method for using in a composite material as a filler, were synthesized with the production conditions of 5 ml/s CO_2 flow rate, 1.0 m^3/h $Ca(OH)_2$ suspension flow rate, with 5 L reaction chamber volume, 30 cm reaction chamber length, at 800 rpm stirring rate and 20 ºC, by using shower. The synthesized particles with these conditions were quite small and cubic, hallow shaped. They were monodisperse particles and their surface areas were large and for the industrial applications.

REFERENCES

Ahn, Ji Whan, Joo, Sung Min, Kim, Hyung Seok, Kim, Dae Hun, Kim, Jong Pyo, & Kim, Hwan. (2003). Influence of Final Crystal with Synthesis of Basic Calcium Carbonate by Carbonation Process. *Materials Science Forum, 439*, 244-253.

Ahn, Ji Whan, Kim, Jung Ah, You, Kwang Suk, Kim, Hwan, Cho, Hee Chan, & Lee, Im Chan. (2007). The Effect of Initial Hydration Temperature on the Characteristics of Calcium Hydroxide and Aragonite Precipitated Calcium Carbonate. *Solid State Phenomena, 124-126*, 815-818.

Beck, R.; Andreassen, J. P. (2010). The onset of spherulitic growth in crystallization of calcium carbonate. *Journal of Crystal Growth, 312*(15), 2226-2238.

Burns, J. R., & Jachuck, R. J. J. (2005). Monitoring of CaCO3 production on a spinning disc reactor using conductivity measurements. *AIChE Journal, 51*(5), 1497-1507.

Cai, H.; Li, S.D. (2003). Reinforcement of Natural Rubber Latex Film by Ultrafine Calcium Carbonate. *J. of App. Pol. Sc., 87*, 982–985.

Carmona, García. (2003). Rhombohedral–scalenohedral calcite transition produced by adjusting the solution electrical conductivity in the system Ca(OH)2–CO2–H2O. *Journal of Colloid and Interface Science, 261*(2), 434-440.

Carmona, J. (2004). The mechanism of precipitation of chain-like calcite. *Journal of Crystal Growth, 262*(1-4), 479-489.

Chen, J. F.; Zheng, C.; Chen, G. T. . (1996). Interaction of Macro and Micromixing on Particle Size Distribution in Reactive Precipitation. *Chem. Eng. Sci., 51*, 1957.

Chen, J.F. ; Wang, Y. H. (2000). Synthesis of Nanoparticles with Novel Technology: High-Gravity Reactive Precipitation. *Ind. Eng. Chem. Res., 39*, 948-954.

Chen, Xue, Zhu, Yanchao, Guo, Yupeng, Zhou, Bing, Zhao, Xu, Du, Yanyan, . . . Wang, Zichen. (2010). Carbonization synthesis of hydrophobic CaCO3 at room temperature. *Colloids and Surfaces A: Physicochemical and Engineering Aspects, 353*(2-3), 97-103.

Chibowski, E., Hotysz, L., & Szcześ, A. (2003). Time dependent changes in zeta potential of freshly precipitated calcium carbonate. *Colloids and Surfaces A: Physicochemical and Engineering Aspects, 222*(1-3), 41-54.

Coto, B.;, Martos, C.;, Peña, J. L.;, Rodríguez, R.;, & Pastor, G. (2012). Effects in the solubility of CaCO3: Experimental study and model description. *Fluid Phase Equilibria, 324*, 1-7.

Cölfen, H. (2003). Precipitation of carbonates: Recent progress in controlled production of complex shapes. *Current Opinion in Colloid and Interface Science, 8*, 23–31.

Dagaonkar, M., Mehra, A., Jain, R., & Heeres, H. (2004). Synthesis of CaCO3 Nanoparticles by Carbonation of Lime Solutions in Reverse Micellar Systems. *Chemical Engineering Research and Design, 82*(11), 1438-1443.

Domingo, C., Loste, E., Gómez-Morales, J., García-Carmona, J., & Fraile, J. (2006). Calcite precipitation by a high-pressure CO2 carbonation route. *The Journal of Supercritical Fluids, 36*(3), 202-215.

Elfil, H., & Roquesb, H. (2001). Role of hydrate phases of calcium carbonate on the scaling phenomenon. *Desalination, 137*, 177-186.

Faatz, M., Gröhn, F., & Wegner, G. (2005). Mineralization of calcium carbonate by controlled release of carbonate in aqueous solution. *Materials Science and Engineering: C, 25*(2), 153-159.

Feng, Bo, Yong, Andrew K., & An, Hui. (2007). Effect of various factors on the particle size of calcium carbonate formed in a precipitation process. *Materials Science and Engineering: A, 445-446*, 170-179.

García-Carmona, Jesús, Morales, Jaime Gómez, & Clemente, Rafael Rodríguez. (2003). Morphological control of precipitated calcite obtained by adjusting the electrical conductivity in the Ca(OH)2–H2O–CO2 system. *Journal of Crystal Growth, 249*(3-4), 561-571.

Gupta, Ritika. (2004). Synthesis of Precipitated Calcium Carbonate Nanoparticles Using Modified Emulsion Membranes. *Georgia Institute of Technology - Paper Science Engineering*.

Hrnjak-Murgic, Z. ; Jelcic, Z. (2002). Molecular and Morphological Characterization of Immiscible SAN/EPDM Blends Filled by Nano Filler. *Macromol. Mater. Eng. , 287*, 684-692.

Ibrahim, A.R;, Vuningoma, J.B;, Hu, X.;, Gong, Y.;, Hua, Dan, Hong, Yanzhen, . . . Li, Jun. (2012). High-pressure gas–solid carbonation route coupled with a solid ionic liquid for rapid synthesis of rhombohedral calcite. *The Journal of Supercritical Fluids, 72*, 78-83.

Islam, M. S.; Quader, A. K. M. A. . (2008). laboratory-Scale Production of Commercial Grade Calcium Carbonate from Lime-Soda Process. *Chemical Engineering Research Bulletin, 12*, 1-6.

Jiang, Jiuxin, Liu, Jie, Liu, Chang, Zhang, Gaowen, Gong, Xinghou, & Liu, Jianing. (2011). Roles of oleic acid during micropore dispersing preparation of nano-calcium carbonate particles. *Applied Surface Science, 257*(16), 7047-7053.

Johannsen, K.; Rademacher, S. (1999). Modelling the Kinetics of Calcium Hydroxide Dissolution in Water. *Acta hydrochim. hydrobiol., 27*(2), 72-78.

Jung, W. M.;. (2000). Particle morphology of calcium carbonate precipitated by gas-liquid reaction in a Couette-Taylor reactor. *Chemical Engineering Science, 55*, 733-747.

Jung, W. M.;, Sung, H.K.;, Kim, K.S.;, Kim, W. S.;, & Chang, K.C. . (2010). Precipitation of calcium carbonate particles by gas–liquid reaction: Morphology and size distribution of particles in Couette-Taylor and stirred tank reactors. *Journal of Crystal Growth, 312*(22), 3331-3339.

Kanakis, J; Dalas, E. (2000). The crystallization of vaterite on "brin. *Journal of Crystal Growth, 219*, 277-282.

Kang, S. H., Hirasawa, I., Kim, W. S., & Choi, C. K. (2005). Morphological control of calcium carbonate crystallized in reverse micelle system with anionic surfactants SDS and AOT. *J Colloid Interface Sci, 288*(2), 496-502.

Kim, Jeong Hwan, Ahn, Ji Whan, Ko, Sang Jin, Park, Woon Kyoung, & Han, Choon. (2006). Inhibition Mechanism of Magnesium Ion on Carbonation Reaction with Ca(OH)2 and CO2. *Materials Science Forum, 510-511*, 990-993.

Kim, Kyung Nam, Shin, Dae Yong, Son, Se Gu, & Kim, Yong Do. (2005). Synthesis of Calcium Carbonate from Calcium Chlorine Solution Using Homogeneous Precipitation Method. *Materials Science Forum, 486-487*, 542-545.

Konno, Haruo. (2003). Effect of NaOH on aragonite precipitation in batch and continuous crystallization in causticizing reaction. *Powder Technology, 129* 15–21.

Konno, Mitsutaka Kitamura; Haruo. (2002). Controlling factors and mechanism of reactive crystallization of calcium carbonate polymorphs from calcium hydroxide suspensions. *Journal of Crystal Growth, 236*, 323–332.

Laudone, G. M. ; Matthews, G. P. (2004). Observation of Shrinkage during Evaporative Drying of Water-Based Paper Coatings. *Ind. Eng. Chem. Res. , 43*, 712-719.

Lieth, R. M. A. (1930). Preparation and Crystal Growth of Materials with Layered Structures. *Physics and chemistry of materials with layered structures 1*, 161.

Lin, Rong-yi. (2002). Nucleation and growth kinetics in synthesizing nanometer calcite. *Journal of Crystal Growth, 245*, 309–320.

Lin, Rong-yi, Zhang, Jia-yun, & Bai, Yuan-qiang. (2006). Mass transfer of reactive crystallization in synthesizing calcite nanocrystal. *Chemical Engineering Science, 61*(21), 7019-7028.

López-Periago, Ana M., Pacciani, Roberta, García-González, Carlos, Vega, Lourdes F., & Domingo, Concepción. (2010). A breakthrough technique for the preparation of high-yield precipitated calcium carbonate. *The Journal of Supercritical Fluids, 52*(3), 298-305.

Matahwa, H., Ramiah, V., & Sanderson, R. D. (2008). Calcium carbonate crystallization in the presence of modified polysaccharides and linear polymeric additives. *Journal of Crystal Growth, 310*(21), 4561-4569.

Molva, M. (2012). Production of nano CaCO3 by carbonization route. *the Graduate School of Engineering and Sciences of İzmir Institute of Technology*.

Montes-Hernandez, G., Daval, D., Findling, N., Chiriac, R., & Renard, F. (2012). Linear growth rate of nanosized calcite synthesized via gas–solid carbonation of Ca(OH)2 particles in a static bed reactor. *Chemical Engineering Journal, 180*, 237-244.

Monteshernandez, G., Fernandezmartinez, A., Charlet, L., Tisserand, D., & Renard, F. (2008). Textural properties of synthetic nano-calcite produced by hydrothermal carbonation of calcium hydroxide. *Journal of Crystal Growth, 310*(11), 2946-2953.

Nefyodova, I.V. (2000). Hydrothermal growth and morphology of calcite single crystals.

Nehrke, G., Reichart, G., Vancappellen, P., Meile, C., & Bijma, J. (2007). Dependence of calcite growth rate and Sr partitioning on solution stoichiometry: Non-Kossel crystal growth. *Geochimica et Cosmochimica Acta, 71*(9), 2240-2249.

Ogino, T.; Suzuki, T.; Sawada, K. (1987). The formation and transformation mechanism of calcium carbonate in water. *Geochimica et Cosmochimica Acta, 51*(10), 2757-2767.

Oniyama, E.; Wahlbeck , P.G. (1995). Application of transpiration theory to TGA data: calcium carbonate and zinc chloride. *Thermochimica Acta, 250*, 41-53.

Pontoni, D.; Bolze, J. (2003). Crystallization of Calcium Carbonate Observed In-situ by Combined Small- and Wide-angle X-ray Scattering. *J. Phys. Chem. B., 107*, 5123-5125.

Rieger, J.; Thieme, J. (2000). Study of Precipitation Reactions by X-ray Microscopy:CaCO3 Precipitation and the Effect of Polycarboxylates. *Langmuir, 16*, 8300-8305.

Roskill Information Services, Ltd. . (2012). Ground and precipitated calcium carbonate: Global industry markets & outlook. *1st edittion*.

Sonawane, Shirish H., & Gumfekar, Sarang P. (2010). Hydrodynamic Cavitation-Assisted Synthesis of Nanocalcite. *International Journal of Chemical Engineering, 2010*, 1-8.

Tai, Clifford Y. (2001). Crystal growth kinetics of calcite and its comparison with readily soluble salts. *Powder Technology 121*, 60-67.

Tang, Chiu. (2012). High Resolution Powder Diffraction. *Diamond Light Source Ltd.*

Tosun, G. (1988). An Experimental Study of the Effect of Mixing on the Particle Size Distribution in BaSO4 Precipitation Reaction. *In Proceedings of the 6th European Conference on Mixing; BHRA; Cranfield, England*, 161.

Trippa, G., & Jachuck, R. J. J. (2003). Process Intensification. *Chemical Engineering Research and Design, 81*(7), 766-772.

Wei, S. H. (1997). High Surface Area Calcium Carbonate: Pore Structural Properties and Sulfation Characteristics. *Ind. Eng. Chem. Res. , 36*, 2141-2148.

Wu, Guohua, Wang, Yujun, Zhu, Shenlin, & Wang, Jiading. (2007). Preparation of ultrafine calcium carbonate particles with micropore dispersion method. *Powder Technology, 172*(2), 82-88.

Xu, B.A.; Giles, D. E.; Ritchie, I.M. (1998). Reactions of lime with carbonate-containing solutions. *Hydrometallurgy 48*, 205-224.

Ye, Yu Qian, & Chen, Xue Mei. (2011). The Role of Crystal Control Agent in the Formation of Needlelike Calcium Carbonate Nano Particles. *Advanced Materials Research, 236-238*, 2150-2159.

Yuan, Pei-Qing, Cheng, Zhen-Min, Zhou, Zhi-Ming, Yuan, Wei-Kang, & Semiat, Raphael. (2008). Zeta potential on the anti-scalant modified sub-micro calcite surface. *Colloids and Surfaces A: Physicochemical and Engineering Aspects, 328*(1-3), 60-66.

Zhu, Wen Kun, Luo, Xue Gang, Luo, An Kai, & Liang, Xuan. (2010). Synthesis and Characterization of Dumbbell Shaped Calcium Carbonate Induced by Lignin. *Materials Science Forum, 658*, 49-52.